

Fall 2014

# Integrating Pro-Environmental Behavior with Transportation Network Modeling: User and System Level Strategies, Implementation, and Evaluation

Husain M. Abdul Aziz  
*Purdue University*

Follow this and additional works at: [https://docs.lib.purdue.edu/open\\_access\\_dissertations](https://docs.lib.purdue.edu/open_access_dissertations)



Part of the [Civil Engineering Commons](#), and the [Transportation Engineering Commons](#)

---

## Recommended Citation

Abdul Aziz, Husain M., "Integrating Pro-Environmental Behavior with Transportation Network Modeling: User and System Level Strategies, Implementation, and Evaluation" (2014). *Open Access Dissertations*. 228.  
[https://docs.lib.purdue.edu/open\\_access\\_dissertations/228](https://docs.lib.purdue.edu/open_access_dissertations/228)

This document has been made available through Purdue e-Pubs, a service of the Purdue University Libraries. Please contact [epubs@purdue.edu](mailto:epubs@purdue.edu) for additional information.

**PURDUE UNIVERSITY  
GRADUATE SCHOOL  
Thesis/Dissertation Acceptance**

This is to certify that the thesis/dissertation prepared

By H M Abdul Aziz

Entitled  
INTEGRATING PRO-ENVIRONMENTAL BEHAVIOR WITH TRANSPORTATION NETWORK  
MODELING: USER AND SYSTEM LEVEL STRATEGIES, IMPLEMENTATION, AND  
EVALUATION

For the degree of Doctor of Philosophy

Is approved by the final examining committee:

SATISH V. UKKUSURI

SRINIVAS PEETA

AMR A. KANDIL

ANDREW (LU) LIU

To the best of my knowledge and as understood by the student in the Thesis/Dissertation Agreement, Publication Delay, and Certification/Disclaimer (Graduate School Form 32), this thesis/dissertation adheres to the provisions of Purdue University's "Policy on Integrity in Research" and the use of copyrighted material.

SATISH V. UKKUSURI

Approved by Major Professor(s): \_\_\_\_\_

Approved by: DULCY ABRAHAM

08/26/2014

Head of the Department Graduate Program

Date



INTEGRATING PRO-ENVIRONMENTAL BEHAVIOR WITH  
TRANSPORTATION NETWORK MODELING: USER AND SYSTEM LEVEL  
STRATEGIES, IMPLEMENTATION, AND EVALUATION

A Dissertation

Submitted to the Faculty

of

Purdue University

by

H. M. Abdul Aziz

In Partial Fulfillment of the

Requirements for the Degree

of

Doctor of Philosophy

December 2014

Purdue University

West Lafayette, Indiana

For their endless support and love, dedicated to my beloved wife Mumu, my sister Jesmin, and my respected parents Mohammad Afzal Husain and Hafiza Husain.

## ACKNOWLEDGMENTS

I would like to express my gratitude to my advisor and mentor Dr. Satish V. Ukkusuri for all the guidance and supports during my doctoral studies. The higher level of flexibility in conducting research and the encouragement to explore beyond traditional transportation science facets helped me to learn and think critically. I am grateful for his time dedication to discuss research ideas and insightful directions. I sincerely thank Dr. Amr Kandil, Dr. Srinivas Peeta, and Dr. Andrew Liu for being my committee members and their suggestions to improve my work. I am highly thankful to Dr. Julian Romero for his guidance and help on designing and developing the experimental game tool. Thanks to all my lab mates at Purdue that include Samiul, Kien, Binh, Rodrigo, Xinwu, Abdiel, Feng, Xianyuan, Sadri, Pulkit, Wenbo, Qing, and others. It was a wonderful experience at Purdue to meet fellow graduate students and learn from them.

I am grateful to my wife Mumu for her patience, support, and love throughout the graduate school life. My little angel Mariam kept me smiling during the toilsome days of dissertation writing. Finally I express my gratitude to the almighty for granting me success and this achievement.

## TABLE OF CONTENTS

	Page
LIST OF TABLES . . . . .	ix
LIST OF FIGURES . . . . .	xi
ABSTRACT . . . . .	xiii
CHAPTER 1 INTRODUCTION . . . . .	1
1.1 Background and motivation . . . . .	1
1.2 Dissertation objectives . . . . .	3
1.2.1 Objective-1 . . . . .	3
1.2.2 Objective-2 . . . . .	7
1.2.3 Objective-3 . . . . .	9
1.2.4 Objective-4 . . . . .	10
1.2.5 Objective-5 . . . . .	11
1.3 Contributions . . . . .	12
1.4 Dissertation organization . . . . .	13
CHAPTER 2 LITERATURE REVIEW . . . . .	14
2.1 Introduction . . . . .	14
2.2 Effect of Descriptive Information on Travel Choices . . . . .	14
2.2.1 Information and Pro-environmental Behavior . . . . .	14
2.2.2 Willingness-to-pay for emissions . . . . .	16
2.2.3 Influence of information . . . . .	16
2.2.4 Summary . . . . .	17
2.3 Carbon allowance schemes . . . . .	18
2.3.1 Tradable systems . . . . .	18
2.3.2 Market based approaches . . . . .	19
2.3.3 Tradable mobility credits . . . . .	19
2.3.4 Personal carbon allowance . . . . .	20
2.3.5 Summary . . . . .	20
2.4 Signal control schemes with emissions objective . . . . .	21
2.5 Assessment of strategies . . . . .	22
2.6 Summary and conclusions . . . . .	22
CHAPTER 3 GREEN CHOICES IN TRAVEL ACTIVITIES . . . . .	24
3.1 Introduction . . . . .	24

	Page
3.2 Design of experiments and Data . . . . .	25
3.2.1 Travel time and variation in travel time . . . . .	26
3.2.2 Quantifying GHG emissions . . . . .	26
3.2.3 Sample description . . . . .	27
3.3 Methodology . . . . .	28
3.3.1 Random-Parameter Model . . . . .	28
3.3.2 Estimating Trade-off . . . . .	30
3.3.3 Interpreting the trade-off values . . . . .	30
3.3.4 Statistical testing . . . . .	31
3.4 Empirical results . . . . .	32
3.4.1 Route choice models . . . . .	32
3.4.2 Work vs. non-work trips . . . . .	32
3.4.3 Estimation results: Route choice . . . . .	33
3.4.4 Trade-offs in route choice . . . . .	37
3.4.5 Work trips . . . . .	37
3.4.6 Non-work trips . . . . .	41
3.4.7 Summary . . . . .	43
3.4.8 Departure time choice models . . . . .	44
3.4.9 Trade-offs in departure time choices . . . . .	46
3.5 Policy implications . . . . .	49
3.5.1 Provision of information . . . . .	49
3.5.2 Savings in terms of emissions . . . . .	50
3.5.3 Improvement of travel time . . . . .	53
3.5.4 Policies for heterogeneous population . . . . .	54
3.5.5 Flexibility in departure time . . . . .	54
3.5.6 Integrated agent based simulation . . . . .	55
3.6 Concluding remarks . . . . .	55
3.6.1 Key findings . . . . .	55
3.6.2 Limitations and future work . . . . .	56
CHAPTER 4 CARBON ALLOWANCE FOR TRAVEL . . . . .	59
4.1 Introduction . . . . .	59
4.1.1 Personal Mobility Carbon Allowance (PMCA) . . . . .	60
4.1.2 Research goals . . . . .	61
4.2 Why experimental games? . . . . .	62
4.3 Description of the experimental game . . . . .	64
4.4 Game design . . . . .	65
4.4.1 Initial allocation . . . . .	65
4.4.2 Travel decision scenarios . . . . .	66
4.4.3 Trip demand and value of time . . . . .	66
4.4.4 Market: double auction mechanism . . . . .	67
4.5 Development of game . . . . .	69



	Page
4.5.1 Interface design . . . . .	69
4.5.2 Real-time interaction using TCP-IP . . . . .	70
4.6 Data collection . . . . .	70
4.7 Methodology . . . . .	71
4.8 General observations . . . . .	73
4.9 Incorporating market effects . . . . .	74
4.10 Parameter estimates . . . . .	74
4.10.1 Work trips . . . . .	75
4.10.2 Grocery(non-work) trips . . . . .	75
4.10.3 Recreational trips . . . . .	78
4.11 Effect of PMCA on travel decision . . . . .	80
4.11.1 Work trips . . . . .	81
4.11.2 Grocery trips . . . . .	83
4.11.3 Recreational trips . . . . .	83
4.12 Price convergence . . . . .	84
4.13 Market: bids and asks . . . . .	86
4.13.1 Model description . . . . .	86
4.13.2 Zero-Inflated model for asks . . . . .	87
4.13.3 Empirical results . . . . .	87
4.13.4 Correlation between asks and bids . . . . .	89
4.14 Conclusions and future research . . . . .	92
CHAPTER 5 EQUILIBRIUM MODELS FOR PMCA . . . . .	94
5.1 Introduction . . . . .	94
5.2 Multi-class characterization . . . . .	94
5.3 Methodology . . . . .	95
5.3.1 Dynamic network loading . . . . .	96
5.3.2 Cell transmission model . . . . .	96
5.3.3 Travel Time Estimation . . . . .	102
5.3.4 Carbon cost for the trip . . . . .	103
5.3.5 Generalized cost function under PMCA . . . . .	104
5.3.6 Dynamic user equilibrium condition . . . . .	105
5.3.7 Demand satisfaction constraints . . . . .	106
5.3.8 Dynamic user equilibrium (DUE-PMCA) . . . . .	107
5.3.9 Equivalent VI . . . . .	108
5.4 Solution approach . . . . .	109
5.4.1 Basic projection method . . . . .	110
5.4.2 Algorithm to solve decomposed VI . . . . .	111
5.5 Numerical example . . . . .	113
5.5.1 Input parameters . . . . .	113
5.5.2 Trip demand and value of time . . . . .	115
5.5.3 Parameters for cost function . . . . .	115

	Page
5.5.4 X-network . . . . .	115
5.6 Results for Sioux-Falls network . . . . .	122
5.6.1 PMCA-DUE-1 (different carbon reduction) . . . . .	122
5.6.2 Comparison of OD level carbon and travel cost . . . . .	127
5.6.3 Comparison of carbon consumption . . . . .	127
5.6.4 Comparison of path level carbon cost . . . . .	129
5.7 Concluding remarks . . . . .	132
CHAPTER 6 LEARNING BASED TRAFFIC CONTROL . . . . .	135
6.1 Introduction . . . . .	135
6.2 Literature Review . . . . .	137
6.3 Reinforcement Learning Based Algorithms . . . . .	139
6.4 Elements of the RL-based algorithm . . . . .	140
6.4.1 State of the system . . . . .	140
6.4.2 System state of the RL . . . . .	142
6.4.3 Action selection strategy . . . . .	142
6.4.4 $\epsilon$ -greedy method . . . . .	143
6.4.5 soft-max method . . . . .	143
6.4.6 Reward function . . . . .	144
6.4.7 Multi-reward structure . . . . .	144
6.5 Algorithm description . . . . .	144
6.5.1 Notations . . . . .	145
6.5.2 RMART description . . . . .	145
6.5.3 Pseudo Code . . . . .	146
6.6 Implementation and numerical results . . . . .	146
6.6.1 Congestion level variation at intersection level . . . . .	146
6.6.2 Statistical tests . . . . .	150
6.6.3 Performance comparison: Average Delay . . . . .	150
6.6.4 Performance comparison: stopped delay . . . . .	152
6.6.5 Comparison of system wide performance . . . . .	153
6.6.6 Comparison with real time adaptive control . . . . .	154
6.6.7 Value of information sharing among neighbors . . . . .	155
6.7 Emissions estimation using MOVES2010b . . . . .	156
6.8 Summary and concluding remarks . . . . .	158
CHAPTER 7 INTEGRATED EMISSIONS TOOL . . . . .	160
7.1 Introduction . . . . .	160
7.2 EPA Regulated Estimation Tool: MOVES2010 . . . . .	164
7.2.1 Estimation Method in MOVES . . . . .	165
7.2.2 Data input for MOVES . . . . .	166
7.3 Integration with Traffic Simulation . . . . .	167
7.3.1 Applications of integrated tool . . . . .	168

	Page
7.4 Methodology: HC-DTW technique . . . . .	169
7.4.1 Computing DTW measures . . . . .	171
7.4.2 Hierarchical clustering . . . . .	172
7.4.3 Consistency measures . . . . .	174
7.4.4 (Dis)similarity measures . . . . .	175
7.5 Demonstration of the technique . . . . .	175
7.5.1 Comparing the performance of HC-DTW . . . . .	177
7.5.2 Computational time . . . . .	180
7.5.3 Results with two signalized intersections . . . . .	180
7.5.4 Summary of findings . . . . .	181
7.6 Concluding remarks . . . . .	189
CHAPTER 8 CONCLUSIONS . . . . .	191
8.1 Major contributions . . . . .	191
8.2 Future works . . . . .	193
BIBLIOGRAPHY . . . . .	194
VITA . . . . .	218

## LIST OF TABLES

Table	Page
1.1 Route Choice Scenario . . . . .	5
1.2 Departure Time Scenario* . . . . .	6
1.3 Route Choice Scenario under PMCA system . . . . .	8
3.1 Estimates: Route choice for work commute . . . . .	35
3.2 Estimates: Route choice for non-work . . . . .	36
3.3 Trade-off value distributions . . . . .	43
3.4 Results: departure time choice . . . . .	45
3.5 Trade-off value distributions . . . . .	46
3.6 Effect of providing emissions information* . . . . .	49
3.7 Impact of information: city level . . . . .	52
3.8 Effect of reducing travel time: Work trips . . . . .	53
4.1 User group definition . . . . .	67
4.2 Estimates for work trips-all groups . . . . .	76
4.3 Estimates for grocery trips-all groups . . . . .	77
4.4 Estimates for recreational trips-all groups . . . . .	80
4.5 Direct elasticity measures . . . . .	82
4.6 Results: Poisson model for bids . . . . .	88
4.7 Elasticity values: Bids model . . . . .	89
4.8 Results: Zero-inflated Poisson model for asks . . . . .	90
4.9 Elasticity values: Asks model . . . . .	90
5.1 User group definition . . . . .	115
5.2 Parameters for generalized cost function. . . . .	116
5.3 System level results for X-network . . . . .	120
5.4 Comparison between two solution approaches . . . . .	121

Table	Page
5.5 OD level cost comparison . . . . .	128
5.6 Comparison of carbon consumptions at user class level* . . . . .	131
6.1 Description Of Congestion Variation . . . . .	150
6.2 System performance for different control algorithms* . . . . .	151
6.3 Average Delay (seconds) Comparison . . . . .	152
6.4 Comparison of Stopped Delay (seconds) . . . . .	153
6.5 Comparisons of system delay (seconds $\times 10^3$ . . . . .	154
6.6 Comparison with Adaptive (ELQF) Controllers . . . . .	155
6.7 Benefits of information sharing . . . . .	156
6.8 Comparison of Emissions (Network-I) . . . . .	157
7.1 Description of test scenarios: vehicular activity proportions . . . . .	179
7.2 Comparison of estimates for different approaches . . . . .	186
7.3 Computational time comparison . . . . .	187
7.4 Sample results using HC-DTW technique . . . . .	188

## LIST OF FIGURES

Figure	Page
3.1 Trade-offs in work trips: Male group . . . . .	38
3.2 Trade-offs in work trips: Female group . . . . .	39
3.3 Trade-offs in work trips: Bike preference . . . . .	39
3.4 Trade-offs: high income households . . . . .	40
3.5 Trade-offs in non-work trips: Male group . . . . .	41
3.6 Trade-offs in non-work trips: Female group . . . . .	42
3.7 Trade-offs in non-work trips: Bike preference . . . . .	42
3.8 Trade-offs in departure time choice: Male group . . . . .	47
3.9 Trade-offs in departure time choice: Female group . . . . .	47
3.10 Trade-offs in departure time choice: Bike preference . . . . .	48
4.1 Overview of the PMCA scheme . . . . .	60
4.2 Route choice segment of the game . . . . .	65
4.3 Market (double auction) segment of the game . . . . .	68
4.4 Interaction between server and client modules . . . . .	70
4.5 Distribution of estimated parameters: Travel cost . . . . .	79
4.6 Patterns of unit price in the market . . . . .	85
5.1 Fitted relationship between speed and emissions rate . . . . .	114
5.2 Cell representation of X-Shaped Network [109] . . . . .	117
5.3 Results for DUE-1: Coupled constraint problem . . . . .	118
5.4 Results for DUE-2: Coupled constraint problem . . . . .	118
5.5 Results for DUE-3: Coupled constraint problem . . . . .	118
5.6 Results for DUE-1: carbon constraint at OD level . . . . .	119
5.7 Results for DUE-2: carbon constraint at OD level . . . . .	119
5.8 Results for DUE-3: carbon constraint at OD level . . . . .	119

Figure	Page
5.9 Cell representation of SiouxFalls network [109] . . . . .	123
5.10 PMCA-DUE-1 results: 2% reduction from base case . . . . .	124
5.11 PMCA-DUE-1 results: 5% reduction from base case . . . . .	125
5.12 PMCA-DUE-1 results: 7% reduction from base case . . . . .	126
5.13 Path level carbon cost at different carbon caps. . . . .	130
6.1 Algorithm: SARSA . . . . .	147
6.2 Algorithm: RMART . . . . .	148
6.3 Test network for evaluating the signal control algorithms. . . . .	149
7.1 Alignment by DTW . . . . .	163
7.2 Framework: integrated traffic and emissions simulator . . . . .	168
7.3 Link Driving Schedule (LDS) finding methodology . . . . .	170
7.4 DTW optimal path computation . . . . .	173
7.5 Test network: five intersection corridor . . . . .	176
7.6 Link-3 for intersection-1 . . . . .	181
7.7 Link-4 for intersection-1 . . . . .	182
7.8 Link-1 for intersection-4 . . . . .	182
7.9 Link-2 for intersection-4 . . . . .	183
7.10 Link-3 for intersection-4 . . . . .	184

## ABSTRACT

Aziz, H. M. Abdul. Ph.D., Purdue University, December 2014. Integrating Pro-Environmental Behavior with Transportation Network Modeling: User and System Level Strategies, Implementation, and Evaluation. Major Professor: Satish V. Ukkusuri.

Personal transport is a leading contributor to fossil fuel consumption and greenhouse (GHG) emissions in the U.S. The U.S. Energy Information Administration (EIA) reports that light-duty vehicles (LDV) are responsible for 61% of all transportation related energy consumption in 2012, which is equivalent to 8.4 million barrels of oil (fossil fuel) per day. The carbon content in fossil fuels is the primary source of GHG emissions that links to the challenge associated with climate change. Evidently, it is high time to develop actionable and innovative strategies to reduce fuel consumption and GHG emissions from the road transportation networks. This dissertation integrates the broader goal of minimizing energy and emissions into the transportation planning process using novel systems modeling approaches. This research aims to find, investigate, and evaluate strategies that minimize carbon-based fuel consumption and emissions for a transportation network. We propose user and system level strategies that can influence travel decisions and can reinforce pro-environmental attitudes of road users. Further, we develop strategies that system operators can implement to optimize traffic operations with emissions minimization goal. To complete the framework we develop an integrated traffic-emissions (EPA-MOVES) simulation framework that can assess the effectiveness of the strategies with computational efficiency and reasonable accuracy.

The dissertation begins with exploring the trade-off between emissions and travel time in context of daily travel decisions and its heterogeneous nature. Data are collected from a web-based survey and the trade-off values indicating the average



additional travel minutes a person is willing to consider for reducing a lb. of GHG emissions are estimated from random parameter models. Results indicate that different trade-off values for male and female groups. Further, participants from high-income households are found to have higher trade-off values compared with other groups. Next, we propose personal mobility carbon allowance (PMCA) scheme to reduce emissions from personal travel. PMCA is a market-based scheme that allocates carbon credits to users at no cost based on the emissions reduction goal of the system. Users can spend carbon credits for travel and a market place exists where users can buy or sell credits. This dissertation addresses two primary dimensions: the change in travel behavior of the users and the impact at network level in terms of travel time and emissions when PMCA is implemented. To understand this process, a real-time experimental game tool is developed where players are asked to make travel decisions within the carbon budget set by PMCA and they are allowed to trade carbon credits in a market modeled as a double auction game. Random parameter models are estimated to examine the impact of PMCA on short-term travel decisions. Further, to assess the impact at system level, a multi-class dynamic user equilibrium model is formulated that captures the travel behavior under PMCA scheme. The equivalent variational inequality problem is solved using projection method. Results indicate that PMCA scheme is able to reduce GHG emissions from transportation networks. Individuals with high value of travel time (VOTT) are less sensitive to PMCA scheme in context of work trips. High and medium income users are more likely to have non-work trips with lower carbon cost (higher travel time) to save carbon credits for work trips.

Next, we focus on the strategies from the perspectives of system operators in transportation networks. Learning based signal control schemes are developed that can reduce emissions from signalized urban networks. The algorithms are implemented and tested in VISSIM micro simulator. Finally, an integrated emissions-traffic simulator framework is outlined that can be used to evaluate the effectiveness of the strategies. The integrated framework uses MOVES2010b as the emissions simulator.

To estimate the emissions efficiently we propose a hierarchical clustering technique with dynamic time warping similarity measures (HC-DTW) to find the link driving schedules for MOVES2010b. Test results using the data from a five-intersection corridor show that HC-DTW technique can significantly reduce emissions estimation time without compromising the accuracy. The benefits are found to be most significant when the level of congestion variation is high.

In addition to finding novel strategies for reducing emissions from transportation networks, this dissertation has broader impacts on behavior based energy policy design and transportation network modeling research. The trade-off values can be a useful indicator to identify which policies are most effective to reinforce pro-environmental travel choices. For instance, the model can estimate the distribution of trade-off between emissions and travel time, and provide insights on the effectiveness of policies for New York City if we are able to collect data to construct a representative sample. The probability of route choice decisions vary across population groups and trip contexts. The probability as a function of travel and demographic attributes can be used as behavior rules for agents in an agent-based traffic simulation. Finally, the dynamic user equilibrium based network model provides a general framework for energy policies such carbon tax, tradable permit, and emissions credits system.

## CHAPTER 1. INTRODUCTION

### 1.1 Background and motivation

Road transportation is an excitingly complex system that brings together elements from diverse dimensions and at the same time directly impacts our economy, energy resources, and the environment. Transportation sector consumes a large portion of fossil fuel and also acts as a significant contributor of greenhouse gas (GHG) emissions. Road transportation sector contributes 28% (Of which, fossil fuel constitutes about 92%) of the total energy consumption in the United States. The U.S. Energy Information Administration reports that light-duty vehicles (LDVs) are responsible for 61% of all transportation related energy consumption in 2012. This is equivalent to 8.4 million barrels of oil (fossil fuel) per day. Evidently road transportation sector is a major player in context of the global challenges: climate change and peak oil crisis, and there is a timely need to find effective strategies to minimize emissions and energy consumption from road transportation.

Further, vehicles traveling on road networks are a major source of air pollutants including carbon monoxide (CO), nitrogen oxides (NO<sub>x</sub>), particulate matters (PM), and volatile organic compounds (VOCs). In 2011, the transportation sector alone is responsible for about 76% of the total CO emissions and 50% of the total NO<sub>x</sub> [1] emissions in the United States. Further, the US Environmental protection agency (EPA) reports transportation sector as the fastest growing source of greenhouse gas (GHG) emissions indicating 47% net increase from 1990 to 2003 [2].

Different policies and technological advancements exist aiming at reducing the vehicular emissions. However, each has its own limitations and challenges. For instance, regulating the emissions rates of vehicles cannot cap the total amount of emissions or

concentration of a particular pollutant on any link of the network. A vehicle meeting the emissions standard can emit even more compared with the vehicle without meeting the standard [3],[4]. Researchers and technologists are still debating over the life cycle cost of using zero-emissions vehicles like the electric vehicles. A similar situation arises in the use of biofuels that may not be a sustainable choice because of its high dependency on the corn production and for the transportation cost.

Emissions and energy consumptions also depend on travel choices made by the road users. Travel choices can be short term (e.g., choice of mode of transportation, route, departure time, etc.) or long term (e.g., car ownership, residential location choice, travel patterns, and so on). Although household level GHG emissions, either for travel or household utilities are individually insignificant, collectively they make a big difference. Even a moderate change in behavior by altering millions of household level transportation choices will lead to significant reductions in GHG emissions. It has been found that household emissions can be reduced by 20% (approximately 123 million metric tons of CO<sub>2</sub>) by altering energy consumption behavior and use of technologies without compromising the household well being [5]. Previous studies [6, 7, 8, 9] show that route choice decisions can have significant impact on the amount of emissions and energy consumptions in daily trips. Moreover, researchers [10, 11] underscore the effect of mode and departure time choices on travel related GHG emissions. This dissertation primarily focuses on these two important dimensions of the short-term travel decisions: route and departure time choice for daily travel.

The goal of this dissertation is to find and to critically analyze user and system level strategies that influence travel related choices to reduce emissions and energy consumptions from transportation networks. First, we explore the heterogeneous trip decision making process of the road users accounting for emissions and fuel consumption. Then, user and system level strategies to reduce emissions and fuel consumption are proposed using the insights gained from the behavioral dynamics. Finally, we evaluate the strategies through an integrated emissions-traffic simulation framework.

Energy and emissions related policies are designed to bring changes in the behavior of the users in the system. Pro-environmental behavior of the road users may reinforce the policies to get the desired level of success. However some forms of financial incentive or disincentive are needed to achieve the desired policy goals. Designing effective policies requires a close look at the question of what drives behavioral change. Traditional transportation network modeling techniques do not focus on the energy and environmental aspects of travel and the key focus is travel time in most cases. Moreover, the primary goals are not linked with the bigger challenges like climate change and energy crisis. This dissertation integrates the pro-environmental behavior aspects into the network modeling and frames the system goals as inherent components of the broader challenges of minimizing energy and emissions from transportation network.

## 1.2 Dissertation objectives

This section describes the primary objectives of this dissertation. We discuss the motivation behind each objective and outline the general research goals.

### 1.2.1 Objective-1

The first objective is to explore the impact of providing information about emissions for short-term travel choices. Technological advancement in communications allows the users of transportation systems to obtain, process, and use information in their daily trip makings. The dynamics of sustainable travel decisions (e.g., that lead to minimize vehicular emissions for the trip and the road network) can be better explained through the temporal evolution in route and departure time choices.

Moreover, it is important to account for the inherent mechanism of trade-off between travel time and emissions. The least emissions path does not always coincide with least travel time path ([12], [13], [14], [15]). The non-monotone relationship between average speed and vehicular emissions is identified as the major cause([14],[4])

behind this. The least emissions path often leads to excessively high travel time that will not be acceptable to most travelers. Note that, it is possible to have alternative route that can yield less emissions than the least travel time path with acceptable increase in the travel time. Now, the question of interest is that what will be the level of trade-off between travel time and emissions a traveler makes considering the increase in travel time. This can be explained through considering some cases as follows:

- Case 1: A traveler can choose a route with less emissions over less travel time route or adjust departure time because of her consciousness towards sustainability (inherently environment friendly).
- Case 2: A traveler can choose a route with less emissions or adjust departure time only when the difference in travel time between the least travel time route and alternative route with less emissions is below certain threshold value.
- Case 3: The change in behavior can take place only when relevant information is available. For instance, departing seven minutes earlier than usual can save four units of carbon emissions for the trip with acceptable travel time- this information can increase the likelihood of adjusting departure time.

The travel time and emissions level highly depend on the congestion of the network which is not deterministic. The travel time for the same route and departure time can differ for different days of a week, different weeks of a month, or different months of a year. To capture this dynamics, we seek to understand the behavior of users at different network conditions and different information provision through observing a series of travel decision making (i.e., the same trip for a month). Table 1.1 illustrates a route choice scenario where users are provided with information about trip emissions. The CO<sub>2</sub> emissions are obtained by following EPA guidelines (also see section 3.2.2) and considering congestion effects.

The route with least emissions (option *B*) has 17 minutes of travel time, which is a significant increase from the least travel time route *A*. Route *A* is the most attrac-

Table 1.1.: Route Choice Scenario

Route	Travel time (minutes)	Emissions (lbs of CO <sub>2</sub> )
$A$	10	20
$B$	17	9
$\hat{B}$	13	12

tive option to the users in terms of minimizing travel time. An individual does not necessarily desire higher emissions for the trip, however an increase of 7 minutes of travel time (option  $B$ ) may not be acceptable for her. Now, route  $\hat{B}$  has travel time 3 minutes higher than route  $A$ , and emissions 3 lbs higher than route  $B$  could be a choice for a user who is willing to minimize emissions within acceptable additional travel time for the trip. Our hypothesis is that, users will perceive path  $B$  as a significantly high travel time route and may not switch to it. However route  $\hat{B}$  could be a choice with acceptable trade-off between travel time and emissions for a certain group of users. The research questions are as follows:

**Q1:** *What is the likelihood that a user will choose a route with less emissions (not necessarily the least-emissions route) over the least travel time route?*

**Q2:** *How to find the trade-off between emissions and travel time accounting for the variation of taste across the users?*

The trade-off between emissions and travel time is not homogeneous. The trade-off values will be different for different types of road users. Again for the same person, an additional 5 minutes may not be acceptable in the morning commute, however may be acceptable in work-to-home return trip. Therefore, it is necessary to account

for heterogeneity across individuals in the population and within the same individual at different trip types.

Table 1.2 shows an example of departure time choice scenario. Assuming flexibility in the departure time choice an individual can leave earlier or later from her commute from work to home. Departing at a later time can have the benefits of reduced travel time because the congestion may become light. Also, the flow becomes smooth as congestion dissipates and accordingly the speed variations are lower. This results into lower emissions for the trip [16, 17]. Table 1.2 shows that, delaying the departure time by five minutes reduces the travel time by one minute, whereas the CO<sub>2</sub> emissions are reduced by 4 lbs. This is because the speed variation becomes smaller (congestion dissipating vs. congestion free) in the latter case. Considering 20 minutes schedule delay (difference between preferred and actual departure) may not be acceptable to all users. Therefore, we also have a trade-off phenomenon in this case.

Table 1.2.: Departure Time Scenario\*

Option	Departure	Travel time (minutes)	Schedule delay (minutes)	Emissions (lbs of GHG)
1	5:30 pm	25	15	12
2	5:35 pm	24	20	8

\*preferred departure at 5:15 pm

The research questions of interest are:

**Q3:** *What is the likelihood that a user will adjust her departure time to have less emissions (compared to the least schedule delay option) in the trip?*

**Q4:** *How to find the trade-off between schedule delay (departing early or late) and emissions accounting for the heterogeneity across the users?*



The focus here is on two specific short-term travel decision contexts:

- (a) Route choice: (i) Week day morning peak hour home-to-work commute with trip length ranging from 21 to 29 minutes, (ii) Weekend home based recreational trips (assuming, travel alternatives available with less emissions compared with least travel time route)
- (b) Departure time choice: Work-to-home trip during afternoon peak hour (assuming the user has flexibility to adjust departure time)

To conclude, the goals for this research are as follows:

- (I) To understand how road users make a trade-off between emissions and travel time while making a short term travel related decision (route or departure time choice).
- (II) To explore the heterogeneity in trade-off values at different trip contexts (work vs. non-work) and choice scenarios (route vs. departure time).
- (III) To apply the insights from the estimated econometrics models (when emissions related information are provided to users) for designing policies to reduce emissions from road networks.

### 1.2.2 Objective-2

The second objective is to develop and analyze a carbon allowance scheme focusing on personal travel. Recently proposed Personal Carbon Allowance (PCA) schemes are designed on intrinsic incentives aiming at reduced dependency on fossil fuels and capping GHG emissions to a certain level [18]. Each eligible individual in the system gets equal share of carbon units and spends the units for energy consumption for relevant services. Users can sell the leftover units in a market. Demand and availability of carbon units determine the unit price in the market. Two key advantages

of these schemes are: guaranteed level of emissions reduction and revenue neutral market mechanism. With a similar concept we propose a carbon allowance scheme, namely the personal mobility carbon allowance (PMCA) scheme that only deals with the travel activities limited to road transportation. Road users will behave differently when PMCA or similar systems will be in effect. In addition to travel time, the carbon budget will be a significant factor in their travel decisions. The entire perspective of network modeling and transport planning will be changed.

Now we extend the travel choice problem to the context of PMCA system. Consider the following scenario where users make travel decisions within PMCA system and the anticipated amount of carbon credits to be charged is available as pre-trip information.

Table 1.3.: Route Choice Scenario under PMCA system

Route	Travel time (minutes)	Carbon credits (units )
A	10	10
B	17	5
C	13	7

However the PMCA system affects the travel behavior in an entirely different manner due to the existence of carbon market and initial carbon allocation mechanism. The users have to buy carbon credits from the market with real money in case the initial free quota is diminished. At different conditions describing the price and availability of carbon credits, the decision making process of the users will be different. The remaining budget, market price of the credits, and pro-environmental attitudes are few of the influencing factors. Similar scenario can be constructed for the departure time choice.

The PMCA system describes a market where users can buy and sell carbon credits. The travel decisions are highly affected by the availability and market price of carbon

credits in the market. Therefore, it is necessary to explore the dynamics of the market mechanism and apply the insights to understand the decision making process of the users.

The specific research goals are as follows:

- (I) To develop a carbon allowance scheme for personal travel,
- (II) To explore the travel decision making patterns under PMCA scheme,
- (III) To understand the impact of carbon market on travel decision making patterns.

### 1.2.3 Objective-3

The third objective is to formulate and solve dynamic user equilibrium based network models accounting for travel behavior under PMCA scheme. It is important to investigate the dynamics in user behavior, and to estimate the resulting state of the traffic networks under PMCA schemes. This dissertation aims to develop methodologies that can analyze the transportation network states under tradable schemes such as PMCA. Our goal is to develop a multi-user class dynamic user equilibrium model, namely the PMCA-DUE model, incorporating the market based carbon reduction strategy described as personal mobility carbon allowance scheme. The PMCA schemes requires a new generalized cost function and corresponding equilibrium condition accounting for the carbon budget and conditions in the carbon market. Moreover, it is necessary to include the effects of initial allocation of carbon credits, value of travel time, and number of trips in generalized cost function. To conclude the goals are:

- (I) To develop a multi-class dynamic user equilibrium model accounting the for the travel behavior under personal mobility carbon allowance (PMCA) scheme,
- (II) To explore and investigate the flow redistribution (path level) under the PMCA system accounting for several dimensions of heterogeneity across the users,

- (III) To examine the change in travel costs and carbon consumption at OD, user class, and path levels under PMCA system at different allocation levels.

#### 1.2.4 Objective-4

The fourth objective is to develop signal control schemes that can reduce emissions from road networks. The number of stops made near the signalized intersections and stopped delay due to red light contribute significantly to vehicular emissions in urban road networks. In 2011, [19] 56 billion lbs of CO<sub>2</sub> released into the atmosphere because of clogged roads. Our system level goal is to design signal control schemes that can minimize emissions near the signalized intersections. Since traffic environment is inherently dynamic and changes over time, there is a scope to learn for its elements (e.g., signal controllers) through interaction with the environment. Later, controllers can adjust the actions towards a desired state of the system. Among different learning techniques, reinforcement learning (RL) is one of the widely used sample based learning techniques applied to solve the traffic control problem. In RL-based schemes, the agent (i.e., signal controller) learns from the interaction with environment, which is often modeled as Markov Decision Process (MDP). The key advantages of RL algorithms are: the ability to learn from the environment and scalability in terms of implementation as no direct optimization is generally involved. The interactive nature of reinforcement learning algorithms requires a communication interface where the agents (vehicles and controllers) can send and receive information. This also fits well into the recently developed concept of connected vehicle (CV) environment. The goals are as follows:

- (I) To develop signal control algorithms that can minimize emissions and energy consumptions in transportation road networks,
- (II) To apply learning based technique for traffic signal control that can incorporate stopped delay and queue size related goals in the reward function,

- (III) To design the algorithms such a way that the benefits (such as information sharing among signal controllers) of connected vehicle environment can be utilized.

### 1.2.5 Objective-5

The final objective of this dissertation is to develop a policy evaluation framework that integrates traffic and emissions simulators. Like any engineering system, the evaluation of policies is an indispensable part. This research quantifies the emissions of the system in a rigorous manner to find the effectiveness of both user and system level strategies (for instance, finding whether the total carbon emissions is reduced after changing the signal settings of a network). To evaluate all the strategies, one needs to quantify the emissions from the road network. We aim to develop a framework that integrates traffic and emissions simulator. The traffic simulator can be any micro-level simulation that provides second-by-second vehicle activity data. The framework uses EPA developed MOtor Vehicle Emissions Simulator (MOVES) tool to estimation vehicular emissions. Further, our goal is to develop a link driving schedule finding technique based on similarity based clustering that overcomes the general limitations of current approaches. The research goals are as follows:

- (I) To provide an evaluation framework integrating traffic and emissions simulator,
- (II) To develop an efficient technique to find link driving schedules using the trajectories obtained from traffic simulation,
- (III) To develop a tool to assess the effectiveness of user and system level strategies proposed in this dissertation.

### 1.3 Contributions

The dissertation has several broader impacts regarding transportation energy policy and planning literature. The key contributions of this dissertation are as follows:

- **Trade-off between emissions and travel time:** This dissertation explores the heterogeneous trade-off between travel time and emissions in different contexts of daily travel (e.g., route choice, departure time, and so on) through econometric models.
- **Policy design for green transportation:** The insights gained from the collected data and the results of the models can help to design effective policies accounting for the behavioral heterogeneity across the population.
- **Experimental game tool to investigate carbon reduction schemes:** This dissertation develops an experimental game tool to understand the travel decision making patterns and market mechanism under carbon allowance schemes. The tool can be used to analyze similar schemes such as carbon tax, mileage based fees, and emissions credit system.
- **Network level traffic equilibrium models** This dissertation develops dynamic equilibrium models that rigorously analyze the congestion and emissions level of traffic networks under the personal mobility carbon allowance scheme. The developed model accounts for multiple user classes characterized based on value of travel time, income level, relative priority to carbon consumption, and conditions in the carbon trading market of PMCA.
- **Learning based signal control for sustainable mobility:** Learning based signal control schemes aiming at reducing emissions are developed. The algorithms utilizes the communication facility of the connected vehicle environment.
- **Integrated traffic-emissions tool:** This dissertation provides an integrated framework to assess effectiveness of user and system level carbon reduction strategies from road networks.

#### 1.4 Dissertation organization

The rest of the dissertation is organized as follows: chapter 2 provides a critical review of the existing literature on effect of emissions related information on travel choices, tradable systems for road networks, signal control algorithms to reduce emissions, and emissions quantification and monitoring tools. Chapter 3 describes the econometric modeling approach to estimate the trade-off between emissions and travel time patterns. Chapter 4 proposes the PMCA scheme and describes an experimental game approach to collect and analyze the data. Chapter 5 presents the dynamic user equilibrium model incorporating the travel behavior under PMCA scheme. Chapter 6 develops the signal control schemes aiming at cutting down emissions. Chapter 7 describes the integrated emissions-traffic simulator framework and the link driving schedule finding technique. Finally, chapter 8 summarizes the findings and contributions of this dissertation along with future directions.

## CHAPTER 2. LITERATURE REVIEW

### 2.1 Introduction

This chapter presents critical review of the existing literature relevant to the research in this dissertation. The goal of this chapter is to position the proposed research in the current literature in terms of needs and significant contributions.

### 2.2 Effect of Descriptive Information on Travel Choices

The number of studies aiming at exploring the effect of travel time information on route and departure time choice through studying the behavioral dynamics is significant and major studies include (but not limited to) [20],[21], [22],[23], [24],[25]. These works established the fact that travel information can influence the route and departure time choice decisions of the travelers. Chorus [26] has an excellent review of the works and major findings. On the other hand, studies to understand the behavior of travelers when information related to vehicular emissions is available are quite few. However, there are studies that show the effect of information on pro-environmental behavior in context of energy and environment.

#### 2.2.1 Information and Pro-environmental Behavior

Schultz et al. [27] reported a residential energy use study in California. 290 households were given information about their energy use and the average energy use in the neighborhood households. The households with above average energy consumption reduced their residential energy use. However, there was also a boomerang effect. The households with energy use below average actually raise their consumption. To



counteract the boomerang effect the researchers added injunctive messages: smiley emoticons for households with below average and frowning emoticons for the households above average or near average energy consumption. This strategy worked and the consumption levels were restated.

In the study of Heath and Gifford [28], the cost of bus use was reduced by the introduction of a universal-pass to university students. Offering the pass assumed to influence attitudes and perceived behavioral control, and thus intention to change behavior. The study reported 7% decrease in driving alone while bus use was increased by 11%.

Taniguchi et al. [29] investigated the effect of traveler feedback programs (TFP) in Japan. TFPs give travelers (at household level) feedback or feed-forward information that include, GHG emissions from car use, personalized recommendations on car use, travel information (e.g., timetables or maps related to alternative travel options for commuting or shopping) and so on. They reported that TFPs in residential areas of Japan reduced car use by 7.3% to 19.1% and increased public transport use by 30% to 68.9% on average. Based on the effectiveness of TFP techniques it was concluded that goal setting can bring significant changes in travel behavior from car use to more sustainable transport. Later, Grling and Fuji [30] found similar results in context of the TFPs and its impact on travel behavior.

In an online article, Thompson [31] reports an experiment with Southern California Edison customers aimed at reducing residential energy consumption. They provided two types of personalized feedback (to different groups). One was timely e-mails and text messages regarding energy use. The second was an ambient orb, which was placed in the house and glowed red during high energy use and green during low energy use. Whereas the former did not lead to significant change in energy use, the latter led to a 40% reduction during peak periods.

From the studies discussed above we conclude that, providing information can influence pro-environmental behavior of the individuals.

### 2.2.2 Willingness-to-pay for emissions

Findings from various studies also indicate the willingness-to-pay of individuals for environmental causes. In the study of Ortuzar and Rodriguez [32], a stated preference ranking experiment is designed to estimate the willingness-to-pay (WTP) for reducing the amount of atmospheric pollution in a group-based residential location context. WTPs were derived for reductions in the number of days of alert and hence the amount of pollutant concentration at a given location. The WTP came out at about 1% of the family income for reducing one contingency day per year; this is approximately 60% higher than an estimate reported for the city of Edmonton, Canada, but the average PM<sub>10</sub> concentration in Santiago is about six times higher.

Saphores et al. [33] asked households whether or not they were willing to pay nothing, 1%, 5%, or 10% more for green cell phones and computers relative to conventional. They found the average household is willing to pay only a 1% premium.

Choudhury et al.[34] estimated WTP for a variety of environmental improvement scenarios and found that while subjects with higher income have a higher willingness to pay for environmental improvement, this is mostly caused by their lower cost sensitivity rather than their environmentalism. Achtnicht [35] studied car purchase behavior in Germany, and from this estimated a willingness to pay of \$0.22 per pound of CO<sub>2</sub> savings (Euro 349 per tonne).

We can conclude that, individuals (or households) will be willing to pay for the sake of environmental causes such as less emissions, green technologies, and so on.

### 2.2.3 Influence of information

Studies exploring the impact of emissions related information in context of daily travel choices are few. Gaker et al. [36] designed three computer experiments for undergraduate students (N = 312) of University of California, Berkeley: (a) personalized information and route choice, (b) social influences and auto ownership, and (c) social influence, and pedestrian safety. The insights suggest high prospects of using behav-

ioral economics and great potential for influencing transport behavior. Trip specific information regarding greenhouse gas emissions has significant likelihood to increase sustainable behavior. The study quantified the value of green at around \$0.24/lb of greenhouse gas avoided. Making the appropriate unit conversions and estimating a single value of green by using the data from both experiments, it was found that the subjects value reducing their environmental impact at \$0.24/lb of greenhouse gas.

In a second study, Gaker et al. [37] found that subjects are willing to adjust their behavior to reduce emissions, exhibiting an average willingness to pay for emissions reduction, or value of green (VoG), of 15 cents per pound of CO<sub>2</sub> saved. Some conclusions from their study were:

- Individual cannot always process the emissions related information and accordingly the decision process is affected.
- The estimated VoG was consistent across context (the wide range of transport decisions that we presented) and presentation (e.g., whether the information was presented in tons or pounds, or whether a social reference point of the emissions of an average person was provided)
- Heterogeneity across individuals was present in terms of VoG.

#### 2.2.4 Summary

The above discussion identifies several aspects where significant contributions can be made. Although these studies are among the first few that aim to address the effect of emissions related information on travel choices. However, scopes exist to improve and contribute:

- The trade-off between travel time and emissions is not directly addressed.
- Only route choice context is considered, although departure time choice is a critical dimension of choice.

- The heterogeneity across individuals is not addressed and variation in travel context has not been considered.

## 2.3 Carbon allowance schemes

### 2.3.1 Tradable systems

The idea of tradable allowances (or permits) was initially described in Coase [38]. Dales [39] proposed a system of auctioned property rights for the use of natural resources and later Montgomery [40] showed its economic efficient properties. Tradable allowance systems minimize and equalize the marginal cost of compliance across firms without requiring detail information as the market determines the price (Tietenberg[41]). Cap and trade schemes are a special form of tradable allowance systems with an upper limit on total emissions featuring the ability to trade between the users. A well known example is the US sulfur dioxide allowance trading system that requires a coal-fired power plant must own or purchase allowances to pollute the air with SO<sub>2</sub> in order to produce electricity.

The European Union Emission Trading Scheme, Chicago Climate Exchange, and the New England Regional GHG Initiative, Global Warming Solutions Act of 2006 (AB32), and the Kyoto Protocol (Perrels[42]) all apply cap and trade systems to reduce GHG emissions. Fleming [43] first proposed personal tradable carbon permits or domestic tradable quotas (DTQ). Later it was extended to involve all individuals and organizations ([43], [18]) and termed as Tradable Energy Quotas (TEQs). Starkey and Anderson [44] at the Tyndall Centre for Climate Change Research evaluated the feasibility and appropriateness of the DTQ model and identified the potential for further work. Hillman et al. [45] proposed a domestic carbon rationing and trading scheme for individuals. Other works include Fawcett [46], Niemeier et al.[47], Tietenberg [41], and so on. Verhoef et al. [48] introduced tradable permits in context

of road transportation sector. Studies by Kockelman and Kalmanjie [49], Raux [50], Wadud [51] are some examples of the qualitative research. Studies aiming at rigorous mathematical analysis include (but not limited to) Nagurney and Dhanda [52], Nagurney [53], Yang and Wang [54], Wang et al. [55], Nie [56], Wang and Yang [57], Wu et al. [58], and Nie and Yin [59].

### 2.3.2 Market based approaches

Researchers applied marginal cost pricing (MCP) techniques for emissions pricing previously. Yin and Lawphongpanich [4] provided pricing schemes that yield a traffic flow distribution with minimum emissions and also provided a bound on the percent reduction of the emissions by the charging scheme. Recently [60] analyzes emissions reduction scheme with tolls and rebates. They prove the existence of non-negative tolls for acyclic networks even when the link emissions function is not monotone. Researchers also focused on the environmental issues for road networks through generalized traffic equilibrium model with emissions standards as the side constraints [[61], [62], [63]]. Clearly, traditional marginal cost pricing based schemes are investigated by researchers aiming at emissions reduction. Nevertheless, opportunities still exist to explore the possibility of tradable credit schemes as effective instruments to reduce emissions and examine the state of transportation network.

### 2.3.3 Tradable mobility credits

Further, trading schemes are rigorously analyzed as an alternative to tolls on road links [54, 56, 59, 64]. These studies provide insights on the resulting state of the transportation systems in terms of flow distribution and travel time. In most cases, the focus is not on emissions or energy consumption. Only exceptions are the works by [4, 60] that apply marginal cost pricing technique to determine the externalities from emissions and by [65] that provides a tradable emissions credit scheme for transportation network. However, the user behavior patterns are not obtained

from experimental settings, rather based on empirical studies or established principles. Carbon tax is another market based strategy to reduce carbon consumption. A key criticism of carbon tax is the inability to account for heterogeneity in the population [47]. A progressive tax at optimal level theoretically can attain success. However determining the carbon tax at optimal level requires full information and most cases it is challenging. Further carbon tax does not encourage the behavioral changes in the energy consumption behavior (either travel or household) and equity issues arise more often. An alternative to carbon tax is the personal carbon trading scheme.

#### 2.3.4 Personal carbon allowance

The downstream carbon trading schemes aiming at reduction of GHG emissions and energy consumptions at household level (travel and utility) [43, 45, 47] are argued to be successful . One class of these schemes, namely personal carbon allowance (PCA), is found to be promising by the researchers that can cut down GHG emissions in a cost effective way [44, 66, 67, 68]. Most existing studies do not focus on personal travel in depth. For instance, cumulative trips, total vehicle miles traveled, total expenditure for travel, etc. are considered, however no investigation on changes in travel behavior is done either at individual or at system level. This research outlines a personal travel focused carbon allowance scheme, namely the personal mobility carbon allowance scheme, that can effectively reduce carbon consumption from the system by influencing travel behavior.

#### 2.3.5 Summary

The above discussions indicate that improvements can be made in several directions:

- The data collection for conceptual tradable credit or carbon allowance system is challenging. Innovative ways such as developing experimental games can be a potential directions,
- Only a few studies model the dynamics of the auction market which is an important element in the scheme,
- Network levels models are not available in the literature that can assess the impact of carbon allowance schemes for the entire system.

#### 2.4 Signal control schemes with emissions objective

Researchers in the past ([69], [70],[71], [16]) evaluated emissions from the on-road vehicles for different traffic conditions at signalized intersections . Studies ([72], [6], [73]) accentuate on the effect of number of stops and driving styles as major factors of on-road emissions. Traffic signal timing plans directly influence the number of stops made by the vehicles and also affects the driving style (frequent deceleration or stopping at all intersections). It is important to devise signal timing plans with emissions minimization objectives, which will also save fuel. Previous studies ([74], [75]) underscore the importance of proper implementation and evaluation of signal control plans in order to reduce significant amount of GHG emissions and fuel consumption.

Different approaches to optimize signal timing plans to reduce emissions include (but not limited to) simulation based approach, mathematical optimization, learning based approaches, coordinated signal network, and so on. Stevanovic et al. [75] integrated VISSIM and CMEM to optimize and evaluate signal control schemes in terms of fuel consumption and emissions. Park et al. [76] applied stochastic optimization to find sustainable signal timing plans. Umedu et al. Umedu et al. [77] applied self-learning techniques to reduce GHG emissions reduction. With the advancements in the connected vehicle technologies, researchers also deploy and evaluate specific control algorithms aiming at emissions reduction ([78],[79]).

The connected vehicle environment offers potential scopes to design signal control strategies that can yield significant reduction in GHG emissions and fuel consumption of on-road vehicles for signalized intersections. This dissertation particularly focuses on the control algorithms that use connected vehicle technologies and aim at reducing emissions.

### 2.5 Assessment of strategies

One major goal of this thesis is to quantify the emissions from the network and evaluate the proposed emissions reduction strategies. For the integration part we will be using EPA regulated micro-level emissions simulator MOVES2010b. Current literature has only a few works that put efforts to integrate traffic simulators with emissions models. In particular, integration between MOVES and traffic simulator has been attempted by only a few including integration of MOVES with DYNAMIQ [80], with DYNUS-T [81], and more recently the integration of MOVES with TRANSIM by FHWA. Recent works by Song et al.[82], Xie et al. [83], and Hao et al.[84] also aim to provide an integrated framework for traffic simulation and emissions estimation.

### 2.6 Summary and conclusions

This chapter presents critical review of literature on key aspects of this thesis: effect of emissions related information on travel choices, tradable credit systems in the context of personal transport, and signal optimization approaches to reduce emissions. The discussions in the earlier sections suggest that,

- Trade-off between travel time and emissions in the context of daily travel choices (route and departure time choice) still have not been understood and explored at a significant level



- Carbon allowance for personal travel has a lot of prospects and requires development of analytical models within the frameworks of transportation network modeling
- Market mechanism (price setting and credit availability) in tradable systems requires in-depth understanding
- Learning based approaches offers a promising platform to design control schemes with emissions minimization objectives
- Finally, it is necessary to have an assessment tool to evaluate the strategies.

Accordingly, this dissertation aims to address all these potential gaps in the current literature and expect to make significant contributions.

## CHAPTER 3. GREEN CHOICES IN TRAVEL ACTIVITIES

### 3.1 Introduction

Recent advances in information and communications technology (ICT) allow the road users to obtain, process, and use information in their travel decision making processes. Providing information related to travel time and emissions for a travel alternative (e.g., route and departure time choice) can influence the travel decision [20, 21, 37]. Studies show that the travel alternative with least emissions does not always coincide with the travel alternative with minimum travel time [6, 12, 13, 15]. The non-monotone relationship between speed and emissions leads to conflicting travel time and emissions objectives for the road users [4, 6, 85]. If a user is willing to make a travel decision that leads to lower emissions compared with the least travel time route, she may have to travel additional minutes. In the context of route choice, least emissions route can have excessively high travel time that may not be acceptable to most travelers. Again, it is possible to have an alternative route that offers less emissions compared with the least emissions route and *acceptable* travel time compared with the least travel time route. The notion of *acceptable* travel time is heterogeneous and it varies across population and decision contexts. Our particular interest is to explore the level of acceptability in terms of the trade-off between the travel time and emissions.

The research goals are discussed in chapter 1 and a literature review is conducted at section 2.2 in chapter 2. This chapter describes the data collection, methodology, estimation results, and contributions of this study.

### 3.2 Design of experiments and Data

Experiments are useful tools to collect data when it is challenging to find suitable data from real world. In our case, we need to observe travel decisions made by users for similar trips (purpose, length, and time of day) over several weeks. This is challenging in terms of time, facilitation, and cost. For example, the American Time Use Survey (ATUS) reports activity only for a single day with details of the trip decisions and the expenses are quite high. To collect data in an efficient manner we design web-based experiments using the Qualtrics tool. Experiments are commonly used to collect data for behavioral and economic analyses [86, 87, 88]. Using students as subjects often raise questions regarding bias and validity of the results. A recent study by [89] conclude that students are appropriate subject pool for the study of social behavior. Their study critically analyzes behavioral data obtained from both representative sample and self-selected students to reach this conclusion. Please see section 3.6.2 for further discussion.

We collect data from the Purdue undergraduate students. First, we collect general information of the participants that include age, gender, household income, and general questions about daily travel (e.g., are you willing to use bike for your trip from the place where you live to work if there is a safe bike route available?). Second, we present hypothetical daily travel scenarios that include route and departure time choices. The web-based experiments are carefully designed so that the hypothetical travel scenarios mimic real world situations. Note that the methodology is based on stated-preference technique which is one form of experiment [88]. We denote this as experiment because the participants have to take decisions in carefully designed repeating contexts instead of single-shot surveys.

Before releasing the web-based experiments to the subjects, we arranged a session that explains the scenarios.

- We discussed about the congestion on the network (Indianapolis, IN) during the morning and afternoon rush hours. The purpose was to give the students an idea of the network conditions who are not familiar with the network. Also,

we show the maps of the alternative routes (using Google maps) so that they can visualize the travel scenarios

- We asked questions about work commute. Since the subjects are students, we presented to them a scenario where they have an internship that requires morning commute on weekdays. Many undergraduate students do internship at different engineering firms in summer and have the schedule similar to a regular worker.
- For each scenario we provided information on: average travel time, emissions, variation in travel time, and schedule delay (in case of departure time choice). We describe the methodologies used to compute these attributes. The next few sections have details.

### 3.2.1 Travel time and variation in travel time

The origins and destinations in the presented scenarios are real world geographic locations (see appendix). For instance, we asked to make route choice decision for a trip from a residential area in Indianapolis, IN to Indiana Department of Transportation (INDOT) office for a morning home-to-work commute. Travel time information are based on Google maps, Map Quest, and Bing. The variations are captured using the time-of-day map in Google maps that shows travel time variation based on the time of the day.

### 3.2.2 Quantifying GHG emissions

The emissions are based EPA guidelines and findings from literature. The base line emissions factor used is 423 g of CO<sub>2</sub> per mile. The factor is adjusted based on the real world travel time profile. Google maps can provide travel time variation on each link of a network. The distribution of travel time can be used to compute the time dependent emissions for the links and thereafter the emissions for the routes.

The travel condition of the network (please see the network in appendix) determines the speed profiles of the routes. For the same network several scenarios with different travel time and emissions value (i.e., different congestion levels) were presented in the experiment. We also follow the work of [16] to consider the effect of speed. For instance, the emissions rate is significantly different while traveling at 55 mph compared to 65 mph.

### 3.2.3 Sample description

After distributing the web-based experiments we had 120 participants for the study. Each participant has to answer 15 route and 14 departure time choice questions. The questions are segmented randomly (e.g., few questions on route choice and then few questions on departure time choices). The study uses 95 observations after accounting for inconsistent and missing data. Also we have to discard some route and departure time choice responses due to incomplete information. For instance, one respondent filled out the demographic information but did not complete all the questions in the route choice experiment. Finally, we have  $(95 \times 10)$  or 950 observations for route choice and  $(95 \times 8)$  or 760 observations for the departure time choice scenarios.

In our sample, 98% individuals are licensed drivers. We have male and female share as 76% and 24% respectively. 45% indicate they do not use the transit service any time in the week. 35% show preference to use bike for daily commute to work with the condition of safe bike route. 39% of the participants are from high income households (defined to have annual income more \$90,000).

### 3.3 Methodology

Random-parameter models are estimated using the tool NLOGIT. Each participant makes choices for a series of travel scenarios. The same unobserved attributes affect the choice making of an individual for repeated travel scenarios. Therefore, correlations exist in the error terms for same individual making a series of choices. The random parameter models account for the correlation in the repeated observations and treats as panel data (i.e., there are 95 groups of observations each can have 15 route choice scenarios for which the error terms are correlated). Moreover, the heterogeneity across individuals is accommodated by considering parameters as random variables. In addition, random-parameter logit models overcome the inherent limitations of multinomial logit models with fixed parameters.

#### 3.3.1 Random-Parameter Model

We follow the approach as described in [90] and [91] and details can be found in [92]. Consider a function determining the outcome probabilities of the travel choice scenarios as:

$$Z_{ni} = \beta_i X_{ni} + \epsilon_{ni} \quad (3.1)$$

Here,  $Z_{ni}$  is the propensity function for any individual  $n$  chooses the travel alternative (either a route or a departure time)  $i$ .  $X_{ni}$  is the vector of the observable characteristics.  $X_{ni}$  is the generalized term used for alternative specific attributes and individual specific attributes.  $\beta_i$  is the vector of parameters to be estimated and  $\epsilon_{ni}$  is the disturbance (error) terms that are extreme value type-I distributed. The probability can be expressed as (standard multinomial logit):

$$P_n(i) = \frac{\exp(\beta_i X_{ni})}{\sum_i \exp(\beta_i X_{ni})} \quad (3.2)$$

Now, a model with mixing distribution can be defined for which we can describe a density function for vector  $\beta_i$ . The probability can be expressed as [92]:

$$\hat{P}_n^m(i) = \int_X \frac{\exp(\beta_i X_{ni})}{\sum_i \exp(\beta_i X_{ni})} f(\beta|\pi) d\beta \quad (3.3)$$

Now, the probability for  $K$  repeated observations for each individual can be expressed as

$$P_n^m(i) = \int_X \prod_k \frac{\exp(\beta_i X_{ni})}{\sum_{i \in Ik} \exp(\beta_i X_{ni})} f(\beta|\pi) d\beta \quad (3.4)$$

Note that,  $Ik$  is used to account for repeated observations. The probabilities  $P_n^m(i)$  are the weighted average of the standard probabilities where the density function  $f(\beta|\pi)d\beta$  determines the weights. The model reduces to a standard multinomial logit model with  $f(\beta|\pi)d\beta = 1$ . Different distributions such as uniform, triangular, weibull, log-normal or normal can be used to define the density function. Most commonly used are normal and log-normal distributions to define  $f(\beta|\pi)d\beta$ .

Now the log-likelihood function can be written as [92]:

$$LL = \sum_{n=1}^N \left( \sum_{i=1}^I \delta_{ni} \ln[P_n^m(i)] \right) \quad (3.5)$$

Note that  $\delta_{ni} = 1$ , when the choice outcome is  $i$  for individual  $n$ . The mixed logit probabilities  $P_n^m(i)$  are not straightforward to compute and we follow the simulation approach. Equation 4.5 is referred to as the simulated likelihood function as the probabilities are approximated by drawing the values from the density function and averaged to estimate the simulated probability. Simulated probabilities are obtained through Halton sequence (Halton draws). Existing studies [[93], [94]] suggest using Halton sequence is efficient in simulatedbased likelihood approach. The estimates reported here are obtained with 800 Halton draws and the estimates are found to be consistent.

### 3.3.2 Estimating Trade-off

The trade-off between travel time and emissions is computed using the concept of marginal rates of substitution [92]. If we take the ratio of the estimated coefficients for travel time and emissions from the random parameter model, it will give us the marginal rate of substitution between time and emissions. This implies that the trade-off between the attributes (in our case emissions and time) that keeps the same value for the defined function as in equation 5.27. Also note that, the trade-off will be different for different persons and also will be different for the same individual at different contexts (e.g, work trip vs. non-work trips). The marginal rates of substitution of time for emissions (minutes per lbs of CO<sub>2</sub>) can be expressed as:

$$MRS_{TT,EM} = \frac{\frac{\partial Z}{\partial(EM)}}{\frac{\partial Z}{\partial(TT)}} = \frac{\beta_{EM}}{\beta_{TT}} \quad (3.6)$$

### 3.3.3 Interpreting the trade-off values

The values of trade-off between emissions and travel time can be great importance in terms of identifying the users with higher pro-environmental attitudes and to design policies. Consider, the following scenario: route A (25 minutes and 20 lbs of CO<sub>2</sub>) and route B (30 minutes and 15 lbs of CO<sub>2</sub>) With all other contributing factors being the same we can write the propensity function (5.27) as:

$$Z_i = -\beta_{TT} \times TT - \beta_{EM} \times EM + \Delta \quad (3.7)$$

$\Delta$  is the constant term accounting for other factors.

With,  $\beta_{TT} = 5$  and  $\beta_{EM} = 1$  (assuming  $\Delta$  to be fixed), the choice outcome functional value for route A will be higher than route B and accordingly will have the higher probability to be chosen. Now, we have the trade-off as  $\beta_{EM}/\beta_{TT}$  or 0.2 (similar value as we get from Figure 1). This tells us, for route B if we can reduce the travel time to 26 minutes it will have same functional value as route A. Therefore, the probability to choose route B (with less emissions) will be same as route A.



$$Z_A = (-)5 \times 25 + (-)1 \times 20 + \Delta = -145 + \Delta$$

$$Z_B = (-)5 \times 30 + (-)1 \times 15 + \Delta = -165 + \Delta$$

If we can reduce travel time for route B to 26 minutes:

$$Z_B^* = (-)5 \times 26 + (-)1 \times 15 + \Delta = -145 + \Delta$$

This is how the analysis of trade-off will help us to understand the behavior and to design policies (e.g., taking measures to improve travel time for route B). One should note that, the interpretation is highly dependent on the context. We cannot just substitute any amount of travel time with emissions. The model only tells us about the trade-off in the travel decision making for the users in the sample for a particular type of trip (purpose, length, and context).

### 3.3.4 Statistical testing

Different specifications of the models are tested for goodness-of-fit and also for transferability of contexts (work vs. non-work trips). The test follows the approach recommended by [95] using the likelihood ratio statistic. Log likelihood-ratio test is widely used in the literature [96], [97],[98],[94]. The null hypothesis for the test is that the restricted model does not have a significantly lower log-likelihood than the unrestricted model. The test statistic can be calculated using the following equation:

$$\text{Likelihood ratio test statistic} = -2[LL(\beta_{Restricted}) - LL(\beta_{Unrestricted})] \quad (3.8)$$

This statistic is  $\chi^2$  distributed with n degrees of freedom which the difference of estimated parameters in the restricted and unrestricted models. When the test statistic is higher than the value with n degrees of freedom at specified confidence level, one can conclude that the null hypothesis can be rejected.

### 3.4 Empirical results

Random parameter models are estimated for route and departure time choice contexts. Further, separate models are estimated for work and non-work trips. The models assume log-normal distribution for the coefficients of travel time and normal distribution for all other coefficients. Moreover, the models account for the correlation across repeated choices considering the fact that the same individual is responding to several repeated travel choice scenarios. We consider 95 groups(panel data) in the estimation procedure and for each group the models estimate distinct coefficients.

Next few sections discuss the results from the estimated models. The trade-offs between emissions and travel time for both route and departure time scenarios are reported as histograms along with cumulative distribution to demonstrate the heterogeneity across the individuals in the sample.

#### 3.4.1 Route choice models

Random parameter models are estimated using the responses from 10 route choice scenarios. Five of these scenarios are home-to-work commute trips in the morning and the length of the trips ranges from 21 to 29 minutes. The rest five are non-work trips on a weekend day for recreational purpose. The length of the non-work trips ranges from 55 to 65 minutes. It should be noted that, non-work trips can take many different forms and recreational trips represent simply one type of non-work trips.

#### 3.4.2 Work vs. non-work trips

The log likelihood ratio test suggests that the route choice models for work and non-work trips should be modeled separately. The restricted model is estimated including all trips (work and non-work) using 950 ( $10 \times 95$  observations) observations. Now, two separate models are estimated for work trips ( $5 \times 95$  observations) and non-work trips ( $5 \times 95$  observations). The null hypothesis for the test is that, the restricted

model (joint model with work and non-work trips) does not have a significantly lower log-likelihood than the unrestricted models. The test statistic is as follows:

$$\begin{aligned}
 & \text{Likelihood ratio test statistic} \\
 &= -2[LL(\beta_{AllTrips}) - LL(\beta_{WorkTrips}) - LL(\beta_{Non-workTrips})] \\
 &= -2[-905.8 + 436.2 + 460.4] = 18.4
 \end{aligned}$$

This statistic is  $\chi^2$  distributed with (18+12-19) or 11 degrees of freedom which the difference of estimated parameters in the restricted and unrestricted models. From the  $\chi^2$  distribution curve we compute the probability and conclude that with 92.3% (computed from  $\chi^2$  distribution) confidence interval the null hypothesis can be rejected. Note that, 95% and 99% confidence intervals are more common in the literature. However, we reject the null hypothesis at 92.3% confidence interval because of the intuitive behavioral difference in work and non-work trips. Previous studies [99, 100, 101, 102, 103] provide evidences of behavioral differences for trips with different purposes. Based on the test results, this research estimates separate models for work and non-work trips.

### 3.4.3 Estimation results: Route choice

Table 3.1 and table 3.2 report the estimates from the route choice model for work and non-work trips respectively. The model specification include travel time and emissions attributes specific to male, female, individuals who prefer bike for commute, use transit at least three times a week, and individuals who are from high income (more than \$90,000 per year) households.

#### *Model results (work trips):*

For work trips, the coefficients for travel time specific to male and individuals who prefer bike for commuting are found to be log-normally distributed with statistically significant standard deviations. Note that the sign of travel time is adjusted to account for the log-normal distribution. This reflects the intuition that no traveler wants

to increase her travel time. The  $p$ -values for the standard deviations are greater than 0.01. Small sample size (95 observations) can be one of the reasons for having high  $p$ -value. Nevertheless, we keep the same specification because the heterogeneity in the effects of travel time on route choice (and other travel decisions) is intuitive and can be found in the literature ([104, 105, 106]).

The coefficients for emissions specific to male, individuals who prefer bike for commute, and individuals from high income households are found to be normally distributed. This implies heterogeneity across sample. For instance, the participants from high-income households have different patterns of route choices when emissions information is provided. Inputting the mean and standard deviation values in the Normal curve we find 53% of the participants from high-income households are more likely to have less emissions in their choice of route and the rest 47% are more like to choose route with higher emissions (low travel time). Further, we found the coefficient for variation in travel time to be normally distributed.

*Model results (non-work trips):*

For non-work trips, we found the coefficients for travel time specific to male individuals to be log-normally distributed. Due to intuition behind heterogeneity in travel time effects we keep the variable in the specification. The coefficients for emissions specific to male and female groups are normally distributed with statistically significant standard deviations. The results for work and non-work trips are similar with the exception that high-income effect is not found to be significant for emissions.

The next sections report the distribution of trade-off values between emissions and travel time.

Table 3.1.: Estimates: Route choice for work commute

<b>Explanatory variable</b>	<b>Estimate</b>	<b>t-statistic</b>
Alternative specific constant-1	0.811	4.42
Alternative specific constant-2	0.278	1.1
Travel time (in minutes)- if male (Standard deviation-Log Normal)	-0.279 (0.0623)	-4.00 (1.3)
Travel time (in minutes)- if female	-0.243	-2.09
Travel time (in minutes)- if bike is preferred for daily commute (Standard deviation-Log Normal)	-0.074 (0.112)	-1.88 (1.44)
Travel time (in minutes)- if transit is used at least twice a week	-0.117	-1.8
Emissions (in lbs of CO <sub>2</sub> )- if male (Standard deviation-Normal)	-0.183 (0.209)	-6.02 (1.76)
Emissions (lbs of CO <sub>2</sub> )- if bike is preferred for daily commute (Standard deviation-Normal)	-0.394 (0.267)	-2.88 (1.74)
Emissions (in lbs of CO <sub>2</sub> )- with high income (Standard deviation-Normal)	-0.019 (0.210)	-0.22 (1.63)
Variation in travel time (Standard deviation-Normal)	-0.126 (0.285)	- 0.78 (1.69)
Log likelihood value at zero	-461.615	
Log likelihood value at convergence	-436.2	
Number of observations	475 (95 groups)	

Table 3.2.: Estimates: Route choice for non-work

<b>Explanatory variable</b>	<b>Estimate</b>	<b><i>t</i>-statistic</b>
Alternative specific constant-1	0.052	0.27
Alternative specific constant-2	0.227	1.6
Travel time (in minutes)- if male (Standard deviation-Log Normal)	-0.18 (0.123)	-4.2 (1.3)
Travel time (in minutes)- if female	-0.179	-2.01
Travel time (in minutes)- if transit is used at least twice a week	-0.059	-1.2
Emissions (in lbs of CO <sub>2</sub> )- if male (Standard deviation-Normal)	0.01 (0.235)	0.08 (2.91)
Emissions (in lbs of CO <sub>2</sub> )- if female (Standard deviation-Normal)	0.045 (0.347)	0.23 (2.45)
Emissions (lbs of CO <sub>2</sub> )- if bike is preferred for daily commute	-0.207	-2.4
Variation in travel time	-0.261	- 2.26
Log likelihood value at zero	-484.34	
Log likelihood value at convergence	-460.4	
Number of observations	475 (95 groups)	

#### 3.4.4 Trade-offs in route choice

Figures 1 through 4 show the frequency distribution of trade-offs between travel time and emissions specific to work trips. Also, we report the cumulative frequency in the same graph. The estimates from the model are specific to different groups (e.g., male, female, high income groups). Random parameter models provide distinct coefficient for each person in the sample. We compute the net effects to quantify the exact trade-off values for each group of interest. For instance, to compute the net effects for the male individuals (work trips) in the sample:

$$\beta_{Net, Male}^{emissions} = MaleIndicator \times (\beta_{male}^{emissions} + \beta_{bike}^{emissions} + \beta_{HighInc.}^{emissions}) \quad (3.9)$$

The interpretation should be based on the definition in equation 5.27 that describes the propensity of choosing a particular route. The value of MRS simply indicates the trade-off between attributes to keep the same functional value in propensity equation (section 3.3.3). For instance, trade-off value of  $y$  minutes per lb of CO<sub>2</sub> for a person in the sample indicates that, the individual shows preference to travel additional  $y$  minutes for each lb of CO<sub>2</sub> emissions reduction for a defined travel context with the following conditions: (a) Purpose and time: morning home-to-work trips, (b) mode of transport: personal vehicle, (c) trip length: ranging from 21 to 30 minutes.

#### 3.4.5 Work trips

Findings for work trips indicate that, on average the trade-off value for a female (1.37 minutes/lb of CO<sub>2</sub>) is higher than that (1.29 minutes/lb of CO<sub>2</sub>) of a male. In other words, the additional travel time for a lb of CO<sub>2</sub> a traveler considers during route choice decision making is higher for female compared to male (for work trips with length ranging from 21 to 30 minutes). Further, the average trade-off value for individuals who prefer bike for daily commute is higher compared to male individuals and lower compared to female individuals.

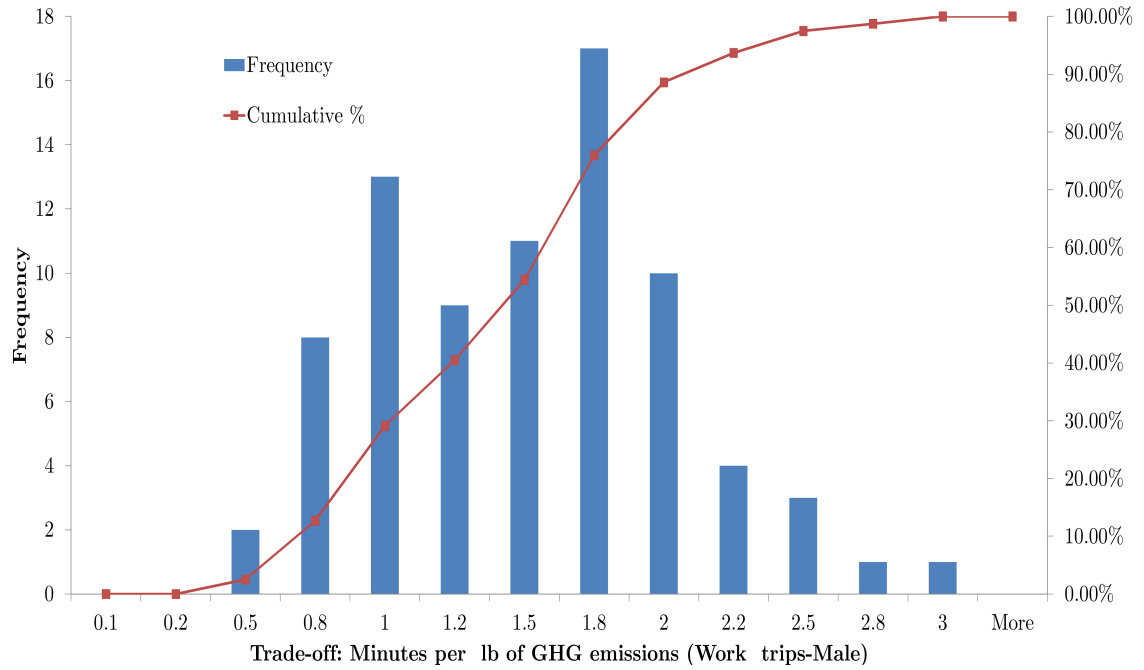


Figure 3.1.: Trade-offs in work trips: Male group

Preference for bike for daily commute does not show increased value for the trade-off value. Someone willing to use bike for commute may not consider higher (compared to who do not prefer bike for commute) additional travel time while making a route choice decision. One interesting finding is that, the average trade-off value for the individuals from high income (greater than \$90,000 per year) is higher compared to the average values for specific groups male, female, who prefer bike. Participants from high income households may have exposed to more educational activities that emphasizes on climate change, energy crisis, and impacts of CO<sub>2</sub> emissions on our lives. Also, the rich people are also believed to have higher social responsibility in context of environment and sustainability. In our case, the level of education regarding climate change, social responsibility, and awareness may be the driving factor for higher trade-off value for participants from high income households.



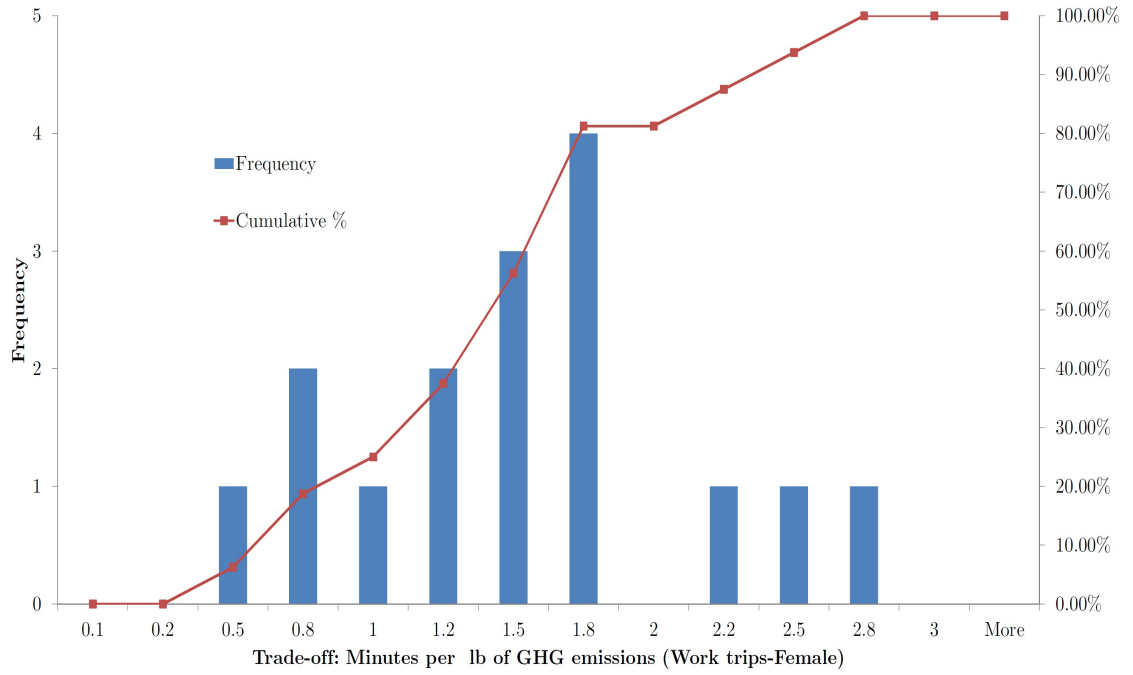


Figure 3.2.: Trade-offs in work trips: Female group

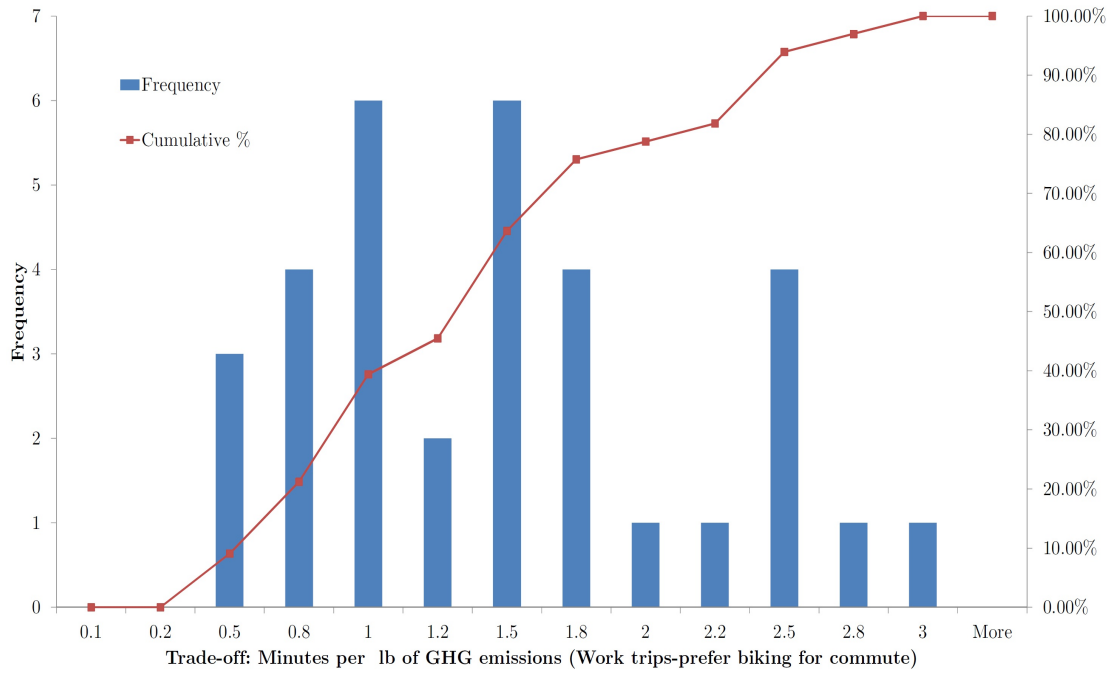


Figure 3.3.: Trade-offs in work trips: Bike preference

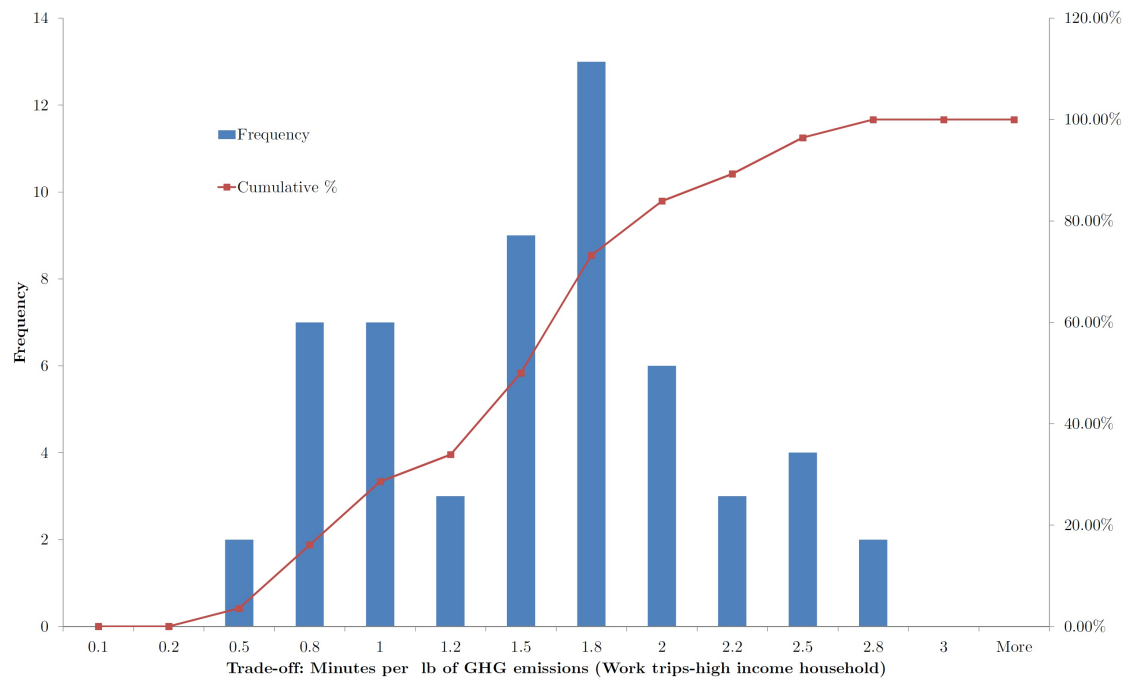


Figure 3.4.: Trade-offs: high income households

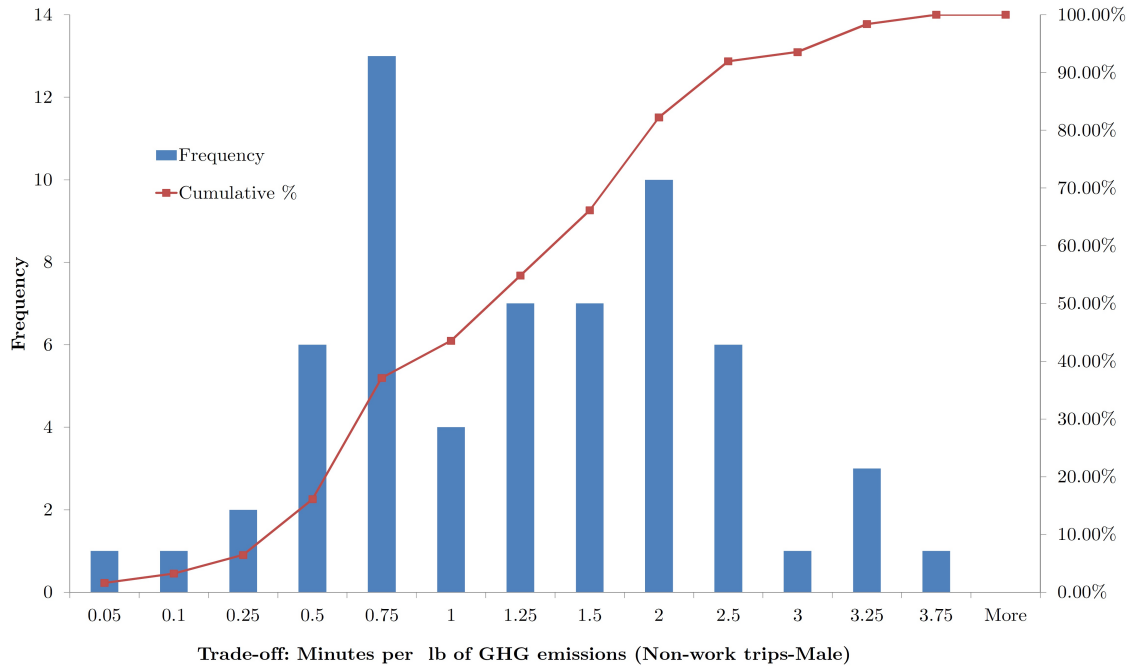


Figure 3.5.: Trade-offs in non-work trips: Male group

### 3.4.6 Non-work trips

Figures 5 through 7 show the frequency distribution of trade-off values for specific groups in our sample. Similar to work trips, the average trade-off value for a female (1.38 minutes/lb of  $\text{CO}_2$ ) is higher compared to a male (1.29/lb of  $\text{CO}_2$ ). Further, both values are higher than those found for work trips.

Again, the average trade-off value specific to the group that prefers bike for daily commute is lower compared to female individuals and higher compared to male individuals. Again, preference for biking does not necessarily indicate consideration for additional travel time to have less emissions along the trip.

Observing the values for work and non-work trips, one can see that for non-work trips participants show preference to travel higher additional minutes for each lb of  $\text{CO}_2$  savings along the trip. This is intuitive because non-work trips (referring only to recreational trips on weekend) are more malleable in terms of travel behavior [103] and the schedules are more flexible.

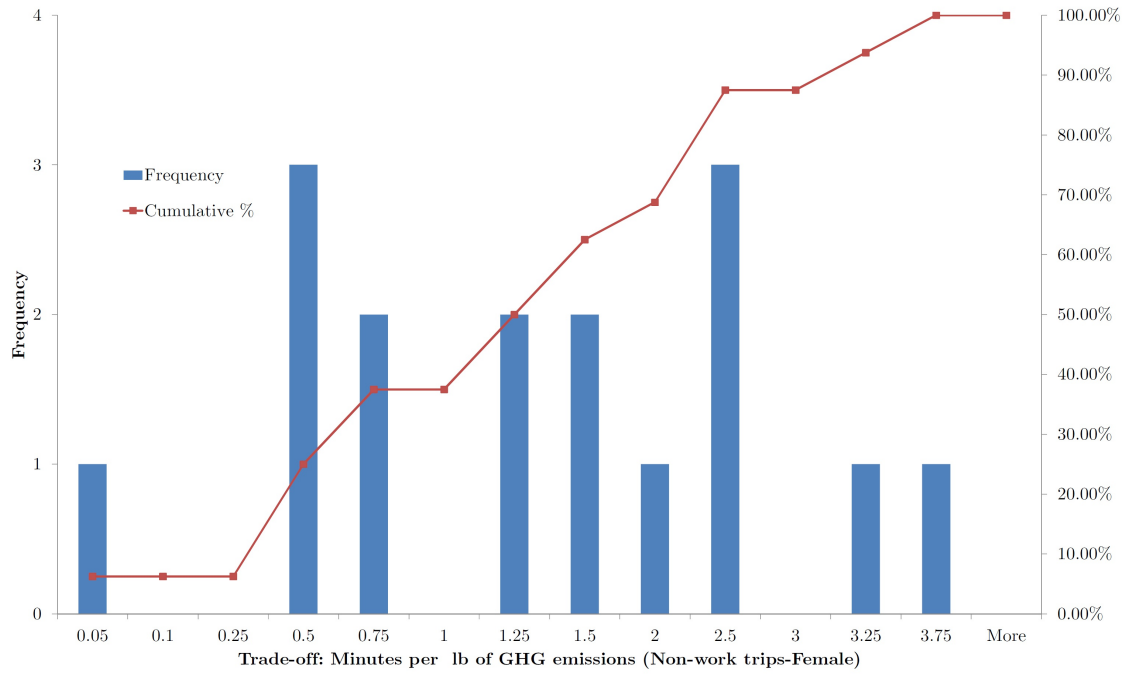


Figure 3.6.: Trade-offs in non-work trips: Female group

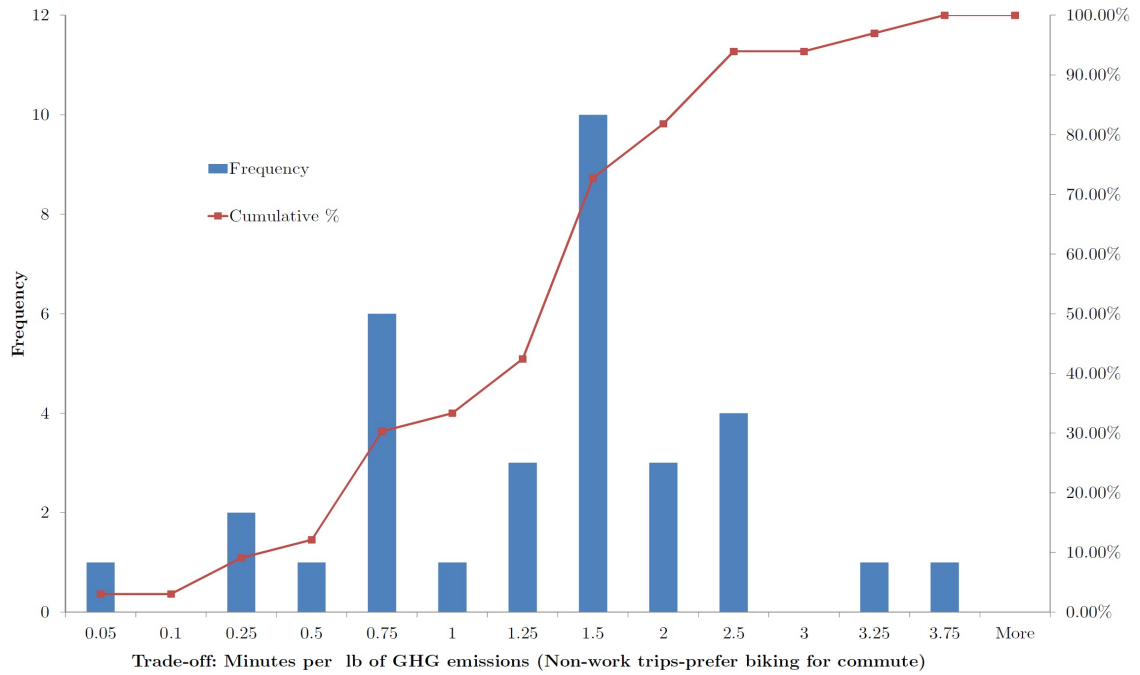


Figure 3.7.: Trade-offs in non-work trips: Bike preference

## 3.4.7 Summary

Table 3.3.: Trade-off value distributions

Context	Trade-off value (minutes per lb of CO <sub>2</sub> )		
	Average	Min.	Max.
Male (work trips)	1.284	0.43	2.87
Male (non-work trips)	1.298	0.04	3.63
Female (work trips)	1.36	0.367	2.61
Female (non-work trips)	1.38	0.02	3.41
Bikers (work trips)	1.33	0.367	2.87
Bikers (non-work trips)	1.31	0.02	3.40
High Income (work trips)	1.41	0.43	2.77

[36] estimated willingness-to-pay as \$ 0.24 per lb of CO<sub>2</sub> savings in context of route choice. The expected wage rate of students in California is about \$ 8.00 per hour. Using these values, the equivalent trade-off is about 1.8 minutes per lb CO<sub>2</sub>. Recently, [37] found the average value of green (willingness to pay per lb of GHG emissions) as 15 cents per lb of CO<sub>2</sub> from their analysis using data from undergraduate students in California. Using these values, the equivalent trade-off is about 1.13 minutes per lb CO<sub>2</sub>. As we see from table 3.3, the values obtained from our model are similar to the findings from other researchers.

### 3.4.8 Departure time choice models

Random parameter models for departure time choice are estimated for work-to-home trips during afternoon rush hour. Table 3.4 reports the estimates from the departure time choice model. Coefficients of travel time specific to male and female groups, and schedule delay specific to Asian ethnicity are found to be random parameters with significant standard deviations. The signs of the coefficients indicate that, on average routes with less travel time and less schedule delay are more preferable. The model also reports the distribution of coefficients for the sample (distinct parameter for each panel). Coefficients of emissions specific to male individuals is found to be normally distributed. This implies that for certain portion of the sample the coefficient is negative and for the rest the coefficient has a positive sign. The net effects of emissions and travel time for a certain group can be computed using equation 3.9. In addition, we found coefficients for travel time and emissions specific to ethnicity, income, and area-grownup to be significant.

Table 3.4.: Results: departure time choice

<b>Explanatory variable</b>	<b>Estimate</b>	<b>t-statistic</b>
Alternative specific constant-1	-0.849	-1.79
Alternative specific constant-2	-0.129	-0.766
Travel time (in minutes)- if male (Standard deviation-log normal)	-0.151 (0.119)	-3.55 (2.5)
Travel time (in minutes)- if female (Standard deviation-log normal)	-0.535 (0.235)	-1.59 (2.83)
Travel time (in minutes)- if grown up in suburb	-0.114	-2.43
Travel time (in minutes)- Asian ethnicity	-0.365	-4.35
Travel time (in minutes)- Caucasian ethnicity	-0.150	-2.83
Emissions (in lbs of CO <sub>2</sub> )- if male mean (normal distribution)	-0.092	-0.805
Standard deviation	0.271	7.06
Emissions (in lbs of CO <sub>2</sub> )- if female	-0.226	-2.03
Travel time- if grown up in suburb	-0.114	-2.44
Travel time- if Asian	-0.347	-4.34
Emissions- if white	-0.187	-1.65
Emissions- if bike is preferred	-0.164	-1.57
Schedule delay (in minutes)- high income group	-0.025	- 1.97
Schedule delay (in minutes)- if bike is preferred	-0.041	- 1.97
Schedule delay (in minutes)- if white	-0.045	- 3.29
Schedule delay (in minutes) - if Asian mean (normal distribution)	-0.067	-1.7
Standard deviation	0.071	3.1
Log likelihood value at zero	-834.945	
Log likelihood value at convergence	-672.461	
McFadden Pseudo $\rho^2$	0.195	
Number of observations	760 (95 groups)	

### 3.4.9 Trade-offs in departure time choices

Figures 3.8, 3.9, and 3.10 show the distribution of trade-offs between schedule delay and emissions. Schedule delay is defined as the amount of time a person adjusts by departing early or late for the destination (see table 1.2). The trade-off values exclude the effects of travel time. Results indicate that the trade-off values are higher than those found for route choice contexts. This implies that an individual, with similar attributes as in our sample, is more likely to consider higher additional minutes when adjusting departure time compared with altering route choices. Further, the average trade-off value is higher for male individuals compared to female. Similar to the case of route choice scenario, the trade-off value for the individuals, who show preference for bike to commute to work, is lower than the average value (male and female groups). Also, we observe a hike around the trade-off value around the range 3.75 minutes per lb for female group. The number of female individuals is relatively small (about 30%) in our sample. This may cause less variation in the trade-off values. For male group, the trade-off values constitute a large share ranging from 3.75 to 5 minutes per lb of CO<sub>2</sub>. Similar trend is found for the trade-off distribution for the group who prefer bike for commute to work. Table 3.5 summarizes the results.

Table 3.5.: Trade-off value distributions

Context	Trade-off value (minutes per lb of CO <sub>2</sub> )		
	Average	Min.	Max.
Male	3.82	1.78	7.8
Female	3.71	2.34	4.55
Bikers	3.65	1.78	5.61



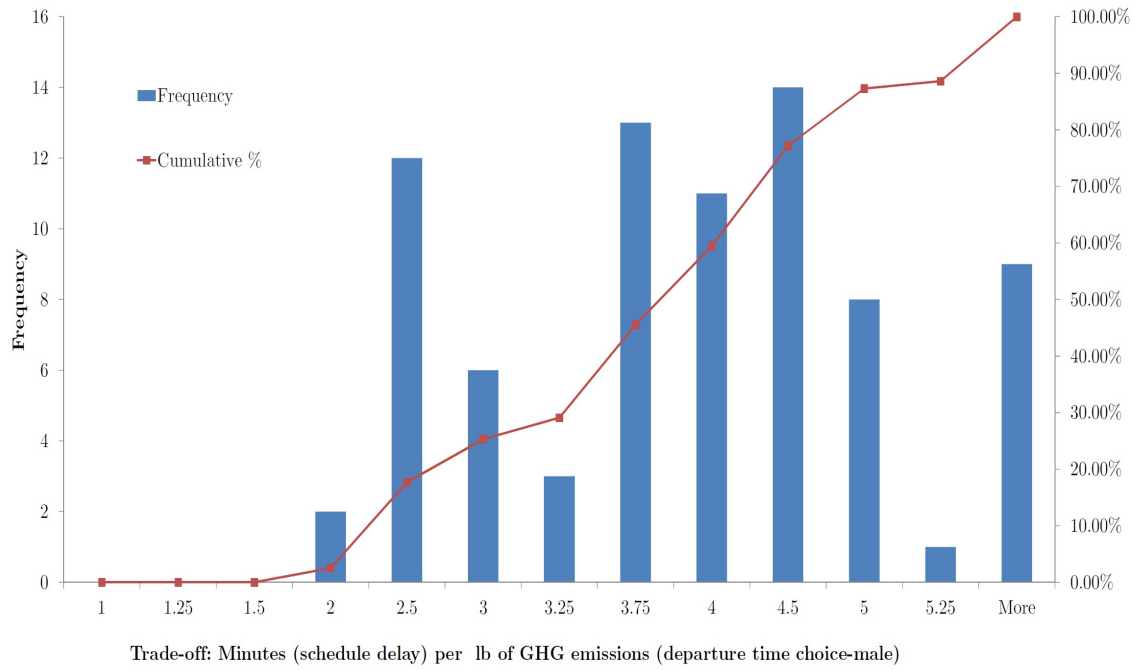


Figure 3.8.: Trade-offs in departure time choice: Male group

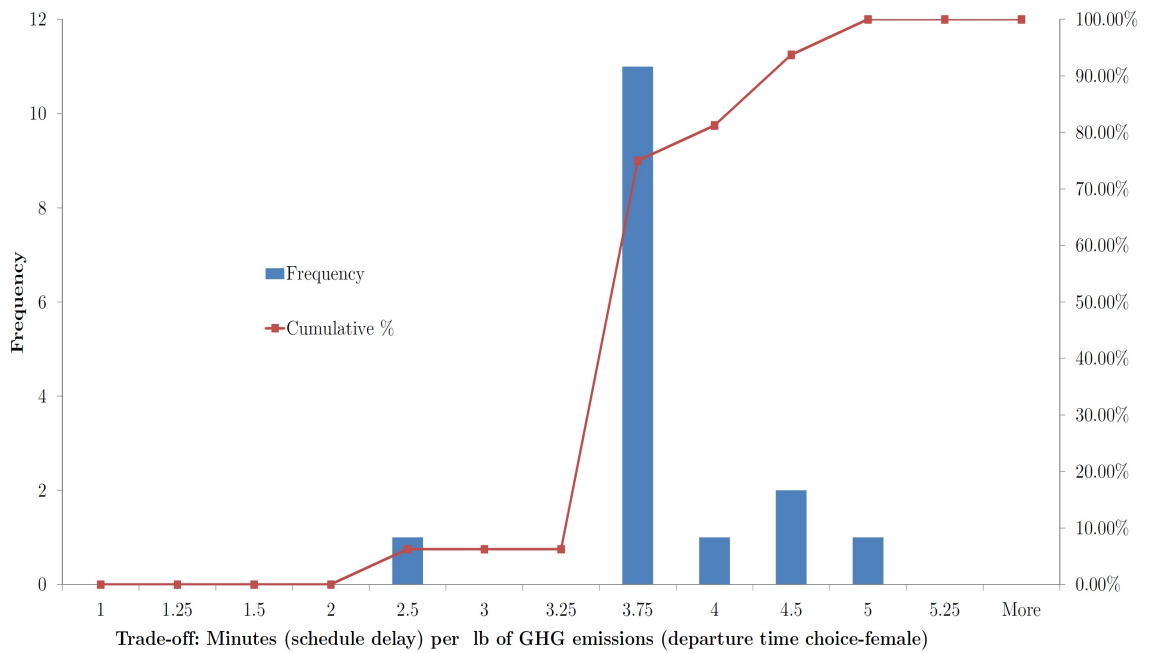


Figure 3.9.: Trade-offs in departure time choice: Female group

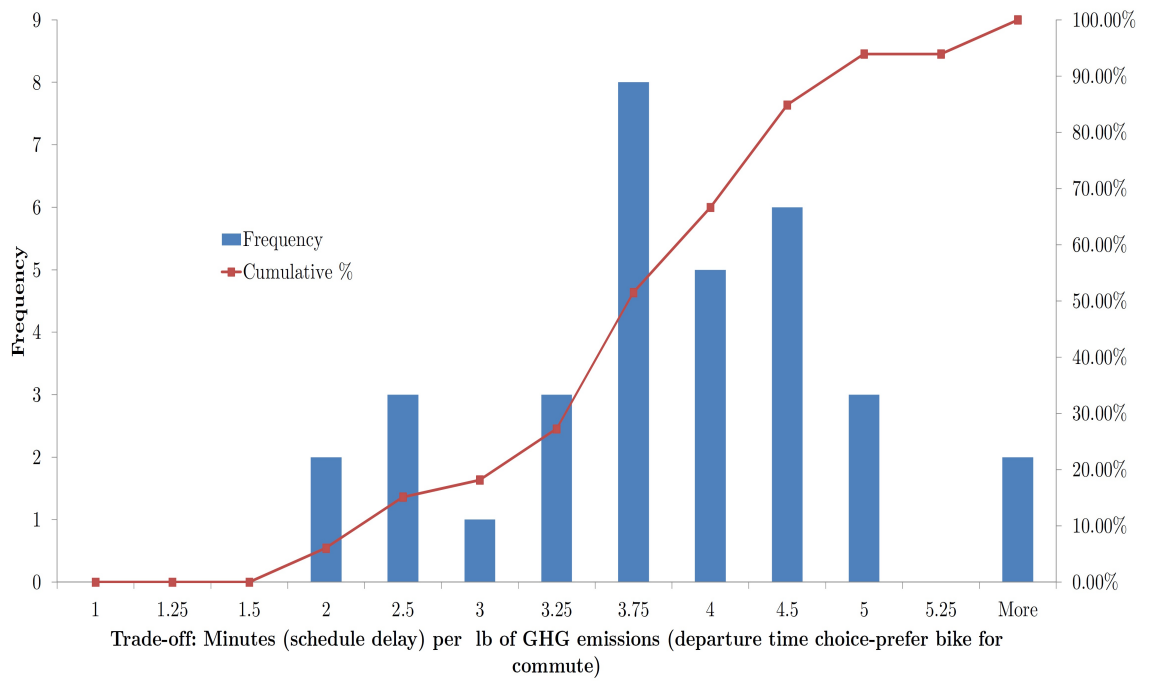


Figure 3.10.: Trade-offs in departure time choice: Bike preference

### 3.5 Policy implications

#### 3.5.1 Provision of information

This research shows that providing emissions related information can influence the travel decisions and accordingly can lead to significant reduction of CO<sub>2</sub> emissions. To demonstrate, we apply the estimates from the models (section 7.5) and approximately quantify the savings in terms of CO<sub>2</sub> emissions. We must acknowledge that, this is an approximation of the CO<sub>2</sub> emissions without accounting for the transferability issues. With our assumptions (justified by the census data), we demonstrate possible reduction in emissions when information regarding emissions for the trip are provided to the users.

At the beginning of the experiment, participants were asked to make travel choices when information about the emissions along the trip is not available. Later, we presented the hypothetical travel scenarios (as described earlier in section 3.2) before the participants with emissions information. The estimated random parameter models (section 7.5) that provide us with the most likely outcome in terms of travel decisions when emissions related information are available.

Table 3.6.: Effect of providing emissions information\*

Information on emissions	Route-1 Share	Route-2 Share	Route-3 Share
NO	92%	8 %	0
YES	86 %	5 %	9 %
(work trips)			
YES	78 %	3 %	19%
(non-work trips)			

\*Route-1: Least travel time with highest emissions

Route-2: Moderate travel time with moderate emissions

Route-3: Highest travel time with least emissions

### 3.5.2 Savings in terms of emissions

Now, we provide an example to demonstrate how much emissions can be reduced for the network. Our collected sample has two unique attributes:

1. Participants are within the age group ranging from 20 to 24 years.
2. The education level is near bachelor's degree in civil engineering.

Purdue University is located in the Tippecanoe county, West Lafayette, Indiana and the American community survey (ACS) provides the data regarding work trips made by the individuals within the age group ranging from 20 to 24 years and with a bachelor's degree. We must acknowledge that, this is a strong assumption that the travel choice making pattern will be similar. Nevertheless, this is only for demonstration purpose to show the benefits of providing emissions related information to the travelers.

We find the work trips made by the individuals from the 2012 ACS survey data with the following attributes:

- age group ranging from 20 to 24 years (about 22% of all work trips)
- either with college or associate degree, or bachelor's degree and mode of transportation to work can be car, truck or van (about 45 % of all work trips)
- commute time ranging from 21 to 29 minutes (about 25% of all work trips)

According to 2012 ACS survey, the estimated number of daily work trips is 83,434 in Tippecanoe county. Now, the number of work trips meeting the above criteria is about 2300 trips per day. In consistent with our travel choice scenarios depicted in our experiment, we assume switching from least travel time route to least emissions

(highest travel time) route saves 5 lbs of CO<sub>2</sub> emissions on average and switching from least travel time to moderate travel time (moderate emissions) route saves 2.5 lbs of CO<sub>2</sub> emissions on average. With these assumptions the following table reports the quantity of CO<sub>2</sub> emissions that can be reduced when emissions related information are available for work trips.

Table 3.7.: Impact of information: city level

Total work trips	2300 per day		
Information on emissions	Route-1 Share	Route-2 Share	Route-3 Share
NO (work trips)	2116	184	0
Base Case emissions <sup>+</sup>	40940 lbs CO <sub>2</sub>		
YES (work trips)	1978	115	207
Daily savings (Morning commute only)		(115 × 2.5) or, 287.5 lbs	(207 × 5) or, 1035 lbs
Total weekly savings (Morning commute only)		6612.5 lbs CO <sub>2</sub>	(16.15 % reduction from base case)
Total Annual* savings (Morning commute only)		167.3 tons CO <sub>2</sub>	

+Assume, 18 lbs of CO<sub>2</sub> on average for the route with least travel time

\*Assume, 253 working days in a year.

With changes in the route choice behavior when emissions related information is available, the network may reach a different equilibrium over time. The direct analogy is the emissions pricing problem where we impose emissions based tolls or credit based pricing, and a new equilibrium (desired) is established [4, 65]. Network equilibrium models [107, 108] can be formulated with generalized cost structure and perception variance when real-time information (either travel time or emissions, or both) is available to the road users. The notion of trade-off will be more prominent when we integrate the route choice models and network equilibrium models.

### 3.5.3 Improvement of travel time

The trade-off values between emissions and travel time can help to design travel time improvement schemes that lead to significant emissions reduction. Note that, the trade-off values are specific to the context that includes (but not limited to): a) trip duration, purpose, and time of day (e.g., short work trip in the morning), b) population mix (e.g., proportion of white and blue collar workers, students, and so on), c) Travel decision scenario (route vs. departure time choice). Further, the availability of alternative travel options and the difference between the least and highest emissions travel options should be accounted for before applying the results from the models.

The results from our estimated model provides insights only for a specific context. The results provide us with a distribution of the trade-off values in the sample. Now, we examine the effect of travel time reduction on route choice decisions. In context of work trips, we keep the same emissions level for the routes and decrease the travel time of the least emissions route to observe the resulting market share. The trade-off values between emissions and travel time help us to decide how much travel time reduction would be effective for this particular context (e.g., the difference in emissions and travel time between the least and highest emissions travel alternatives).

Table 3.8.: Effect of reducing travel time: Work trips

Travel time reduction (in minutes)	Route-1 Share	Route-2 Share	Route-3 Share
No change	51%	31%	18%
0.5	49 %	29 %	22%
0.75	48.38 %	28 %	23.58%
1.0	47.6 %	26.9 %	25.5%
2.0	44 %	22 %	34%
3.0	39.5 %	17.3 %	43.2%

\*Route-1: Least travel time with highest emissions

Route-2: Moderate travel time with moderate emissions

Route-3: Highest travel time with least emissions

Table 3.7 reports the outcome of the scenarios. We reduce the travel time for the least emissions path by values ranging from 0.5 to 3.0 minutes and simulate the probabilities using the results from our estimated models.

#### 3.5.4 Policies for heterogeneous population

Our results indicate that trade-off between emissions and travel time vary across the population. Even the same individual can have different trade-off values at different travel scenarios (route vs. departure time). Therefore, the policies that encourage travel behavior leading to less emissions for the network (similar to scenarios explained in this research) should account for the heterogeneity. For instance, for particular context if the trade-off values are too small, even a big improvement in travel may not bring a significant reduction in emissions. Likewise, different groups of people have different trade-off values and accordingly one need to consider the population mix before consideration of any scheme.

#### 3.5.5 Flexibility in departure time

Figures 3.8 3.9, 3.10 and table 3.5 indicate that users are willing to adjust departure times for their work to home commute trips. Moreover, the average values are higher compared to route choice context. Policies allowing for higher flexibility in terms of departure time from work can help to reduce emissions. Many employers (e.g., Sun Microsystems, BestBuy, PNC Financials) are interested to give flexible schedule to the workers where they can set the start and end time of their weekday work and allow telecommuting(<http://www.careerbuilder.com>)



### 3.5.6 Integrated agent based simulation

The estimated models for route and departure time choice provide us with the probabilities for travel options at specific context. These probability values can be integrated with an agent based simulation that can serve as an effective policy tool. The random parameter models provide choice probabilities for each individual in the sample and can be integrated to the route choice rules in an agent based traffic simulation.

## 3.6 Concluding remarks

This study motivates the analysis of trade-off between emissions and travel time at different contexts of daily travel, describes a mixed logit based framework that accounts for heterogeneity across the sample, and completes the study with a sample collected from Purdue undergraduate students. Random parameter models accounting for correlation across repeated observations are estimated to find the trade-off between emissions and travel. The empirical results show that trade-off values are different for route (home-to-work morning commute) and departure time (work-to-home afternoon commute) choice contexts. Further, the log likelihood ratio test suggests different models for work and non-work (weekend recreational trip, in our case) travel decisions. Further, the trade-off values for route choice contexts estimated from our models are similar as found by [36] and [37].

### 3.6.1 Key findings

The findings are limited to the scope of the data and travel contexts (purpose, length, and type of trips) we have analyzed. Key findings from the empirical results are as follows:

- (a) Female individuals consider higher additional travel time (compared to available alternatives with lower travel time and higher emissions) per lb of GHG emissions in route choice contexts compared to male individuals. Findings are similar for

work and non-work trips (table 3.3). However, for departure time context we see the opposite trend. This research analyzes only few travel choice contexts and accordingly a general conclusion cannot be made.

- (b) For the route choice contexts, the average additional minutes the participants from high income households (annual income greater than \$90,000) are willing to consider is higher than average value in the sample. Level of awareness and exposure to education related to climate change can be the driving factors behind this. In addition, this also indicates to the notion of higher social responsibility of rich people in general.
- (c) One interesting finding is that, the average additional minutes per lb of CO<sub>2</sub> emissions for the group of participants who prefer bike for daily commute (when a safe bike route with convenient length is available) is lower than the average value in the sample. Preference to bike is often considered as an indicator of pro-environmental attitude. Our results show that, preference to bike does not necessarily mean pro-environmental attitude in the context of trade-off between emissions and travel time.
- (d) Our study indicates that, the additional travel time per lb of CO<sub>2</sub> emissions individuals consider in departure time context is higher compared to route choice contexts. This has an important policy implication in terms of flexibility provided by the employer(section 3.5).
- (e) Providing emissions related information prior to daily travel decisions can lead to significant emissions reduction. We do not generalize the results from our study. However, the framework and methodologies can be readily transferred to any travel context for a different population mix.

### 3.6.2 Limitations and future work

The study has few limitations. First, use of sample that includes only students limits the scope of estimated models in terms of generalization and transferability. The insights are only valid for certain population group with characteristics similar to the student sample. However analyses can be done after characterizing population groups by the selected sample attributes. Further data collection is required for a comprehensive analysis for a city or geographic region. Also, the participants made choices in a lab setting and the impact of time or money constraints is minimal. To address this issue, we have designed the experiments incorporating real world network, travel time variations, and emissions estimation (see screen shots in the appendix). Finally, the conclusions are not directly transferable to policy making for general population of traffic users. However the results help us to understand the impact of providing information about emissions to travelers. The distribution of trade-off values indicate heterogeneity exists in willingness to consider additional travel time to save emissions. This can serve as a basis for designing policies that motivate individual to save emissions.

Student samples are often characterized with selectivity bias. A recent study by [89] indicates that self-selected students are appropriate for behavioral experiments with least bias. We plan to collect data to obtain a larger and representative sample in near future.

Second, we only consider three travel choice scenarios. It would be useful to collect data for additional travel contexts (i.e., range of travel activities along the day) and analyze the trade-off values.

Third, we consider route and departure time choice separately, however studies [23, 109] suggest it is important to consider the coupled choice of departure time and route choice. As a future extension, we plan to collect data and estimate joint choice models.

Nevertheless, this research is one of the first studies focusing on the trade-off between emissions and travel time using econometric models. The framework can be transferable for any particular study for general road networks. We demonstrate the

use of trade-off values in terms of finding effective policies that can help to reduce emissions from transportation network (section 3.5). To conclude, this research contributes to find effective policies for emissions reduction from road transport (e.g., information provision, flexible departure time), to assess the policies (e.g., what-of scenario with travel time improvement), and to explore the inherent heterogeneity in terms of pro-environmental behavior (trade-off as minutes per lb of CO<sub>2</sub> emissions) across the users of transportation network.

## CHAPTER 4. CARBON ALLOWANCE FOR TRAVEL

### 4.1 Introduction

This chapter proposes personal mobility carbon allowance scheme, collects the data using an on-line experimental game, and analyzes data with econometric models. We propose personal mobility carbon allowance (PMCA) scheme that allocates carbon credits to users at no cost based on the emissions reduction goal of the system. Users can spend carbon credits for travel and a market place exists where users can buy or sell credits. To understand this process, a real-time experimental game tool is developed where players are asked to make travel decisions within the carbon budget set by PMCA and they are allowed to trade carbon credits in a market modeled as a double auction game. Random parameter models are estimated to examine the impact of PMCA on short-term travel decisions.

The downstream carbon trading schemes aiming at reduction of GHG emissions and energy consumptions at household level (travel and utility) [43, 45, 47] are argued to be successful . One class of these schemes, namely the personal carbon allowance (PCA), focuses on cutting down household level carbon consumptions [44, 66, 67, 68]. Two key advantages of PCA schemes are: emissions reduction target and revenue neutrality. Moreover these policies are identified as soft policies because no restriction on personal mobility is imposed directly. The idea presented here is conceptually similar to the Tradable Energy Quotas (TEQs) [18] with the key difference that our focus is only on personal travel and we study at a finer level of travel behavior rather than aggregate trips or vehicles-miles-traveled measures.

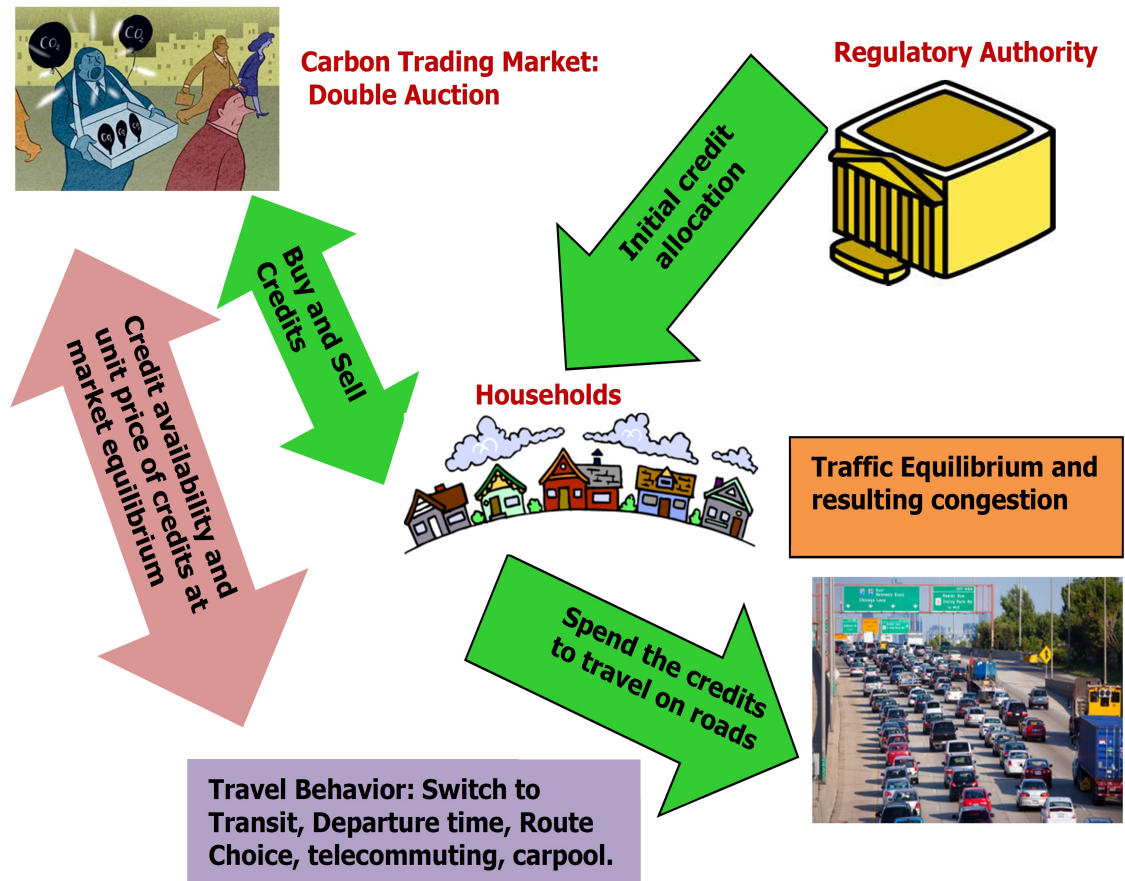


Figure 4.1.: Overview of the PMCA scheme

#### 4.1.1 Personal Mobility Carbon Allowance (PMCA)

PMCA scheme allocates each eligible (e.g., all taxpayers) household within the system boundary a fixed number of carbon credits to spend for travel activities at no cost. The allocation interval can be each week or each month depending on the scope of the system. Figure 4.1 describes all elements of a PMCA scheme that include: distribution authority, travelers (users), carbon market, and the collective travel patterns that decide the transportation network state in terms of congestion and emissions.

The government or an authority regulates the distribution. A third party energy committee decides the total carbon cap for the system. The carbon cap changes

each year. For instance, the cap can be set to have 2%, 5%, 7% carbon reduction from the base case for the consecutive three years. The carbon credits can be spent to purchase any form of energy or fuel sources required for personal transportation. Transit systems and air travel can be considered separately. The air fare and transit pass can include the carbon cost for users. A carbon rating system sets the carbon credit cost based on the carbon contents of the energy sources. For instance, refueling at gas station and recharging the battery of an electric vehicle both will cost carbon credits. Further, a carbon market exists where households can sell (surplus) or buy (additional) carbon credits. The demand and trading patterns determine the price of unit carbon credit.

Under PMCA scheme the road users consider the carbon cost in addition to travel cost associated with the travel alternative (e.g., route and departure time choice) . The travel decisions are influenced by the carbon budget and the current price of unit carbon credit. It is intuitive that the decision making process will not be homogeneous. Users with different values of travel time are likely to have different patterns of travel behavior.

#### 4.1.2 Research goals

Section 2.3 in chapter 2 has a discussion on the relevant works in the literature and the general research goals are described in section 1.2.2. This research aims to address the limitations of previous studies relevant to carbon allowance and trading schemes. Existing works [51, 110, 111, 112] have explored different aspects of household level carbon trading schemes qualitatively. The scope of most of these studies are limited to aggregate level analysis of behavioral change and they do not capture the changes in travel decisions or patterns at household or individual level. Additionally, the data used are obtained in the form of either opinions or responses from questionnaire based surveys [113, 114, 115].

Further, a key limitation of these approaches is the absence of the carbon market. Modeling carbon market requires interaction among all individuals (households) in the market and questionnaire based settings are not able to do that. This is important because the trading behavior determines the price of carbon credit in the market. The price affects the travel decisions. Assuming a fixed carbon price will not be appropriate to investigate the evolving travel patterns under household level carbon schemes. Finally, the resulting travel patterns are not analyzed rigorously with behavioral models based on econometrics.

Major goals of this research are as follows:

- (a) To develop and design an interactive experimental tool with integrated trading market to collect data for PMCA scheme,
- (b) To estimate cost functions accounting for heterogeneity in the users, and to investigate the influence of carbon credit cost and market conditions on travel decision making,
- (c) To investigate the patterns of unit price of carbon credit, and to explore the asks-bids patterns in the trading market.

#### 4.2 Why experimental games?

Understanding PMCA scheme requires observations from real world systems where the scheme is being implemented and the evolved travel and market behavior can be observed. Personal carbon allowance schemes are relatively new and no effective implementation at household level can be found to the best of the authors' knowledge. The only carbon trading study we are aware of is the carbon health evaluation project in Norfolk Island which lies in the Pacific Ocean between Australia, New Zealand and New Caledonia. This is the world's first carbon trading pilot project conducted by Southern Cross University in a *closed system* island environ-



ment(<http://www.norfolkislandcarbonhealthevaluation.com/>). Collecting real world data is challenging and expensive both in terms of money and time.

An alternative to the collection of the real-world data is conducting laboratory experiments with human subjects. In the experiment, a group of participants interact with each other in a controlled environment. The incentives for specific actions are designed in such a way that one can investigate the evolution of certain behavior patterns at individual and collective level. Note that laboratory experiments do not require any prior assumptions on the behavior of the participants. Rather the behavior patterns are observed and analyzed from the experimental data.

Experimental economics offers a suitable way to collect *field* data for behavioral analysis. Nobel Laureate Vernon Smith first emphasized on the applicability of well designed experiments to analyze theories involving human behavior and market interactions [116]. The experiments can be run with a controlled, uniform group of subjects. The utility (cost) functions that are imposed upon the subjects allow for heterogeneity among the subjects. The basic unit of analysis for PMCA is a household. For example, in the context of a PMCA scheme, we will allow some subjects have a higher value of time and a higher trip demand, which would lead to a higher demand for personal carbon credits and other subjects (say blue collar workers) who make mandatory trips due to their work situation. Our analysis puts focus on qualitative rather than quantitative results, i.e., trends and patterns in the data that allow behavioral characterization rather than absolute magnitudes. An experiment will likely not be able to tell us that a given scheme can lower energy use by 35%, more realistically; it will tell us that imposing a certain scheme will lead to lower energy use, a relative sense of the savings across different populations and how they impact differentially among different user groups. Though it may not be perfect, it provides the only reasonable way to analyze the effect of untested schemes such as PMCA on a given population.

The incentive for the game is designed so that the primary objective of the players is to minimize travel cost within the carbon budget. At the same time the players

get additional points from buying and selling in the markets. This is to replicate the behavior of the road users (households) under PMCA scheme. Since subjects' choices are incentivized, it is expected that they will make choices with the goal of maximizing points they earn in the experiment. For each player the cost function and travel demand will be different based on the assigned group. This points to an important feature of experimental economics. Since the subject pool will likely be a homogeneous set of students, the only way that we can study behavior of a heterogeneous population is by *imposing* specific utility (cost) functions on the subjects. For example, subject  $A$  may have a value of time  $\zeta_{Aj} = 10$  for trip  $j$  while subject  $B$  only has a value of time  $\zeta_{Bj} = 2$  for trip  $j$ . Though the individual subjects may be identical, we have imposed utility functions on them such that individual  $A$  values time more than individual  $B$ . Because of these different utility functions, we are able to study heterogeneous groups. To impose heterogeneity, we will have different types (or income levels) of subjects. Different types of subjects will vary in three different ways: their initial level of money, their value of time, and the number of trips they make per week.

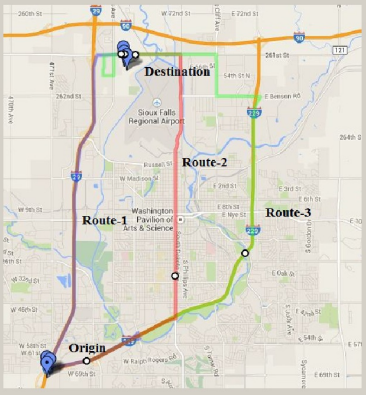
The next few sections describe the experimental setup, and details of the game interface development for travel choices, and the double auction framework.

### 4.3 Description of the experimental game

The experimental game comprises making choices for daily trips and participation in a double-auction based carbon credit market. The trip decision segment involves making route and departure time choices with available information on travel cost, carbon credit cost, and travel time variation (figure 4.2). The temporal horizon of the game depends on the scope of the problem. This study collects data for a five week horizon. A player makes travel choices on each week based on available information. Each player starts the game with certain amount of carbon credits and money. After making a travel decision, the corresponding carbon credits are deducted from the player's carbon account (figure 4.2). The available money can be used to buy credits

Work commute (Weekdays) [2 Trip(s)]

No. of trips left = 6



Choose a travel option: 2 Trips

Option	Time (min)	Carbon	Time Var.	Cost
6:45 am Route-1	34	39	4	280
6:45 am Route-3	37	31	3	316
7:00 am Route-1	43	25	4	322.4
7:00 am Route-2	48	21	2	489.6
7:10 am Route-3	55	17	2	596

6:45 am Route-1  
 6:45 am Route-3  
 7:00 am Route-1  
 7:00 am Route-2  
 7:10 am Route-3

Confirm and Proceed

Total Money (Account) = 500  
 Total Credits (Account) = 429  
 Total Cost (in Francs) = 1622.0  
 Price( unit Carbon Credit) = 21

Figure 4.2.: Route choice segment of the game

in the market. While making a decision players can see the remaining carbon credits and remaining money to buy credits from the market (figure 4.2). After making all travel choices for the week, all players enter in a double-auction based market. The market allows the players to buy and sell credits. The unused credits are rolled over and each player gets new credits before making choices for the next week.

#### 4.4 Game design

This section describes different features and design aspects of the experiment that include initial carbon allocation, design of travel choice scenarios, travel cost functions, and mechanism of double-auction market.

##### 4.4.1 Initial allocation

To set the initial allocation of carbon credits, we follow the target-based approach that sets goal to reduce GHG emissions from baseline (existing state). The analysis

of the test network with associated conditions such as demand, multiple user groups, and route availability provides us with the baseline GHG emissions for the system. The baseline emissions can be converted into equivalent number of carbon credits. For instance, we set a goal to reduce the emissions by 10% (choice by policy maker) and distribute the equivalent carbon credits among all users.

#### 4.4.2 Travel decision scenarios

We designed the travel choice scenarios for the bi-directional Sioux-Falls network. Sioux-Falls is located in South Dakota, USA. Using Google maps, the initial travel time values are obtained. The travel time values between different origin-destination pairs were systematically varied to reflect varying congestion states. The experiment presents travel scenarios on three basic types: work, non-work(grocery), and recreational trips. Non-work trips constitute a large set with numerous specific purposes and we Only consider grocery trips because of its higher frequency in the daily trip decisions. Ideally, the experiments should be conducted with all trip purposes. However conducting an experiment including all trip types and with a time horizon of four weeks requires more than 2 hours. It is challenging to find participant with a time commitment more than 2 hours.

#### 4.4.3 Trip demand and value of time

Number of trips for user groups representing different income levels are obtained from the 2009 National Household Travel Survey data and are listed in table 5.1. The income brackets are modified so that there are five groups and the number of weekly trips are determined from the survey data. The experiments in this study have players representing three income groups.

To account for the heterogeneity in travel cost for each income class we use the value of travel time (VOTT) for trips specific to purpose. The VOTT values are obtained from the guidelines provided by FHWA [117]. For the ease of conduct-

ing experiments, the number of total trips are proportioned with the same relative difference among the groups.

Table 4.1.: User group definition

<b>User Group</b>	<b>Income Range</b>	<b>Work Trips</b>	<b>VOT</b>	<b>Grocery Trips</b>	<b>VOT</b>	<b>Rec. Trips</b>	<b>VOT</b>
Group-1	\$20,000 - \$39,999	4	7.2	7	5.8	3	6.1
Group-2	\$40,000 - \$59,999	6	12.0	8	9.6	4	10.2
Group-3	\$60,000 - \$99,999	7	18.0	10	14.4	5	15.3

#### 4.4.4 Market: double auction mechanism

Carbon market plays an important role in the PMCA scheme. At the beginning of the game each player receives a fixed amount of money that can be spent to buy carbon credits. The players collectively participate in a market where they can buy or sell their carbon credits. The market takes the form of a double-auction where players can post bids (offers to buy) and asks (offers to sell).

Double auction mechanism ([116]) is commonly used in market experiments in context of experimental economics. Studies confirm that convergence using double auction mechanism occurs quickly in a variety of environments, even with very few traders in the market [118]. For a more detailed survey on the history of double auction experiments in economics see [119]. In a double auction market buyers post bids and sellers post asks, which are all listed publicly in order. Each time a player submits a bid or an ask, it will be added to a queue of offers, the most competitive (highest bids and lowest asks) will be shown to all players (figure 4.3). If a bid (or ask) is submitted that is higher (lower) than the lowest ask (highest bid) A transaction takes place when a buyer is willing to pay the price equal or more than the ask listed top in the ask table.

Remaining Time: 09:16

**Bid Table (Buyers)**

Bid-Price	Quantity
21	5
0	0
0	0
0	0
0	0
0	0
0	0
0	0
0	0
0	0
0	0

**Ask Table (Sellers)**

Ask-Price	Quantity
23	1
0	0
0	0
0	0
0	0
0	0
0	0
0	0
0	0
0	0
0	0

**Transactions log**

Price	Quantity
0	0
0	0
0	0
0	0
0	0
0	0
0	0
0	0
0	0
0	0

Bid Price:

Bid Quantity:

Bid

Sell Price:

Sell Quantity:

Sell

**Your Bids:**

Your bid (P)	Quantity
21	5
0	0
0	0
0	0
0	0

Price (B):

Quantity (B):

Cancel Bid

**Your Asks:**

Your Ask (P)	Quantity
23	1
0	0
0	0
0	0
0	0

Price (A):

Quantity (A):

Cancel Ask

Credits (Account):109

Available Credits (Sell):108

Money (Account):500

Available Money (BUY):395

Carbon Credits (Sold):0

Carbon Credits (Bought):0

Figure 4.3.: Market (double auction) segment of the game

The transaction takes place in units. A buyer does not have to buy all the units a seller offers with a particular ask. After the transaction the money and carbon credits balance are adjusted for the buyer and the seller. The transaction price is also shown to all users through the transaction table (figure 4.3). The duration of market segment depends on the state of the game. At early weeks when players are just participating in the market for first time we use a higher duration (e.g., 7 minutes) and later a smaller duration (e.g., 3 minutes) is used. All remaining carbon credits and money will carry over to the next session.

#### 4.5 Development of game

The game is developed using Python language. With compiled binaries and required dynamic libraries, one can run the game in machines running on Windows, Linux, and MacOS. The game application has two parts: client and sever. The players interact (travel choices and auction) in client part. The server part communicates (bi-directional) with all players. For example, each client sends the server information on bids and asks. The server processes the queues of bids and asks, and broadcasts the bid and ask tables to all the clients (i.e., the players). TCP-IP protocols are used to facilitate communication between the server and a client.

##### 4.5.1 Interface design

The interface is designed using PyQt4 and TKInter library. PyQt is commonly used to develop interface for cellphone, tablets, and general applications. PyQt4 allows to convert the code to a standalone application. We keep the development framework flexible so that the same module can be used for similar problems in the future.

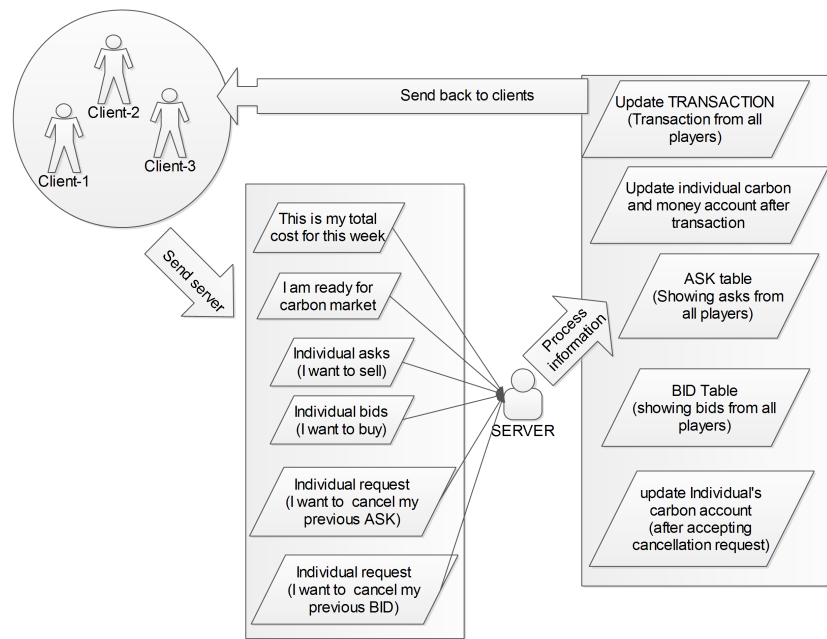


Figure 4.4.: Interaction between server and client modules

#### 4.5.2 Real-time interaction using TCP-IP

The communications between the server and the client(s) is facilitated using TCP-IP protocol. the SocketServer and Socket libraries are used. To allow for faster communication and least packet drop, we run the sessions in private LAN network. Figure 4.4 shows the interactions between the server and client(s).

#### 4.6 Data collection

The game participants were graduate students of Purdue University. A brief description of the personal mobility carbon allowance scheme is provided to all participants before starting the game. The rules of the auction are explained. Further, we conduct a demo session where each player learns how to make travel choices and



how to participate in the market. This is done to make sure that each player knows all the rules. Two types of incentives were provided to the players. First, lunch is provided for each session. Second, winner from each group is offered a 25\$ gift card.

The experiments were conducted on multiple days and each day has three or more sessions. A participant can attend one or more sessions. We have at least nine players for each session. This is important because the market would not have a realistic presentation with fewer participants. The highest number of players of a session was 15. Multiple sessions were conducted on five days. However, not all data are used for the model estimation. The data used from the sessions where players have already participated at least in two sessions prior to this session. This is to ensure that the players are familiar with rules and they possibly have learned how to manage carbon budget optimally.

#### 4.7 Methodology

Using the data obtained from the experiments, we estimate the parameters of the (dis)utility or generalized functions of travel cost accounting for heterogeneity across user groups in the system. Mixed logit (random parameter) models are used to estimate parameters of utility functions describing decision making process [90, 91, 92]. Each utility function is specific to a user group characterized based on income level, value of travel time, and number of trips made. Further characterization is made based on trip purpose (e.g., work vs. non-work trips), congestion level, and carbon credit allocation in the scheme. Denote,  $\Psi_{i,m}$  as the generalized (dis)utility function (or the generalized cost of travel) for an individual  $i$  choosing the travel alternative (combination of departure time and route)  $m$  in one of her trip making instances. For simplicity, we present the formulation for a specific trip purpose, congestion level, initial credit allocation and for a specific user group. Accordingly, the notations that characterize the user group, congestion level, and carbon credit allocation are omitted.

Now,  $X_{i,m}$  is the generalized vector for observed attributes specific to the alternative and the individual making the choice.

$$\Psi_{i,m} = \beta_m X_{i,m} + \zeta_{i,m} \quad (4.1)$$

$\beta_m$  is the vector of parameters to be estimated and  $\zeta_{i,m}$  is the error terms that are extreme value type-I distributed. For any travel decision instance we observe the following attributes:  $TT_m$ : the travel time associated with option  $m : \{r, t\}$ ,  $CC_m$ : the carbon cost in terms of units of credits associated with option  $m$ ,  $RB_i$ : remaining carbon credits for individual  $i$  prior to making decision,  $H_i$ : available money for individual  $i$  to purchase carbon credits from the market. Incorporating these attributes, the utility function can be written as:

$$\Psi_{i,m} = \beta_m^{TT} TT_m + \beta_m^{CC} CC_m + \beta_m^{RB} RB_i + \beta_m^H H_i + \zeta_{i,m} \quad (4.2)$$

Now a model with mixing distribution is defined for which we describe a density function  $f(\beta|\xi)$  with parameters  $\beta_m$ .  $\xi$  vector of parameters of the density function (mean and variance). The probability that individual  $i$  chooses option  $m$  is expressed as [92]:

$$\hat{P}_i(m) = \int_X \frac{\exp(\beta_m X_{i,m})}{\sum_m \exp(\beta_m X_{i,m})} f(\beta|\xi) d\beta \quad (4.3)$$

Since the players make decisions for similar trips for several weeks, we have repeated observations. The probability for  $K$  repeated observations for each individual is

$$P_i(m) = \int_X \prod_k \frac{\exp(\beta_m X_{i,m})}{\sum_{m \in M^k} \exp(\beta_m X_{i,m})} f(\beta|\xi) d\beta \quad (4.4)$$

Note that,  $M^k$  is the set that contains repeated observations. The probabilities  $P_i(m)$  are the weighted average of the standard probabilities where the density

function  $f(\beta|\xi)d\beta$  determines the weights. Different distributions such as uniform, triangular, weibull, log-normal or normal will be used to define the density function. Most commonly used are normal and log-normal distributions to define  $f(\beta|\xi)d\beta$ .

Now the log-likelihood function is:

$$LL = \sum_{i=1}^I \left( \sum_{m=1}^M \delta_{i,m} \ln[P_i(m)] \right) \quad (4.5)$$

Note that  $\delta_{i,m} = 1$ , when the choice outcome is  $m$  for individual  $i$ . The mixed logit probabilities  $P_i(m)$  are not straightforward to compute. Simulated likelihood functions are approximated by drawing the values from the density function and averaged to estimate the simulated probability [92, 93] This models provide us with the estimates for  $\beta_m^{TT}$ ,  $\beta_m^{CC}$ ,  $\beta_m^{RB}$  and  $\beta_m^H$  for each group specific to trip type, demand level, and initial credit allocation. The estimates from this behavioral model will be used to integrate with PMCA based dynamic traffic equilibrium model which is the focus of the next section.

#### 4.8 General observations

Experiments with different settings show some interesting findings of the PMCA scheme. We vary the number of players for each group for different sessions. With fewer players in the Group-1 (low travel demand) the number of credits available for buying went down in the market. Although the players from Group-3 offered very high price to buy credits, very few credits were available to purchase in the market. After investigating the data from multiple sessions we identified two reasons behind this to happen.

- (a) The players from the low income group are mostly selling the surplus credits. If there are too many high-income players and too few low-income players, the extra credits sold away too soon.
- (b) Even some low income players are not willing to sell. Since they always can make trips with reasonable travel time, not enough credits are available to sell.

Also, hoarding behavior was found among some players particularly in Group-3 characterized by moderate travel demand. The players were saving credits for future use so that they can make the trips with smaller travel cost.

Our experiments also reflect the learning behavior of participants over time. After examining the budget data for the players we find that the allocation of carbon budget improves over time. Most players have a better allocation of money and credits after the first session. Each session comprises five weeks of decision making (route and participation in the credit market).

#### 4.9 Incorporating market effects

The available carbon credits and disposable money are included in the cost function to incorporate the effect of carbon market into the travel decision making process. We assume the users participate in the market after each week. Within a week the unit price of credit does not change. Given a fixed unit price, the available carbon credit and the disposable money are more likely to influence the travel decisions. Disposable money refers to the amount of money a user can spend in the market to buy credits. Each group has a different disposable money allocation with the high income group having more. The market condition also impacts the available credits to spend to travel. The amount of credit depends on the transactions a user makes in terms of buying and selling. For instance, although started with same initial allocation a user can have significantly higher number of carbon credits based on her transactions in the market. Accordingly the travel decisions she will be making can be significantly different from a user from the same group. Accounting for these effects, we include available credits and disposable income as explanatory variables in our cost function specification. The estimation procedure will be discussed in details in section 4.10.

#### 4.10 Parameter estimates

The data from the experiment allows us to estimate models for different user groups specific to trip purpose. Nine distinct models are estimated for three user groups characterized by the income level and three trip purposes: work, grocery (non-work), and recreational trips. In our experiments users from all groups make similar types of trips in the same network. The trip length is identical, however the number of trips made weekly and the perceived cost as a function of VOTT is distinct for each user group. The next sections describes the estimation results.

#### 4.10.1 Work trips

Table 4.2 reports the estimation results for work trips. The signs of travel cost parameters can be explained intuitively. For work trips, users from all classes prefer lower travel cost in their travel choices. This parameter is found to have normal distribution for Group-1. Figure 4.5 shows an example regarding the interpretation that can be made for random parameters. Using the mean and standard deviation we see (figure 4.5-yellow region) that more than 92% of the area lies on the left of zero that indicates preference for lower travel cost in travel option.

Results show that, users from Group-2 and Group-3 on average are more likely to have less carbon credit cost in their travel options. For Group-1 the parameter for carbon cost is found to be normally distributed. Using the mean and standard deviation value we find that 65% of the sample has positive sign and the rest 35% have negative sign(prefer less carbon cost). Users from Group-1 have fewer trips to make compared with other groups. This may lead to results that a certain portion of the sample have positive sign for carbon cost parameter.

#### 4.10.2 Grocery(non-work) trips

Table 4.3 reports the estimation results for grocery (non-work) trips. For grocery trips, the estimated parameters for travel cost specific to Group-2 and Group-3 have different signs for different parts of the sample population. The distribution curves of

Table 4.2.: Estimates for work trips-all groups

Variable	Group-1		Group-2		Group-3	
	Estimate	<i>t</i> -stat	Estimate	<i>t</i> -stat	Estimate	<i>t</i> -stat
Constant-1	2.742	0.4	4.522	1.12	-4.805	-0.816
Constant-2	2.924	0.45	3.691	0.987	-3.584	-0.696
Constant-3	2.583	0.4	3.301	0.911	-2.307	-0.468
Constant-4	1.202	0.19	2.312	0.657	-1.329	-0.282
Travel cost	-0.031	-1.89	-0.0066	-2.24	-0.011	3.66
(S. D.)	(0.022)	(2.33)	-	-	-	-
Carbon cost	0.056	0.64	-0.113	-2.73	-0.057	-0.835
(S. D)	(0.144)	(3.26)	-	-	(0.166)	(2.59)
Credits relative						
to allocation	-3.34	-0.48	-0.031	-0.005	2.521	0.34
(S. D)	(2.92)	(1.6)	(3.754)	(1.89)	(7.75)	(2.4)
Money relative						
to allocation	-0.197	-1.51	-0.144	-0.225	1.02	1.03
(S. D)	(0.149)	(1.83)	(1.307)	(2.38)	(2.06)	(2.56)
Halton draws		800		800		800
LL(Restricted)		-177.04		-209.22		-180.26
LL(Convergence)		-65.44		-168.29		-154.41
McFadden $R^2$		0.63		0.196		0.16
Observations		110		130		112

the random parameters show that the areas on the left of zero are 20% and 27% for Group-2 and Group-3 respectively. These segments of the sample prefer less travel costs in their choices whereas for the rest of the sample the direction is opposite. The estimated parameter of carbon cost for Group-2 has a negative sign indicating that preference for lower carbon cost in the travel options. For Group-3 the carbon cost

Table 4.3.: Estimates for grocery trips-all groups

Variable	Group-1		Group-2		Group-3	
	Estimate	<i>t</i> -stat	Estimate	<i>t</i> -stat	Estimate	<i>t</i> -stat
Constant-1	-11.98	1.88	7.13	2.54	4.71	1.08
Constant-2	-9.89	-1.78	7.17	2.61	4.77	1.6
Constant-3	-7.09	-2.05	5.12	3.2	5.16	1.85
Constant-4	-3.67	-2.09	3.75	1.6	2.56	1.52
Travel cost	-0.024	-1.17	0.0009	0.305	0.005	1.43
(S. D)	(0.015)	(1.85)	(0.0011)	(1.55)	(0.008)	(2.83)
Carbon cost	0.46	2.39	-0.132	-1.89	-0.109	-0.98
(S. D)	-	-	-	-	(0.079)	(1.23)
Credits relative						
to allocation	3.466	0.514	-0.499	-0.23	-0.244	-0.091
(S. D)	(12.7)	(1.6)	(3.25)	(2.37)	(3.17)	(1.61)
Money relative						
to allocation	0.459	1.3	-1.633	-1.85	-0.733	-1.72
(S. D)	(0.471)	(1.44)	-	-	-	-
Halton draws		800		800		800
LL(Restricted)		-177.04		-209.23		-180.25
LL(Convergence)		-53.34		-168.23		-154.61
McFadden $R^2$		0.69		0.196		0.142
Observations		110		130		112

parameter is found to have a normal distribution with 92% of the area on the left side of zero indicating the users are more likely to have less carbon cost. The carbon cost parameter for Group-2 is fixed and has a negative sign.

These findings show a derived outcome of the travel decision behavior under PCA scheme. Due to carbon budget constraints the users are more likely to save carbon

credits on their non-work (e.g., grocery) trips. The trend is more prominent in higher income groups (Group-2 and Group-3) with higher travel demand. However due to the equal allocation feature, the users from Group-1 with low trip demand have sufficient carbon credits and the carbon saving trend is not found (positive sign of carbon cost parameter).

#### 4.10.3 Recreational trips

Table 4.4 reports the estimation results for recreational trips. The parameters for travel cost are found to be random with negative mean for Group-1 and Group-2. The distribution curves show that the splits in the sample 50.7-49.3%, and 50.2-49.8 % for Group-1 and Group-2 respectively. The parameters of carbon cost for Group-1 is found to be random with a split 99-1%. For group-2 this parameter is fixed with a negative sign. For Group-1 and Group-2, we conclude that carbon saving trend is dominant, however travel cost saving pattern is different for different segment of the sample as found in the distribution curve.

For Group-3 the travel cost parameter is random with 11-89% split and carbon cost parameter is fixed with a negative sign. With higher travel demand and limited budget it is intuitive that users from Group-3 are more likely to choose travel options that can save carbon credits.

The sign and distribution (if random) of an estimate tell us only the direction of impact on the cost function. The level of impact on the probability of making a particular travel decision cannot be assessed. A more effective way to explore the results is to estimate the elasticity values and then infer the change in probabilities when an explanatory variable changes from base case. The next section reports the elasticity values and discuss the impact of PMCA scheme on travel decision making.



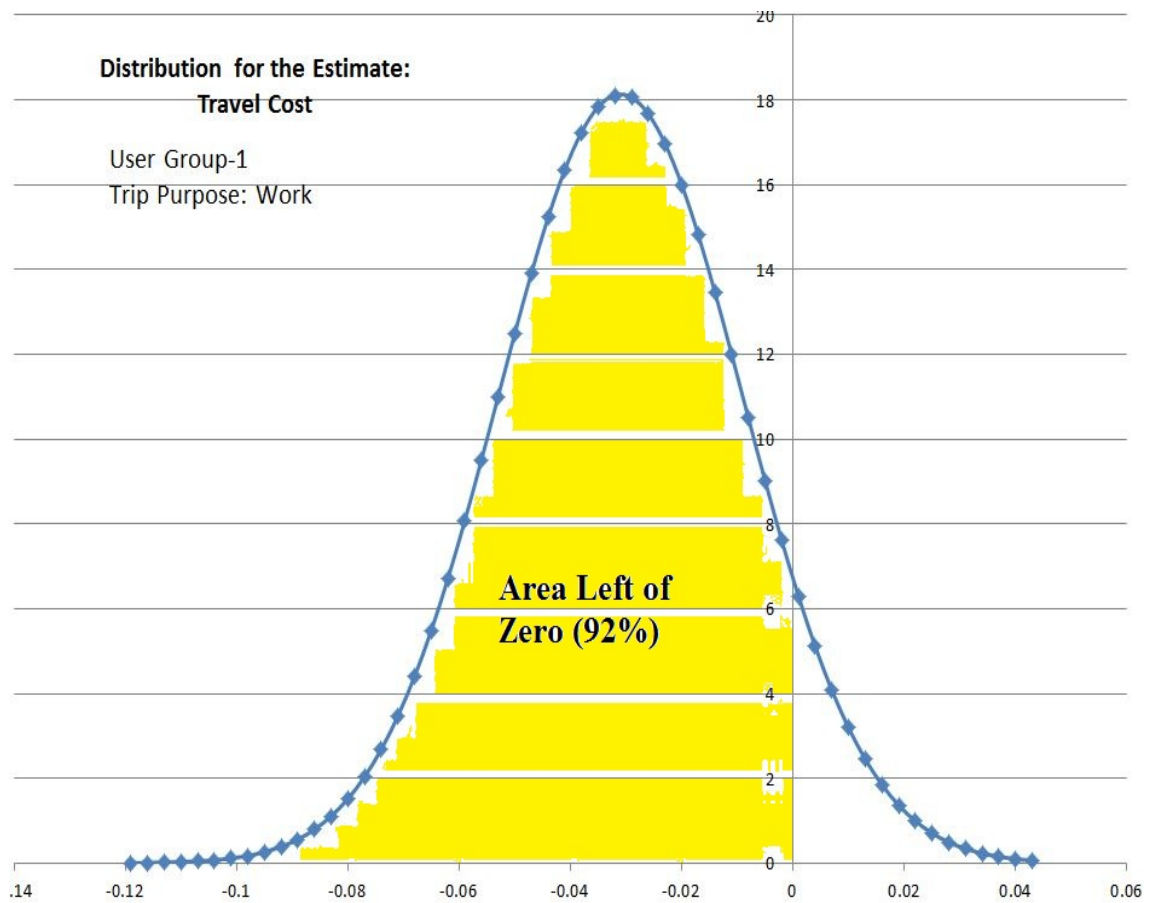


Figure 4.5.: Distribution of estimated parameters: Travel cost

Table 4.4.: Estimates for recreational trips-all groups

Variable	Group-1		Group-2		Group-3	
	Estimate	<i>t</i> -stat	Estimate	<i>t</i> -stat	Estimate	<i>t</i> -stat
Constant-1	28.29	1.73	3.93	1.16	11.33	1.64
Constant-2	21.35	1.1	3.67	1.54	8.63	1.67
Constant-3	17.62	1.02	1.09	0.611	6.44	1.88
Constant-4	-	-	0.896	0.76	5.12	1.93
Travel cost	-0.0006	-0.01	-0.0003	-0.046	0.016	2.01
(S. D)	(0.031)	(1.86)	(0.061)	(2.49)	(0.013)	(1.68)
Carbon cost	-0.18	-0.98	-0.162	-2.61	-0.173	-1.53
(S. D)	(0.062)	(1.64)	-	-	-	-
Credits relative						
to allocation	6.23	1.65	10.65	1.5	24.12	1.56
Money relative						
to allocation	-0.091	-0.96	1.198	1.61	6.084	1.03
(S. D)	(0.129)	(1.52)	-	-	(2.742)	(1.1)
Halton draws		200		800		800
LL(Restricted)		-76.246		-103.004		-90.13
LL(Convergence)		-30.348		-82.26		-51.35
McFadden $R^2$		0.601		0.20		0.43
Observations		55		64		56

#### 4.11 Effect of PMCA on travel decision

Elasticity values are well accepted way to infer the impact of explanatory variables on the dependent variable in choice models [92]. In our case, the dependent variable is the travel choice defined as a joint decision of departure time and route. The elasticity values help us to determine the effects of travel cost, carbon cost, available credits, and disposable money on travel decisions made by the users under PMCA

scheme. An elasticity measure of  $\kappa_j^x$  for a variable  $x$  on option  $j$  indicates that 1% change in variable  $x$  will change (increase or decrease based on sign) the probability of choosing option by  $\kappa_j^x\%$ . Elasticities are defined as  $\kappa_j^x = \frac{\partial P_j}{\partial x} \times \frac{x}{P_j}$ . Here  $P_j$  is the probability of choosing travel option  $j$  and  $x$  is the variable of interest. A value less than 1 implies the choice is inelastic to the changes in the variable in consideration.

Table 4.5 reports the elasticity values each group (see definition of each at section 5.1) specific to trip purpose. The values are computed based on the results in the tables 4.2, 4.3, and 4.4. The results are organized by groups and trip purposes. The elasticity values reported here are averaged over all observations. The next subsections discuss the results specific to trip purpose:

#### 4.11.1 Work trips

It is intuitive to find that group-3 (high VOTT and income) is the most sensitive to a change in the travel cost compared with other groups. With 1% increase in the travel cost the probability of choosing that travel option decreases by 4.8% for group-3. Further, we find group-1 (low VOTT and income) and group-3 are inelastic to change in carbon cost. This may be resulting from two facts: (i) group-1 users have fewer trips (but with equal carbon allocation) to make in the week compared with other groups and (ii) the highest VOTT for group-1 is also assigned for work trips. On the other hand, the VOTT of work trips for group-3 very high and it is more likely that carbon cost has less priority compared with travel cost.

The effects of available carbon credits and disposable money are significant for group-3. Elasticity values indicate that 1% increase in available carbon credits and disposable money increases the probability of choosing a particular travel option (with all other variables unchanged) by 2.23% and 2.76% respectively. Available money and credits are indirect measures of reliability and market effects. With a fixed travel choice, an individual with more money to spend in the carbon market has a higher likelihood to choose that option compared with another individual with

less money to spend in the market. Likewise, the effects of available carbon credits can be explained.

Table 4.5.: Direct elasticity measures

Variable	Average (Direct) Elasticity		
	Group-1	Group-2	Group-3
Work Trips			
Travel cost	-2.9	-3.02	-4.8
Carbon credits cost	-0.8	-2.5	-0.63
Available carbon credits relative to initial allocation	-1.15	0.13	2.23
Available disposable money relative to initial allocation	-0.46	0.11	2.76
Grocery Trips			
Travel cost	-0.98	0.52	1.14
Carbon credits cost	6.67	-2.96	-1.65
Available carbon credits relative to initial allocation	2.92	0.04	0.03
Available disposable money relative to initial allocation	3.91	-0.72	-1.13
Recreational Trips			
Travel cost	5.18	-0.79	3.66
Carbon credits cost	-6.56	-7.02	-6.03
Available carbon credits relative to initial allocation	1.38	0.29	-1.09
Available disposable money relative to initial allocation	0.009	0.53	2.57

#### 4.11.2 Grocery trips

It is interesting to see that a rise in travel cost increases the probability of choosing the travel option for group-3. This can be explained when we carefully examine the elasticity value specific to carbon cost for group-3. The elasticity value indicates that 1% increase in the carbon cost reduces the probability of choosing the travel option by 1.65%. Unlike the work trips, group-3 users are highly sensitive to carbon cost. Grocery trips are characterized with lower VOTT values and it is more likely that users would spend fewer carbon credits for grocery trips compared with work trips. As a result, group-3 users are more likely to choose travel options with less carbon cost and to have a lower priority for travel cost which is reflected by the elasticity value. Moreover, group-2 users are more sensitive to change in carbon cost compared with group-3 users. Although the initial carbon allocation is equal for all groups, the disposable money to spend in carbon market is less for group-2 users. Since the likelihood to buy more credits from market is low (less money compared with group-3), group-2 users are more sensitive to changes in carbon cost for grocery trips.

#### 4.11.3 Recreational trips

The elasticity values specific to carbon cost are much higher for recreational trips. This is valid for all groups. It is more likely that a travel option with high travel cost but low carbon cost is preferred by all groups in context of recreational trips. Moreover we observe that available money affects the choice significantly (an elasticity value of 2.57). Group-3 users are more sensitive to disposable money for recreational trips. For instance, an individual from group-3 may not be willing to choose a travel option that has high carbon cost. However the same individual having higher disposable money to buy credits from the market will have a higher probability (an increase by 2.57%) to choose the same travel option.

#### 4.12 Price convergence

This section investigates the convergence of unit price (carbon credit) in the double auction based market. Our experiment has four auction sessions and the average duration of the auction is 3.5 minutes. We allow longer duration in the earlier sessions (5-7 minutes) and smaller duration (3 minutes) in the ending sessions. Even though we have explained the rules of the market before the game session, it is more likely that participants would spend more time at earlier sessions to understand the mechanism and making bidding or asking decisions. On the other hand, during the end sessions the participants have already ideas about the price in the market and have experiences on ask or bid decision making. Therefore, the duration get smaller for the end sessions. This section reports three cases of the experimental sessions.

Figure 4.6 shows the patterns of changes in unit price for three cases as defined earlier. Each row in figure 4.6 illustrates a case. In case-1 (row 1 in figure 4.6) we have many participants from group-3 (higher travel demand, but equal allocation as group-1). As a result the demand for carbon credits is higher from the very beginning. However the supply is not high because group-1 participants are few. Session-1 exhibits low price to high price at the end of auction. Session-2 and session-3 start with a higher price. This is because the participants are aware of the market conditions at that point and asking price goes up for credits. The final session shows stable price for the last 7 intervals indicating convergence of price.

Case-2 (row 2 in figure 4.6) refers to a case where we have high number of group-1 users compared with group-2 and group-3. At the beginning session the price is stable at lower values. During session-2 we see a rise in the price. It is interesting to see the stable low price during the last two sessions. It indicates that supply is higher than demand in the market and the price goes down. Group-1 users are more likely to have spare carbon credits to sell in the market. With higher trip demand, high VOTT, and more disposable money to spend, group-3 users are more likely to buy credits from the market. Since case-2 has fewer group-3 users, it is possible that

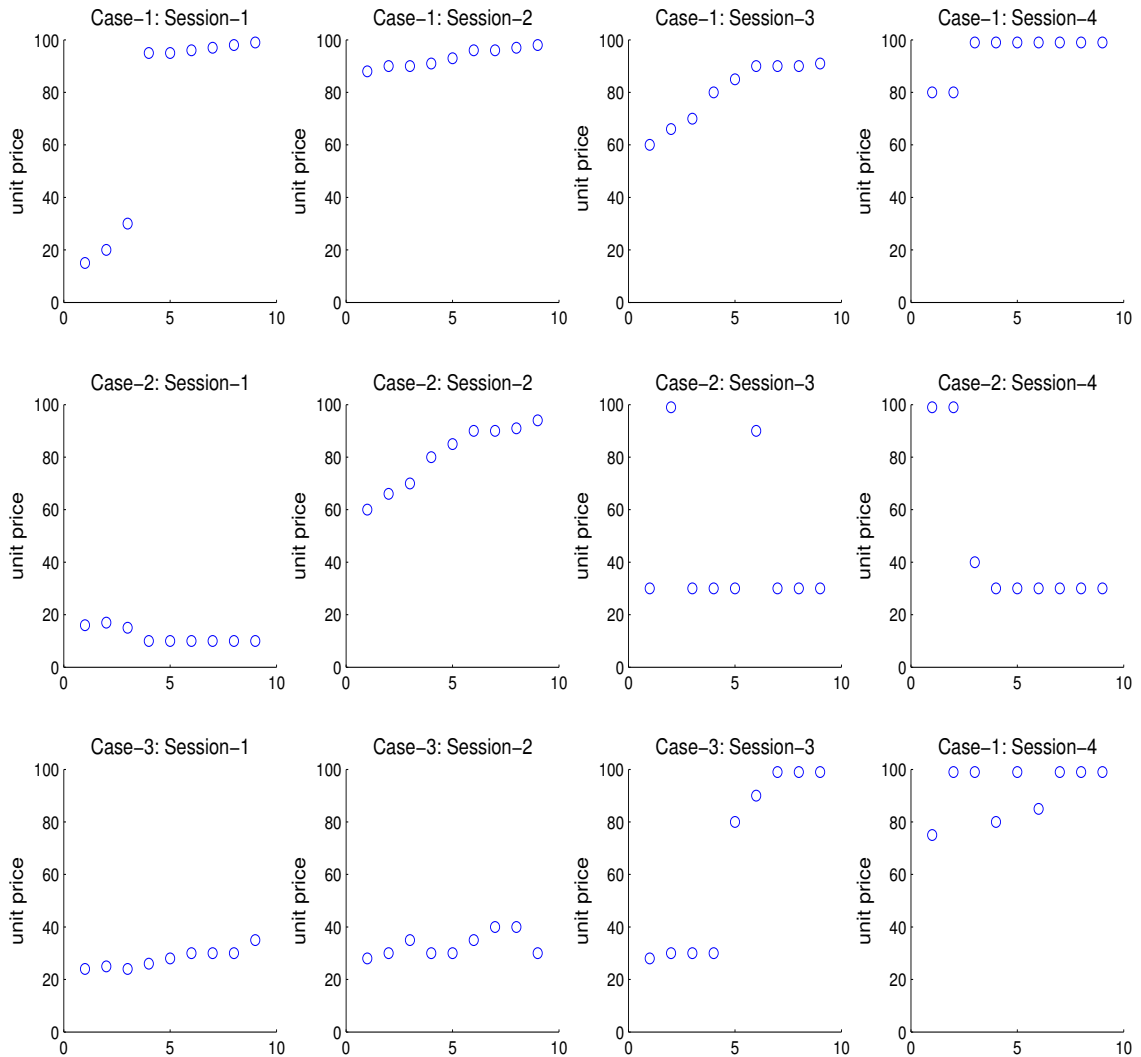


Figure 4.6.: Patterns of unit price in the market

market has many sellers but fewer buyers. Accordingly we see a pattern where the unit price goes down and stay stable for the session.

Case-3 (row 3 in figure 4.6) represents a more generalized case where we have equal share of group-1 and group-3 users. The first two sessions indicate low unit price and then in session-3 the price goes up. The high price remains stable during session-4. This pattern indicates the general response of the market as the number of available credits gets low. At the beginning with more credits available in the market the price

remains low. During the last sessions the demand for credits goes up, however the supply does not increase. Accordingly we see stable high price for carbon credits.

#### 4.13 Market: bids and asks

This section provides a framework to estimate the total number bids or asks a player would make in the auction session of the experimental game. Under PMCA scheme, each individual allocates the available carbon credits for personal travel. After each week all players participate in an auction for carbon credits where they can sell and buy credits. The trading actions in a particular session primarily include bid, ask, and the transaction. The total number of bids and asks for a player in the auction depends on various factors. The primary factors are mostly related to travel demand, market conditions, and value of travel time. To estimate the expected number of total bids and total asks by an individual in a particular session we approach with count data models. Since the total number of bids and asks are non-negative integers and can be considered as count data.

##### 4.13.1 Model description

Denote  $\lambda_j$  as the Poisson parameter for individual  $j$  that we define as the expected number of bids an individual  $j$  will place in an auction session. Poisson parameters  $\lambda_j$  is a function of a set of explanatory variables that include available carbon credits, available money to spend in the market, the current price of carbon credit, number of left trips, and so on. Assuming log-linear model the functional form can be expressed as:

$$\begin{aligned}\lambda_j &= \exp(\beta \mathbf{X}_j) \\ \Rightarrow LN(\lambda_j) &= \beta \mathbf{X}_j\end{aligned}$$



$X_j$  defines the set of explanatory variables for individual  $j$  and  $\beta$  are the vector of estimable parameters. According to the Poisson regression model, the probability  $P(u_j)$  of having  $u_j$  number of bids by a household  $j$  can be written as:

$$P(u_j) = \frac{\exp(\lambda_j)\lambda_j^{u_j}}{u_j!} \quad (4.6)$$

$\lambda_j$  is the expected number of bids by household  $j$  during an auction session with the relationship  $E(u_j) = \lambda_j = \exp(\beta\mathbf{X}_j)$ . Standard maximum likelihood methods can be used to find the parameters  $\beta$ . The likelihood function can be expressed as:

$$L(\beta) = \prod_j \frac{\exp(-\exp(\beta\mathbf{X}_j))(\exp(\beta\mathbf{X}_j))^{u_j}}{u_j!} \quad (4.7)$$

The log of this function is commonly used to estimate the parameters. A caveat with the Poisson model is the assumption that mean and variance are equal. A general approach to resolve this is to check the dispersion parameter for the data to be used for estimation. When the dispersion parameter is different from zero with statistical significance, one should use the negative binomial model instead.

#### 4.13.2 Zero-Inflated model for asks

Due to high frequency of zero asks in our data set, we test the data for the suitability of using zero-inflated model. The Vuong test statistic is found to be 2.62 ( $> 1.96$ ), and zero-inflated Poisson model will be appropriate for the asks. Zero-inflated Poisson model accounts for two distinct states: zero count state, and normal count state. A zero count state refers to a situation where the likelihood of an event is extremely rare. More details can be found in [92]. We estimated a Poisson model for the bids and a zero-inflated Poisson model for the asks using a set of data obtained from our experiments.

#### 4.13.3 Empirical results

We identified several variables as the contributing factors for asks and bids placed by the users. The variables include: the number of trips left, available carbon credits

relative to initial allocation, available money relative to initial allocation, price of unit carbon credit, and income level. Table 4.6 shows the results from the Poisson model for bids. The signs of the estimated parameters indicate the effect on the average number of bids placed by a player in the game. More available money increases the likelihood to place bids. Further, the income indicators have intuitive directions. Being a player from the low income groups reduces the average number of bids to be placed. Increase in price also lowers the average number of bids.

Table 4.6.: Results: Poisson model for bids

Variable	Estimate	<i>t</i> -stat.
Constant	1.737	4.01
Credit consumption level	0.011	2.32
Available money	$0.452 \times 10^{-4}$	3.32
Price of unit credit	-0.008	-5.07
Indicator- High income	0.162	1.04
Indicator-Low income	-0.966	-5.98
Number of trips left	0.0033	1.6
Log likelihood (restricted)		-357.48
Log likelihood (convergence)		-258.48
McFadden		0.28
Total observations		49

Table 4.7 shows the average elasticity values of the variables. We observe that being a player of the high-income group increases the mean number of bids by 1.826. Further, 1% increase in available money to spend in the market increases the mean number of bids by 0.0005. The increase in credit consumption level also has similar impacts. Higher consumption level is an indirect indicator of higher travel demand or suboptimal usage of carbon credits. Both can lead to buying more carbon credits.

Table 4.7.: Elasticity values: Bids model

Variable	Elasticity
Credit consumption level	0.127
Available money	0.0005
Price of unit credit	-0.0967
Indicator-High income	1.826
Indicator-Low income	-10.923
Number of trips left	0.0377

Table 4.8 reports the results from zero-inflated Poisson model for asks. Unlike the bids model we observe that being a player from low income group has a positive impact on the average number of asks. For a player from mid-income group the direction is opposite. Also higher credit consumption level leads to lower average number of asks to be placed. It is obvious that, with higher consumption the surplus credits will be fewer and accordingly the number of asks will be few.

Table 4.9 shows the elasticity values obtained from the zero-inflated Poisson model. The values indicate that 1% increase in credit consumption level decreases the mean number of asks by 0.0389. Also, belonging to mid-income group reduces the number of mean asks by 0.6015. On the contrary, being a player from low-income group increases the mean number of asks by 2.23.

#### 4.13.4 Correlation between asks and bids

The number of bids and asks placed by an individual can be correlated. For instance, an individual with high trip demand may place high number of bids and at the same time the number of asks will be few (if not zero). However the correlation value ( $R^2$ ) in our data set is 0.065 which is very small. We have a small sample and the experiment continues for only five weeks. With a larger sample, it may be possible

Table 4.8.: Results: Zero-inflated Poisson model for asks

Variable	Estimate	<i>t</i> -stat.
Constant	8.267	12.1
Credit consumption level	-0.047	-6.98
Available money	-0.0000504	-7.74
Price of unit credit	-0.0472	-6.98
Indicator- Mid income	-0.729	-2.51
Indicator-Low income	2.708	7.59
Number of trips left	0.0018	0.567
(Standard deviation)	-0.0115	-7.712
Log likelihood (restricted)		-949.0233
Log likelihood (convergence)		-92.899
McFadden		0.9
Total observations		49

Table 4.9.: Elasticity values: Asks model

Variable	Elasticity
Credit consumption level	-0.0389
Available money	-0.0365
Price of unit credit	-0.000042
Indicator- Mid income	-0.6015
Indicator-Low income	2.233
Number of trips left	0.00147

to have a high correlation. Different methodologies exist to account for correlation in count data models. Poisson log-Normal models and Copula-based models are two prominent directions that accounts for correlation and have been used by researchers.

MVPLN model is proposed by Chib and Winkelmann [120]. An MVPLN model accommodates both positive and negative correlations in the data. Studies [121, 122] show that MVPLN models provide better statistical fit and predictions compared with univariate Poisson and negative binomial models. Copula-based models are recently gaining attentions in economics and other areas including transportation science, behavior modeling, traffic safety analysis and so on. Copulas can be specified parametrically with joint distributions obtained from given marginals. The unobserved factors behind the decision to make asks and bids can be correlated and can be captured through a copula. Details can be found in [123, 124].

#### 4.14 Conclusions and future research

This research describes a market based strategy to reduce carbon consumptions originating from personal travel. The personal mobility carbon allowance scheme (PMCA) scheme is based on the conventional cap-and-trade system with a different scope. The successful implementation of the carbon allowance schemes [18, 68] requires a comprehensive understanding of the change in travel behavior in context of personal trip decision making. Further, it is challenging to obtain data for PMCA because there is still not real world implementation and a pilot study would be significantly expensive. Aiming at understanding the travel behavior we develop an experimental tool where the elements of PMCA can be designed and data can be obtained. Further, travel behavior patterns are analyzed by estimating cost functions specific to user groups and trip type and by estimating elasticities to determine the effect of travel option attributes and market conditions on travel choices.

The PMCA scheme is a novel market based strategy to reduce carbon consumptions originating from personal travel. This research contributes to literature in several ways. First, the developed game is a handy tool to collect data for cases that require interaction among users in real time. the developed game can collect data for cases that require interaction among users such as carbon tax schemes and trading systems. Without a market integration, analysis of the tradable schemes is incomplete.

Second, the sensitivity analysis using the estimates mode random parameter models provides insights on the effect of travel option attributes and market conditions on travel choices. The probability as a function of travel and demographic attributes can be used as behavior rules for agents in an agent-based traffic simulation.

Finally, the PMCA scheme can be extended to combine energy consumptions in household utility and personal travel. Instead of focusing on travel we can explore the general energy consumption behavior. The market component will be same. However more decisions have to be incorporated in the first segment of the experimental game developed here. The question of interest would the be evolving patterns of energy

consumptions as a result of interaction between travel and household energy related activities.

## CHAPTER 5. EQUILIBRIUM MODELS FOR PMCA

### 5.1 Introduction

The previous chapter outlines the PMCA scheme and developed an experimental game to collect data. Further the generalized cost functions are estimated with random parameter models. This chapter motivates the necessity of system level assessment when PMCA scheme is implemented. The cost functions can be incorporated in a network wide user equilibrium model to assess the travel time and emissions (carbon consumptions) for the network. The research goals are outlined in section 1.2.3 and section 2.3 describes relevant existing works.

This research offers novelty in several ways and addresses limitations of previous works. First, our focus is on the emissions and energy consumption in addition to travel time. Second, the generalized cost function explicitly considers the effect of PMCA and budgeting behavior of households. Third, the integrated framework combines the decision making process at household level and the impact on the system at network level in terms of congestion and emissions accounting for heterogeneity at originating from the dynamics of carbon trading. Finally, this is one of the first network equilibrium models capturing the impacts of carbon allowance scheme at household level.

### 5.2 Multi-class characterization

The primary heterogeneity originates due to income level, trip demand, and driving patterns. The value of travel time (VOTT) is often used an indirect measure for income level [49, 125, 126, 127]. Further, carbon consumption through fuels are directly influenced by the driving patterns of the users on the road. Generally, higher



fluctuation in the speed profile leads to higher emissions in traffic networks [16, 71]. Finally, emissions (accordingly the carbon consumption) from on-road vehicles depend on the congestion state of the network. The congestion state of a traffic network is highly dominated by the travel choices [6] by the users( e.g., route and departure time choice) of the network. The emissions in a highly congested network is significantly different from that of a non-congested network. Modeling the effect of congestion on carbon credit cost and its impact on route and departure time choice behavior is central in this research and we have a detailed discussion in the methodology section. Also, the travel decisions are impacted by trip purpose, length of the trip, and time-of-the-day.

The travel decision of an user also depends on the remaining carbon credits in her quota at that particular point of time. Additional carbon credits are added at the end of the week as per PMCA system. A traveler with higher credits (with a predefined budget for personal travel and household energy consumption) is more likely to have less sensitivity for the emissions (i.e., carbon credit spending) at the end of the week. Based on this attributes mentioned above we define each user class based on five attributes:(a) value of travel time (VOTT), (b) purpose of trip making (e.g., work vs. non-work), (c) available carbon credits prior to making the trip decision, (d) remaining money to spent in the carbon market to buy or sell credits, and (e) value of carbon credits relative to travel time cost.

### 5.3 Methodology

This section describes a multi-user based dynamic network equilibrium model under PMCA scheme. The DUE-PMCA model gives us the resulting path flow pattern specific to OD pairs and user groups in the network when PMCA scheme is in effect. The next few sections provide details on the key components of the model that include: the network loading model, travel time estimation, quantification of  $\text{CO}_2$

emissions to find carbon credit consumption, characterization of multi-user classes, and the dynamic user equilibrium conditions under PMCA.

### 5.3.1 Dynamic network loading

Our formulation embeds a spatial queue based traffic flow model, namely the cell transmission model (CTM), that computes the travel cost and carbon credit cost for the paths in the network. The cell transmission model is originally proposed by [128, 129]. However many variants of the model exist in the literature [130] and CTM is widely used as dynamic network loading models. This research follows the models by [131] and [132]. The key differences are as follows:

- (a) Generalized cost structure to capture PMCA attributes. Carbon credit cost is considered in addition to travel cost.
- (b) Heterogeneity in the population: value of time, value of carbon, and carbon credit market attributes such as unit price of carbon credit and credit availability. This leads to dynamic equilibrium model for multi-user groups.
- (c) DUE formulation with coupled carbon-cap constraint reflecting the target emissions reduction in the PMCA scheme.

### 5.3.2 Cell transmission model

The CTM divides each link of the network into finite number of homogeneous cells. Each cell has a length at least equal to the distance traveled in a single time interval at free flow speed. Also, the time horizon is finite and discretized into a number of intervals.

- (a) Notations and symbols:

*Indices:*

- $w$ : index of origin-destination pairs,  $w \in \mathbb{W} : \{1, \dots, W\}$ ;  
 $p$ : index of paths,  $p \in \mathbb{P} : \{1, \dots, P\}$ ;  
 $i, j, k$ : index of cells;  
 $t$ : index of discrete time intervals,  
 $m$ : index of user group,  $m \in \mathbb{M} : \{1, \dots, M\}$  .

*Parameters:*

- $\alpha_1^m$ : unit cost of travel time for user class  $m$ ;  
 $\alpha_2^m$ : unit cost of early arrival for user class  $m$ ;  
 $\alpha_3^m$ : unit cost of late arrival for user class  $m$ ;  
 where  $\alpha_2^m < \alpha_1^m < \alpha_3^m$ ;  
 $t^{*w}$ : preferred arrival time for O-D pair  $w$  (this is same for all user classes);  
 $\beta_T^m$ : Estimated parameter for travel time cost for class  $m$ ;  
 $\beta_C^m$ : Estimated parameter for carbon cost class  $m$ ;  
 $\beta_R^m$ : Estimated parameter for the effect of remaining carbon budget for class  $m$ ;  
 $\beta_H^m$ : Estimated parameter for the effect of available money for class  $m$ ;  
 $d^{w,m}$ : total demand from O-D pair  $w$  for class  $m$ ;  
 $\varsigma$ : infinitesimal flow to avoid zero denominator;  
 $t_e$ : maximum departure time (loading time);  
 $t_f$ : maximum time horizon (network clearance time);  
 $N^i$ : jam density of cell  $i$ ;  
 $Q^i$ : flow capacity out of cell  $i$ ;  
 $\delta$ : ratio of backward to forward shockwave propagation.

*Sets:*

- $C$ : set of cells;
- $C_O$ : set of ordinary cells;
- $C_R$ : set of source cells;
- $C_S$ : set of sink cells;
- $C_D$ : set of diverging cells;
- $C_M$ : set of merging cells;
- $E$ : set of links or cell-connectors;
- $E_O$ : set of ordinary links;
- $E_D$ : set of diverging links;
- $E_M$ : set of merging links;
- $\Gamma_i^{-1}$ : set of predecessors of cell  $i$ ;
- $\Gamma_i$ : set of successors of cell  $i$ ;
- $M$ : set of all user classes;
- $W$ : set of all O-D pairs;
- $P^w$ : set of paths for O-D pair  $w$ ;
- $P$ : set of all the paths,  $P = \cup_{w \in W} P^w$ ,
- $T_e$ : set of all departure time intervals,  $T \triangleq \{0, \dots, t_e\}$
- $T_f$ : set of all time intervals,  $T_f \triangleq \{0, \dots, t_f\}$ .

*Variables:*

- $x_{p,t}^{i,m}$ : cell occupancy of cell  $i$  at time  $t$  on path  $p \ni i$  for user class  $m$ ,
- $y_{p,t}^{i,j,m}$ : flow from cell  $i$  to cell  $j$  at time  $t$  for the flow on path  $p \ni (i, j)$
- $\bar{x}_t^i$ : aggregate cell occupancy of cell  $i$  at time  $t$ ,
- $\bar{y}_t^{i,j,m}$ : aggregate flow from cell  $i$  to  $j$  at time  $t$ ,
- $\tilde{x}_t^{i,j}$ : aggregate cell occupancy at diverging cell  $i$  at time  $t$  proceeding to cell  $j$ ,
- $r_{p,t}^m$ : departure rate at time  $t$  for the flow using path  $p$  for user class  $m$ ,
- $TT_{p,t}$ : travel time for the flow using path  $p$  at time  $t$ ,

An ordered pair of cells  $(i, j)$  represents a link and an ordered collection of links or an ordered collection of cells represents a path (similar to [132]). Also, a cell  $i \in p$

implies that path  $p$  must contain cell  $i$  and a link  $(i, j) \in p$  implies that path  $p$  must go through link  $(i, j)$ .

(b) Initialization:

At the beginning of the simulation ( $t = 0$ ), the cell occupancies are set to zero for all paths and for all user classes in the network.

$$x_{p,0}^{i,m} = 0, \quad \forall i \in C, p \in P, m \in M; \quad (5.1)$$

$$y_{p,0}^{i,j,m} = 0, \quad \forall (i, j) \in E, p \in P, m \in M. \quad (5.2)$$

Source cells ( $C_R$ ):

During network loading vehicles get into the source cells according to the demand pattern  $r_{p,t}^m$ . Based on the capacity (in and outflow rate), vehicles move to the next cell. For each path  $p \in P$  containing source cells  $i \in C_R$ , the occupancy updates can be expressed as:

$$x_{p,t}^{i,m} = r_{p,t-1}^m + x_{p,t-1}^{i,m} - y_{p,t-1}^{i,j,m}, \quad \forall j \in \Gamma_i, t = \{1, \dots, t_e + 1\}, m \in M, \quad (5.3)$$

$$x_{p,t}^{i,m} = x_{p,t-1}^{i,m} - y_{p,t-1}^{i,j,m}, \quad \forall j \in \Gamma_i, t = \{t_e + 2, \dots, t_f\}, m \in M. \quad (5.4)$$

Now, each O-D pair has unique demand values for each user class  $m \in M$  of the network. The cumulative departure rate should be equal to the total demand for a OD pair.

$$\sum_{p \in P^w} \sum_{t=0}^{t_e} r_{p,t}^m = d_w^m, \quad \forall w \in W, m \in M; \quad (5.5)$$

$$\sum_{m \in M} d_w^m = d_w, \quad \forall w \in W. \quad (5.6)$$

Ordinary cells ( $C_O$ ):

An Ordinary cell,  $i \in C_O$  has one incoming link and one outgoing link. The following equation updates the cell occupancy of an ordinary cell for a user class  $m \in M$ :

$$x_{p,t}^{i,m} = x_{p,t-1}^{i,m} + y_{p,t-1}^{k,i,m} - y_{p,t-1}^{i,j,m}, \quad \forall p \ni i, k \in \Gamma_i^{-1}, j \in \Gamma_i, t = \{1, \dots, t_f\}. \quad (5.7)$$

Also, if  $i$  not part of path  $p$ , then  $x_{p,t}^{i,m} = 0$ .

Diverging-merging cells ( $C_D$ ):

The occupancy of any diverging and merging cell,  $i \in C_D \cup C_M$  for a user class,  $m \in \mathbb{M}$  is updated as follows:

$$x_{p,t}^{i,m} = x_{p,t-1}^{i,m} + \sum_{k \in \Gamma_i^{-1}} y_{p,t-1}^{k,i,m} - \sum_{j \in \Gamma_i} y_{p,t-1}^{i,j,m}, \quad \forall p \ni k, i, j; k \in \Gamma_i^{-1}; j \in \Gamma_i; t = \{1, \dots, t_f\}. \quad (5.8)$$

Sink cells ( $C_S$ ):

A sink cell  $i \in C_S$  has limited in-flow capacity  $Q^s$ , however the storage capacity is unlimited ( $N^s \rightarrow \infty$ ). The cell occupancy  $x_{p,t}^{i,m}$  equals with the cumulative arrivals of path  $p$  in the period from 0 to  $t$  for user class  $m \in \mathbb{M}$ .

$$x_{p,t}^{i,m} = x_{p,t-1}^{i,m} + y_{p,t-1}^{k,i,m}, \quad \forall i \in C_S; p \ni i; k \in \Gamma_i^{-1}; t = \{1, \dots, t_f\}. \quad (5.9)$$

Ordinary links ( $E_O$ ):

At the aggregate flow level, we have:

$$\bar{y}_t^{i,j} = \min(\bar{x}_t^i, Q^i, Q^j, \delta(N^j - \bar{x}_t^j)) \quad \forall (i, j) \in E_O; t = \{1, \dots, t_f\} \quad (5.10)$$

At the disaggregate level, we use the proportion of path-based cell occupancy  $x_{p,t}^{i,m}$  and aggregate cell occupancy  $\bar{x}_t^i$  to determine the path flow  $y_{p,t}^{i,j,m}$

$$y_{p,t}^{i,j,m} = \min(\bar{x}_t^i, Q^i, Q^j, \delta(N^j - \bar{x}_t^j)) \times \frac{x_{p,t}^{i,m}}{\bar{x}_t^i + \varsigma} \quad \forall (i, j) \in E_O; p \ni i; j \in \Gamma_i; t = \{1, \dots, t_f\} \quad (5.11)$$

Here  $\varsigma > 0$  is an infinitesimal number used to make sure that the denominator is different from 0.

Diverging links ( $E_D$ ):

The updates are similar to Ukkusuri et al. [109] and aggregate occupancies are computed as follows:

$$\tilde{x}_t^{i,j} = \sum_{\forall p \ni (i,j), m \in M} x_{p,t}^{i,m} \quad \forall i \in C_D; j \in \Gamma_i; t = \{1, \dots, t_f\} \quad (5.12)$$

$$\bar{x}_t^i = \sum_{j \in \Gamma_i} \tilde{x}_t^{i,j} \quad \forall i \in C_D; t \in \{1, \dots, t_f\}, \quad (5.13)$$

For the diverging flows:

For all  $i \in C_D; j \in \Gamma_i; t = \{1, \dots, t_f\}$ ,

$$\bar{y}_t^{i,j} = \min(\tilde{x}_t^{i,j}, Q^j, \delta(N^j - \bar{x}_t^j)) \times \min \left( 1, \frac{Q^i}{\sum_{j' \in \Gamma_i} (\min(\tilde{x}_t^{i,j'}, Q^{j'}, \delta(N^{j'} - \bar{x}_t^{j'})))} + \mu \right) \quad (5.14)$$

Ukkusuri et al. [109] use the proportional rule to obtain the flow for each path from each O-D pair:

$$y_{p,t}^{i,j,m} = \bar{y}_t^{i,j} \times \frac{x_{p,t}^{i,m}}{\tilde{x}_t^{i,j} + \varsigma} \quad \forall i \in C_D; p \ni i; j \in \Gamma_i; t \in \{1, \dots, t_f\} \quad (5.15)$$

Merging links ( $E_D$ ):

The updating for merging links are computed by the following equations:

For all  $i \in C_M; k \in \Gamma_i^{-1}; t = \{1, \dots, t_f\}$ ,

$$\bar{y}_t^{k,i} = \min(Q^k, \bar{x}_t^k) \times \min \left( 1, \frac{\min(Q^i, \delta(N^i - \bar{x}_t^i))}{\sum_{k' \in \Gamma_i^{-1}} (\min(Q^{k'}, \bar{x}_t^{k'}))} + \varsigma \right). \quad (5.16)$$

The flow for each path of each O-D pair can be computed as:

$$y_{p,t}^{k,i,m} = \bar{y}_t^{k,i} \times \frac{x_{p,t}^{k,m}}{\bar{x}_t^k + \varsigma} \quad \forall i \in C_M; p \ni i; k \in \Gamma_i^{-1}; t \in \{1, \dots, t_f\} \quad (5.17)$$

### 5.3.3 Travel Time Estimation

Travel time computation is a critical element for both DUE formulation. Most of the previous works only compute the travel time without considering schedule delay [133, 134]. More recently, the notion of schedule delay is accounted for in the DUE and DSO framework [131, 132, 135]. Our proposed model requires the computation of average travel time. [136] and [131] provide details on computing average travel time within the path-based CTM model. For the completeness of our discussion we mention the equations from [132].

$$\nu_{p,t,t'} = \max \left( 0, \sum_{h=0}^t r_{p,h} - x_{p,t'}^s \right),$$

$$\forall p \in P; s \in p \cap C_S; t = \{0, \dots, t_e\}; t' = \{t, \dots, t_f\} \quad (5.18)$$

$$TT_{p,0} = \frac{\sum_{h=0}^{T_f-1} (\nu_{p,0,h} - \nu_{p,0,h+1})h}{r_{p,0} + \mu}, \forall p \in P \quad (5.19)$$

$$TT_{p,t} = \frac{\sum_{h=t}^{T_f-1} (\nu_{p,t,h} - \nu_{p,t,h+1} + \nu_{p,t-1,h+1} - \nu_{p,t-1,h})(h-t)}{r_{p,t} + \mu},$$

$$\forall p \in P; s \in p \cap C_S; t = 0, \dots, T. \quad (5.20)$$

Users from all classes experience the same travel time. Therefore, the average travel time computation is not specific for a class.

$$r_{p,h} = \sum_{m \in M} r_{p,t}^m, \quad (5.21)$$

$$x_{p,t'}^s = \sum_{m \in M} x_{p,t'}^{s,m}. \quad (5.22)$$



Now, the max operator can be replaced by the following complementarity conditions:

$$0 \leq \nu_{p,t,t'} \perp \nu_{p,t,t'} - \left( \sum_{h=0}^t r_{p,h} - x_{p,t'}^s \right) \geq 0$$

$$\forall p \in P; t = \{0, \dots, t_e\}; t' = \{t, \dots, t_f\}. \quad (5.23)$$

### 5.3.4 Carbon cost for the trip

The carbon credit cost to travel in a traffic network is inherently heterogeneous and depends on several attributes pertaining to the vehicle, the user (driver) behavior, traffic conditions, and atmospheric attributes such as humidity, wind speed, temperature profile. Previous researchers [16, 17] estimated the relationship between average trip speed and CO<sub>2</sub> emissions. The emissions on a link can be expressed as polynomials.

$$\psi_e = a_0 + a_1 * v_p + a_2 * (v_p)^2 + a_3 * (v_p)^3 + a_4 * (v_p)^4 + \dots \quad (5.24)$$

Where,  $a_j$ s are the coefficients,  $v_p$  is the average trip speed.  $\psi_e$  is the total CO<sub>2</sub> emissions for the trip. Relationships also exist for electric vehicles. Based on the data from Tesla Motors, the average CO<sub>2</sub> from EVs is about 12.6 g/km. [137] use the following equation to compute the energy requirement from EV:

$$EC_{EV} = 1.79*10^{-8}*(v)^4 - 4.073*10^{-6}*(v)^2 + 3.654*10^{-4}*(v)^2 - 4(v)^4 - 0.0109v + 0.2372$$

The steps to compute carbon cost for a path are as follows:

- *Step 1:* Compute the average travel time  $TT_{p,t}$  for the path with departure time  $t$
- *Step 2:* Estimate the average speed  $V_{p,t}$  using the trip length  $l_p$
- *Step 3:* Use the appropriate emissions estimation equation based on engine type

- *Step 4:* Convert the emissions into carbon credit using proper factor (in our case 100 g of CO<sub>2</sub> = 1 carbon credit)

The path level carbon cost can be computed as follows:

$$CC_{p,t} = \alpha_1 v_{p,t}^4 - \alpha_2 v_{p,t}^3 + \alpha_3 v_{p,t}^2 - \alpha_4 v_{p,t} + \alpha_5. \quad (5.25)$$

$\alpha_1, \alpha_2, \alpha_3, \alpha_4,$  and  $\alpha_5$  are input parameters that depend on type of engine, geographical location, and atmospheric attributes such as wind speed, temperature profile, *etc.*

$v_{p,t}$ : Average speed of the trip when a user departs at time  $t \in T_f$  on path  $p$ .

$$v_{p,t} = \frac{\sum_{i \in I_p} L_i}{TT_{p,t}} \quad (5.26)$$

$I_p$ : set of all cell index constituting path  $p$ ,

$L_i$ : Length of cell  $i$ . Next we describe the generalized cost function and its parameters for each user class.

### 5.3.5 Generalized cost function under PMCA

Consider an individual  $i \in \mathbb{I} : \{1, \dots, i, \dots, I\}$ , with total  $N$  trips (set of trips  $\mathbb{N} = \{1, \dots, n, \dots, N\}$ ). For any trip  $n \in \mathbb{N}$ , an individual chooses travel option  $\hat{k}$  from the set of all feasible travel options to make the trip defined as  $\mathbb{K} = \{1, \dots, \hat{k}, \dots, \hat{K}\}$ . Each travel option has two dimensions: path  $p$  and departure time  $t$ , and is associated with a cost in carbon credits  $CC_{\hat{k}}$  and a travel cost  $TC_{\hat{k}}$ . The generalized cost function is specific to a user group characterized based on income level, value of travel time, and number of trips made. Further characterization is made based on trip purpose (e.g., work vs. non-work trips), congestion level, and carbon credit allocation in the scheme. Denote,  $\Psi_{i,\hat{k}}$  as the generalized cost of travel for an individual  $i$  choosing the travel alternative (combination of departure time and path)  $\hat{k}$  in one of her trip making instances. For simplicity, we present the formulation for a specific trip purpose, congestion level, initial credit allocation and for a specific user group. The notations that characterize the user group, congestion level, and carbon credit allocation are omitted. For any travel decision instance we observe the following attributes:

$TC_{\hat{k}}$ : the travel time cost associated with option  $\hat{k}$ ,

$CC_{\hat{k}}$ : the carbon cost in terms of units of credits associated with option  $\hat{k}$ ,

$RB_i$ : remaining carbon credits for individual  $i$  prior to making decision,

$H_i$ : available money for individual  $i$  to purchase carbon credits from the market.

Incorporating these attributes, the generalized trip cost function, when travel option  $\hat{k}$  is chosen, can be written as:

$$\Psi_{i,\hat{k}} = \beta^{TC} TC_{\hat{k}} + \beta^{CC} CC_{\hat{k}} + \beta^{RB} RB_i + \beta^H H_i \quad (5.27)$$

With data on the travel decisions for all options  $\hat{k} \in K$  for all trips, the coefficients  $\beta_m^{TC}, \beta_m^{CC}, \beta_m^{RB}, \beta_m^H$  can be estimated for each group  $m \in M$ . To collect data we designed experiments and have estimated the coefficients using random parameter models (please see the previous chapter). The parameters are estimated specific to each user class and each trip type. The generalized cost  $GC_{p,t}^m$  when departing at time  $t \in T_e$  on path  $p \in P^w$  for OD pair  $w \in W$  by a user in group  $m \in M$  can be expressed as:

$$GC_{p,t}^m = \beta_m^{TC} TC_{p,t}^m + \beta_m^{CC} CC_{p,t} + \beta_m^{RB} RB_m + \beta_m^H H_m \quad (5.28)$$

Note that, each path is unique, therefore we do not use the OD index  $w$ . Also, the remaining carbon budget and money are only specific to the user class and independent of the current travel option  $(p, t)$ . Only travel cost is specific to a user class  $m \in M$  because the value of travel time and the penalties for early and late arrival at destination is different for each group.

### 5.3.6 Dynamic user equilibrium condition

The dynamic user equilibrium (DUE) condition for PMCA-DUE specific to a user class is defined as follows:

The generalized cost of each path between an O-D pair is equal and minimum at any departure time interval with non-zero departure rate for the paths.

In other words, at equilibrium there is no incentive for a user belonging to a particular class to switch path and departure time (i.e., travel option). While this definition of network equilibrium is similar to dynamic equilibrium problems in the literature [130, 132], a key difference is that the generalized cost in our case is a function of carbon credit consumption and the accommodation of user heterogeneity in formulation.

For each user class  $m \in M$  and OD pair  $w \in W$  in the network we have the following dynamic equilibrium condition:

$$\begin{aligned} 0 &\leq r_{p,t}^m \perp GC_{p,t}^m - GC_{p,t}^{g*} \geq 0, \\ \Rightarrow 0 &\leq r_{p,t}^m \perp \beta_m^{TC} TC_{p,t}^m + \beta_m^{CC} CC_{p,t} + \beta_m^{RB} RB_i + \beta_m^H H_i - GC_{p,t}^{m*} \geq 0 \end{aligned} \quad (5.29)$$

The travel cost  $TC_{p,t}^m$  is computed as follows:

$$TC_{p,t}^m = \alpha_1^m TT_{p,t} + \alpha_2^m e_{p,t} + \alpha_3^m l_{p,t} \quad (5.30)$$

### 5.3.7 Demand satisfaction constraints

At equilibrium the departure rate for all paths must accumulate to the demand for the O-D pair.

$$0 \leq GC_{p,t}^{m*} \perp \sum_{p \in P_w} \sum_{t=0}^{t_e} r_{p,t}^m - d_w^m \geq 0, \quad \forall w \in W, m \in M \quad (5.31)$$

This constraint is similar to [109, 138] with the addition of user class level constraint.

At equilibrium we have,

$$\sum_{p \in P_w} \sum_{t=0}^{t_e} r_{p,t}^m - d_w^m = 0, \quad \forall w \in W, m \in M \quad (5.32)$$

The equations that compute  $e_{p,t}$  and  $l_{p,t}$  can be transformed into equivalent complementarity conditions (see [138]).

### 5.3.8 Dynamic user equilibrium (DUE-PMCA)

PMCA scheme is continuous in nature. With a choice of interval for the auction it can continue for years. The model presented here assumes a weekly auction format. A user only participates in the auction after a week. The price changes after each week, however the remaining carbon credits and money continue to change as users make travel decisions during the week. The model divides the time horizon into multiple segments. This segmentation helps to run the model efficiently compared with a single analysis with a very long time horizon (e.g., entire day or week). We refer to such segment as a DUE-episode. For instance, the morning peak hour (6 am to 9 am) is a DUE-episode. DUE-PMCA formulates the model with multiple DUE-episodes as required by the time horizon. For instance, a typical week day can have several DUE-episodes covering all travel activities from the 4 am to 12 midnight. Each DUE-episode is distinct in terms of demand and purpose of the trips. For instance, a DUE-episode for 12 noon-2 pm will have higher grocery trips.

Define a finite time horizon  $\{1, 2, \dots, \pi, \dots, \Pi\}$  and a set of DUE-episodes for the horizon  $\{E_1, E_2, \dots, E_\pi, \dots, E_\Pi\}$ . Each episode  $E_{pi}$  follows the conditions as described by the equations 5.29 and 5.31. Now we introduce a necessary constraint for the DUE-PMCA model that reflects the carbon consumption cap for the system. PMCA schemes are designed to meet targets such as reducing the carbon consumption by 5% from the base case. To meet this requirement, carbon credits equivalent to 95% of the base case are distributed among the users. Therefore the model needs to ensure that the total carbon consumption for all episodes should not exceed 95 % of the base consumption.

$$\sum_{E_\pi: \pi \in \{1, \dots, \Pi\}} \sum_{t \in T_f} \sum_{m \in M} \sum_{w \in W} \sum_{p \in P^w} CC_{p,t}^m * r_{p,t}^m \leq \Theta \quad (5.33)$$

In equation 5.33,  $\Theta$  defines the desired threshold for carbon consumption. Equation 5.33 is a coupling constraint for all the DUE-episodes in considered in the model. Now the entire model can be presented as follows:

For each episode  $E_\pi$ :

**A1.** DUE Condition:

$$0 \leq r_{p,t}^m \perp \beta_m^{TC} TC_{p,t}^m + \beta_m^{CC} CC_{p,t} + \beta_m^{RB} RB_i + \beta_m^H H_i - GC_{p,t}^{m*} \geq 0$$

**A2.** Demand satisfaction:

$$0 \leq GC_{p,t}^{m*} \perp \sum_{p \in P_w} \sum_{t=0}^{t_e} r_{p,t}^m - d_w^m \geq 0, \quad \forall w \in W, m \in M$$

**A3.** Travel time computation (equation 5.20)

**A4.** Carbon cost computation (equation 5.25)

**A5.** Non-negativity constraints

Coupling constraint:

**B.** carbon cap:

$$\begin{aligned} \sum_{E_\pi: \pi \in \{1, \dots, \Pi\}} \sum_{t \in T_f} \sum_{m \in M} \sum_{w \in W} \sum_{p \in P^w} CC_{p,t}^m * r_{p,t}^m &\leq \Theta \\ \Rightarrow \sum_{\pi=1}^{\Pi} \theta_\pi &\leq \Theta \end{aligned}$$

$\theta_\pi$ : Total carbon consumption for an episode  $\pi$ .

### 5.3.9 Equivalent VI

For each DUE episode we can write the complementarity formulation in a compact format:

$$0 \leq r_{p,t}^m \perp GC_{p,t}^m - GC_{p,t}^{m*} \geq 0 \quad \forall p \in P^w, w \in W, t \in T_e. \quad (5.34)$$

The demand satisfaction and non-negativity constraints can be represented as follows:

$$\Omega \triangleq \left\{ \sum_{p \in P_w} \sum_{t=0}^{t_e} r_{p,t}^m - d_w^m = 0, \mathbf{r} \geq 0 \quad \forall w \in W, m \in M \right\} \quad (5.35)$$

Now define the  $\theta$  as the total carbon consumption for the episode and it should be non-negative. The equivalent VI formulation for a single DUE-episode will be:

$$\mathbf{GC}^T(\mathbf{r} - \mathbf{r}^*) \geq 0, \quad \mathbf{r}^* \in \Omega \quad (5.36)$$

$$0^T(\theta - \theta^*) \geq 0, \quad \theta^* \in \mathbb{R}_+ \quad (5.37)$$

Now for a PMCA-DUE problem with  $\Pi$  DUE-episodes we can have:

$$\begin{aligned}
\mathbf{GC}_1^T(\mathbf{r}_1 - \mathbf{r}_1^*) &\geq 0, & \mathbf{r}_1^* &\in \Omega_1, \\
0^T(\theta_1 - \theta_1^*) &\geq 0, & \theta_1^* &\in \mathbb{R}_+, \\
\mathbf{GC}_2^T(\mathbf{r}_2 - \mathbf{r}_2^*) &\geq 0, & \mathbf{r}_2^* &\in \Omega_2, \\
0^T(\theta_2 - \theta_2^*) &\geq 0, & \theta_2^* &\in \mathbb{R}_+, \\
&\dots\dots\dots \\
&\dots\dots\dots \\
\mathbf{GC}_\pi^T(\mathbf{r}_\pi - \mathbf{r}_\pi^*) &\geq 0, & \mathbf{r}_\pi^* &\in \Omega_\pi, \\
0^T(\theta_\pi - \theta_\pi^*) &\geq 0, & \theta_\pi^* &\in \mathbb{R}_+, \\
&\dots\dots\dots \\
&\dots\dots\dots \\
\mathbf{GC}_\Pi^T(\mathbf{r}_\Pi - \mathbf{r}_\Pi^*) &\geq 0, & \mathbf{r}_\Pi^* &\in \Omega_\Pi, \\
0^T(\theta_\Pi - \theta_\Pi^*) &\geq 0, & \theta_\Pi^* &\in \mathbb{R}_+, \\
\sum_{\pi=1}^{\Pi} \theta_\pi &\leq \Theta.
\end{aligned}$$

Now we denote,

$$\Omega_\theta \triangleq \left\{ \sum_{\pi=1}^{\Pi} \theta_\pi \leq \Theta \right\} \quad (5.38)$$

Also define,  $Y = [\mathbf{r}_1, \theta_1, \mathbf{r}_2, \theta_2, \dots, \mathbf{r}_\pi, \theta_\pi, \dots, \mathbf{r}_\Pi, \theta_\Pi]^T$ ;

$\mathbf{C} = [\mathbf{GC}_1, 0, \mathbf{GC}_2, 0, \dots, \mathbf{GC}_\pi, 0, \dots, \mathbf{GC}_\Pi, 0]^T$  and

$\Omega : \{\Omega'_1 \times \Omega'_2 \times \dots \times \Omega'_\pi \times \dots \times \Omega'_\Pi \times \Omega_\theta\}$ . Now the system of VIs can be represented in a compact format.

$$\mathbf{C}^T(\mathbf{Y} - \mathbf{Y}^*) \geq 0, \quad \mathbf{Y}^* \in \Omega \quad (5.39)$$

The solution of the  $VI(\mathbf{C}, \Omega)$  will be the solution of formulation **AB**

#### 5.4 Solution approach

This section describes the solution approaches to solve the DUE-PMCA problem. In the previous section, we have shown that the original problem can be transformed into a variational inequality (VI) problem. This section proposes solution methods for the equivalent VI problem. Challenges associated with the solution technique mostly arise with the nature of the cost function that is non-differentiable, non-convex, and non-monotone. The reason is that we obtain the cost function from the CTM simulation. Commonly used commercial solvers such as KNITRO and PATH are not able to solve this problem for reasonable sized networks. Addressing this issue, this research approaches with derivative-free algorithms, namely the projection algorithm, to solve the equivalent VI problem.

We propose two approaches to solve the problem. The first approach is to use the basic projection algorithm to solve the VI problem with coupling constraints of carbon cap. The second approach is to decompose the original VI problem and solve a series of smaller VI problems where the carbon cap constraints are associated with each individual DUE-episode.

#### 5.4.1 Basic projection method

To solve a  $VI(F, K)$  we compute a sequence of points  $\{u^i\}_{i=1}^{\infty}$  starting with an initial solution  $x^0$ .

$$u^{i+1} = \Lambda_K[u^i - F(u^i)], \quad \forall i = 1, 2, \dots, \infty \quad (5.40)$$

$\Lambda_K(u)$  denotes the the projection of  $u$  on the feasible region  $K$ . In other words, one defines the projection:

$$\varpi = \arg \min \|z - u\|^2 \quad (5.41)$$

The convergence of the solution requires that  $F$  should be monotone. In our case, the cost function does not have this property and direct convergence cannot be shown. However the feasible region that has only systems of linear equations and inequalities is compact. With this compact feasible region it is possible to show sub sequential



convergence when the VI problem is solved using projection method. [132] has the proof for the case without carbon cap constraint. Since carbon cap constraints are linear in nature and the properties of the feasible region remain the same, the same proof applies for our case.

**Algorithm steps:**

*Data:* Initialize with a feasible  $\mathbf{Y}^0 \in \Omega$

*Step 0:* Set  $i = 0$ .

*Step 1:* Computation:  $CTM(\mathbf{Y}), \mathbf{C}, \mathbf{Y}$

*Step 2:* Find the projection:  $\mathbf{Z}^* = \arg \min_{z \in \Omega} [Z - (\mathbf{Y}^i - \lambda \mathbf{C}(\mathbf{Y}^i))]$ .

*Step 3:* If  $\|\mathbf{Z}^* - \mathbf{Y}^i\| < \xi$ , Terminate. Else,  $\mathbf{Y}^{i+1} = \mathbf{Z}^*$  and Go to Step 1.

Our experience with the basic projection algorithm shows that the algorithm is not efficient to solve large networks and do not meet the error tolerance criterion at most cases. To resolve the issue we propose a decomposed approach where each DUE-episode is solved separately with its distinct carbon cap constraint. The next sections describes the algorithm.

#### 5.4.2 Algorithm to solve decomposed VI

Instead of a coupling constraint for all the DUE-episodes in an analysis we can distribute the carbon caps among the DUE-episodes. This implies that each DUE-episode can be solved separately with its own carbon cap constraints. Further, we assign the carbon caps specific to each user class and each OD pair. A useful property of our problem is that its feasible region  $\Omega$  can be expressed as a Cartesian product of a set of closed and convex linear constraints: demand satisfactory and carbon cap conditions. This naturally leads to a decomposition optimization scheme to solve this problem. The algorithm proposed by [139] decomposes the original VI problem coupled variation inequalities of lower dimensions, with each defined for a user group and origin-destination pair. The algorithm ensures the mapping finds a convergent sequence and it can be proved that such a fixed point is a solution for sub-VI problem.

If we find a set of solutions for all sub-VI problems simultaneously, it can be shown that the combined solution is a solution of the original VI problem.

Algorithm steps ([139]):

*Step 0:* Set counter  $k=0$ . Initialize a feasible departure rate.

*Step 1:* Run the simulation  $CTM(\gamma^k)$  and compute  $TC(\gamma^k), CC(\gamma^k), GC(\gamma^k)$ .

*Step 2:* Decompose  $\gamma^k = (\gamma_1^k, \gamma_2^k, \dots, \gamma_m^k)^T$ .

*Step 3:* Find the  $\lambda^k(\gamma^k)$  that ensures most number of user classes and OD pairs satisfy:  $\|T_i(\gamma_i^k) - T_i(\gamma_i^{k-1})\| \leq \alpha \|\gamma_i^k - \gamma_i^{k-1}\|$ , in which  $T_i(\gamma_i^k) = Pr_{\Omega_i}[\gamma_i^k - \lambda^k(\gamma^k)GC_i(\gamma^k)]$

*Step 4:* Update departure rate  $\gamma_i^k$  using mapping  $T_i$  only for those user classes and OD pairs that satisfy the condition in Step 3. For others that not satisfied, set  $\gamma_j^k = \gamma_j^{k-1}$ .

*Step 5:* If none of the user classes and OD pairs are found satisfy condition in Step 3, set  $\gamma_j^k = \gamma_j^{k-1}, \lambda^k(\gamma^k) = \lambda^{k-1}(\gamma^{k-1})/2$ .

*Step 6:* If  $\|z^* - \gamma^k\| \leq \epsilon$ , terminate the algorithm,  $\gamma^* = z^*$ . Otherwise  $\gamma^{k+1} = \gamma^k$ , Set  $k = k + 1$ , go to step 1.

## 5.5 Numerical example

We solved the PMCA-DUE model with two test networks.

- (a) X-shape network (similar to that used in [109]) with four O-D pairs and three user classes. The network has ten cells and the equilibrium is based on departure time choice only.
- (b) Sioux-Falls network with six O-D pairs and five user classes. The network has 114 cells and 142 links. There are two O-D pairs with three paths, two O-D pairs with two paths, and two O-D pairs with a single path.

Each link in the network is divided into multiple cells. The time step for the simulation is set such that no vehicle can move more than one cell in a single time step. We choose the time step as 60 seconds. With free flow speed 30 miles/hour the maximum length of a cell is 0.5 miles or 0.8 kilometers. Assuming saturation flow as 1800 vehicles per hour per lane the maximum flow rate for a cell is 30 vehicles per time step per lane. At saturated condition the bumper-to-bumper distance is about 10 meter. Therefore, the jam density is  $(0.8 \times 1000) / 10$  or 80 for the cells in the network. Other than source and sink cells we use these parameters for all cells in the network. The ratio to forward to backward shockwave propagation is 0.8 in the analysis. The convergence criterion is the norm of difference between two consecutive solutions. All results in this research are obtained by setting the convergence criterion as 0.05. The optimal value of parameter step size in projection algorithm that produces the best results is different for different problems. We observe that the value is less than 1 in all cases and ranges between 0.1 and 0.625 in our tests.

### 5.5.1 Input parameters

To quantify the carbon cost we extracted a relationship between average path speed and GHG emissions rate (g of CO<sub>2</sub> per mile) using the county level database from EPA-MOVES. We tested our algorithm on Sioux-Falls network which is closer

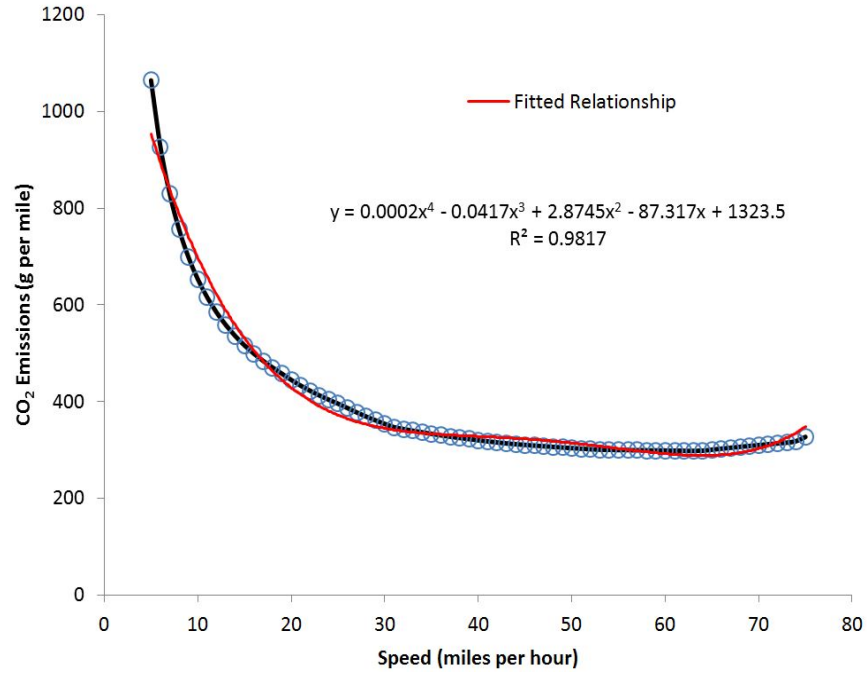


Figure 5.1.: Fitted relationship between speed and emissions rate

in terms of traffic and atmospheric conditions of Minnehaha county of South Dakota in the U.S. EPA-MOVES provides access to county level data that include fuel type and formulation, vehicle age distribution, temperature profile, humidity, and fuel type distribution. With link geometry attributes identical to the Sioux-Falls network, we estimate GHG emissions for different speed levels. A fourth-order polynomial fits the data points and represents the relationship between average path (trip) speed and GHG emissions. The fitted relationship is similar to the empirical relationship obtained in the study by [16]. [137] followed similar approaches to extract functional relationship from EPA-MOVES. The fitted function is as follows:

$$\psi_e = 0.0002v^4 - 0.0417v^3 + 2.8745v^2 - 87.317v + 1323.5. \quad (5.42)$$

Here,  $\psi_e$  = Emissions rate g/mile and  $v$  = Average speed in miles/hour. We used this equation for both X-shape and the Sioux-Falls network.

### 5.5.2 Trip demand and value of time

We consider three income classes with three types of trips for our tests. Number of trips for user groups representing different income levels are obtained from the 2009 National Household Travel Survey data and are listed in table 5.1. To account for the heterogeneity in travel cost for each income class we use the value of travel time (VOTT) for trips specific to purpose. The VOTT values are obtained from the guidelines provided by FHWA [117]. For the ease of conducting experiments, the number of total trips are proportioned with the same relative difference among the groups.

Table 5.1.: User group definition

User Group	Income Range	Work Trips	VOTT Work	Grocery Trips	VOTT Shopping	Rec. Trips	VOTT Rec.
Group-1	\$20,000 - \$39,999	4	7.2	7	5.8	3	6.1
Group-2	\$40,000 - \$59,999	6	12.0	8	9.6	4	10.2
Group-3	\$60,000 - \$99,999	7	18.0	10	14.4	5	15.3

### 5.5.3 Parameters for cost function

Table 5.2 shows the parameters used for cost function. The parameters correspond to: travel cost, carbon cost, effect of remaining carbon credits relative to initial allocation at the point of decision making, and available money to spend in the carbon market relative to initial money.

### 5.5.4 X-network

The X-shape network, originally used in [109], is a small network with diverge and merge cells (figure 5.2). It allows to test the equilibrium with departure time choice. We define a scenario with three DUE episodes characterized by distinct trip

Table 5.2.: Parameters for generalized cost function.

User	$\beta_{TC}$	$\beta_{CC}$	$\beta_{RB}$	$\beta_{HH}$
Class-1	0.031	0.056	-0.42	-0.048
Class-2	0.0066	0.113	3.72	1.163
Class-3	0.011	0.057	2.75	-1.63
Class-4	0.024	0.46	5.23	1.04
Class-5	0.03	0.109	1.52	-1.72

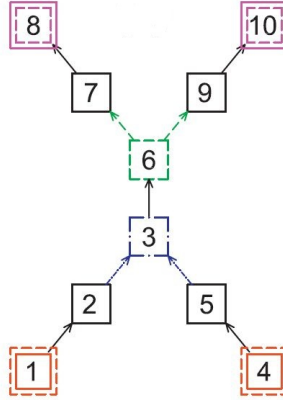


Figure 5.2.: Cell representation of X-Shaped Network [109]

demand for each user class. The carbon cap constraint requires a threshold value for the PMCA-DUE problem as a whole (i.e., coupled with all DUE-episodes). First, we solve three DUE problems without carbon cap constraints separately and compute the carbon consumption. Then we set a 2% reduction goal for the PMCA-DUE and define the constraint such that the total carbon consumption for all three DUE-episodes cannot exceed 98% of the base case. We solve the network following both approaches described earlier in sections 5.4.1 and 5.4.2. Results from two solution approaches are compared to verify whether significant difference exists between the solution approaches.

The figures 5.3, 5.4, 5.5 show the results obtained from basic projection algorithm 5.4.1. The departure rate vs. generalized cost plots show that highest departure rate occurs at lowest cost. This trend is valid for all user classes and O-D pairs. Next, the figures 5.6, 5.7, 5.8 show the results obtained from decomposed VI projection algorithm 5.4.2. No significant differences are found in the cost vs. departure rate plots compared with those obtained from the basic projection algorithm with coupled constraints.

Table 5.3 summarizes the results. The base case represents the problem without any carbon cap, basic refers to the solution obtained by basic projection algorithm

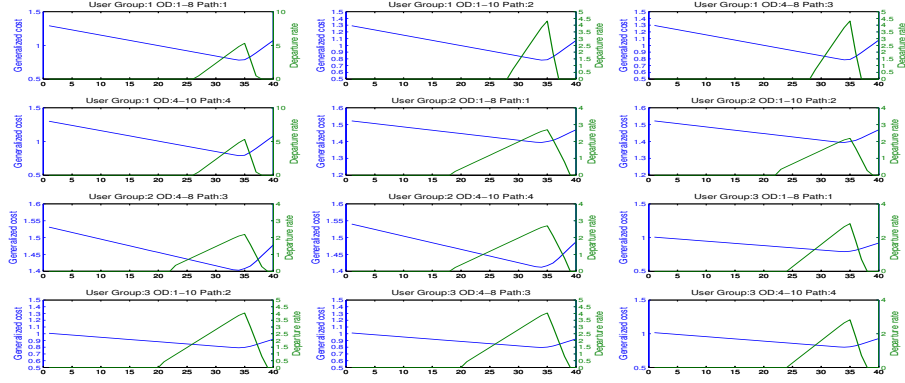


Figure 5.3.: Results for DUE-1: Coupled constraint problem

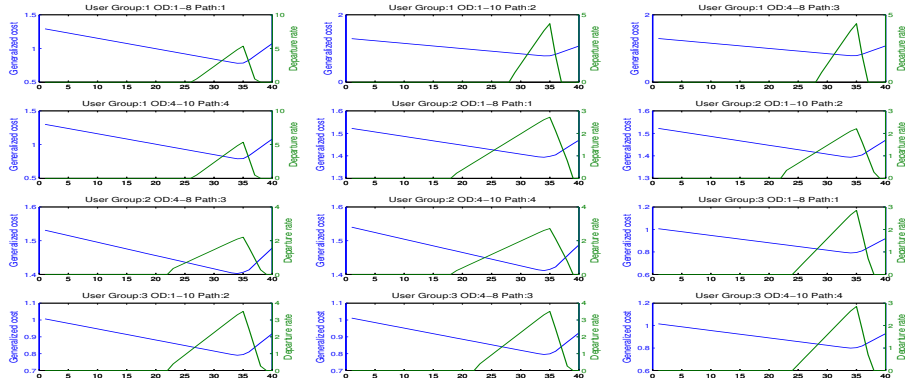


Figure 5.4.: Results for DUE-2: Coupled constraint problem

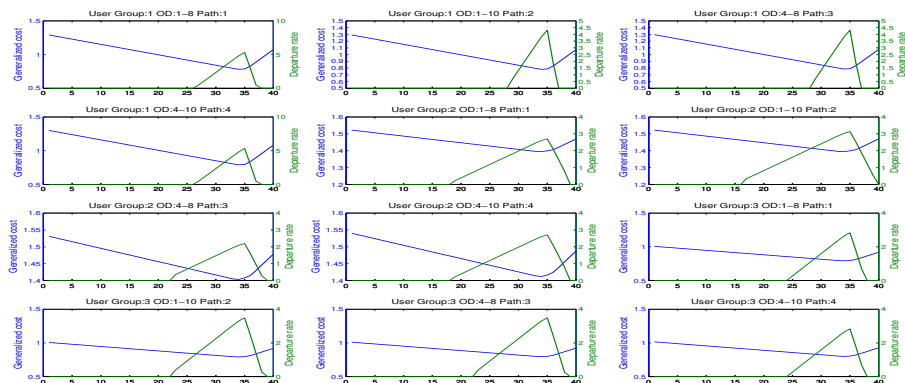


Figure 5.5.: Results for DUE-3: Coupled constraint problem



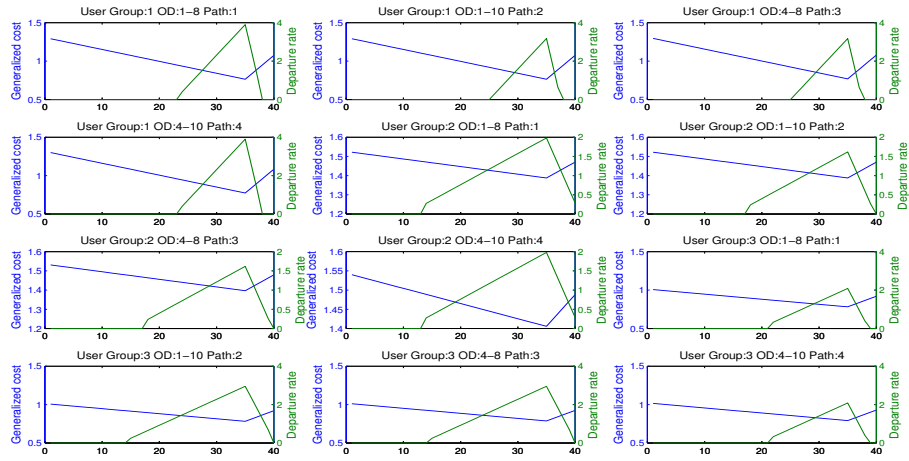


Figure 5.6.: Results for DUE-1: carbon constraint at OD level

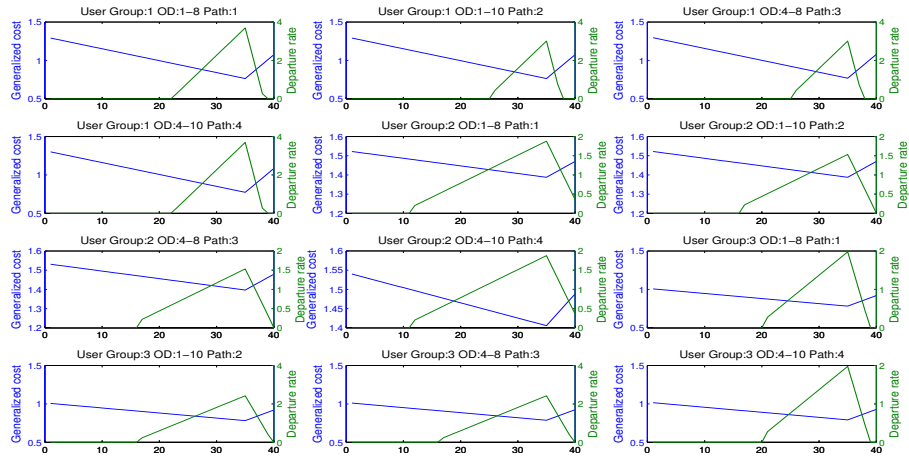


Figure 5.7.: Results for DUE-2: carbon constraint at OD level

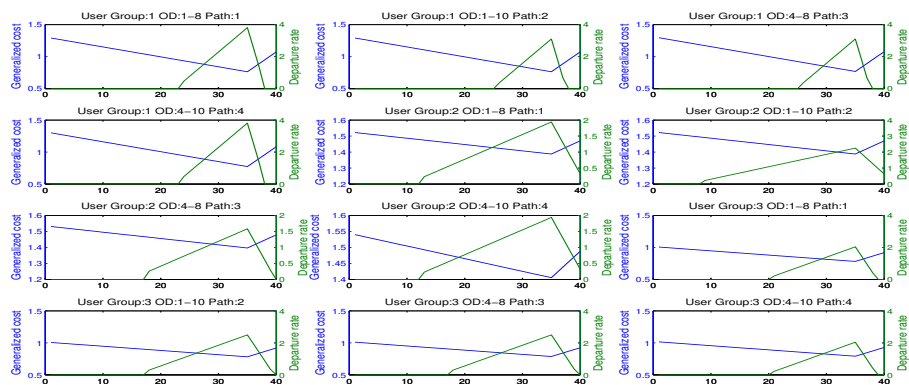


Figure 5.8.: Results for DUE-3: carbon constraint at OD level

and coupled carbon cap constraint, and decomposed refers to the solution obtained by the decomposed VI algorithm with individual carbon cap constraints. At system level we see the total carbon consumption reduced to near 2% for all DUE-episodes. In other words the constraint is not active. It is interesting to see that the travel cost is lower with carbon cap constraint for DUE-1 when compared with the base case. Due to the inclusion of carbon credit cost into the generalized cost, the path flows are redistributed and this may cause a lower total cost compared with the base case. These findings are same for both basic and decomposed algorithms. However for DUE-2 and DUE-3, the travel time costs increase when the carbon cap constraints are introduced. As mentioned earlier, path flow redistribution is one of the possible causes that affects the resulting travel times. In addition, demand levels specific to user classes also affect the travel costs.

Table 5.3.: System level results for X-network

<b>Episode</b>	<b>Carbon cost</b>			<b>Travel cost</b>		
	Base	Basic	Decomposed	Base	Basic	Decomposed
DUE-1	393600	386000	385810	2972	2711	2788
DUE-2	370200	361900	361747	2431	2686	2740
DUE-3	394500	385900	385723	2887	2944	2955

Table 5.4 reports the cumulative carbon cost difference at O-D level for each user class using the results obtained from basic and decomposed algorithms. In the tables, each row represents a user class and each column represents an O-D pair. Each cell value indicates the difference between the solution obtained from basic projection and decomposed algorithm. The purpose of the comparison is to show that the results obtained from decomposed algorithm that solves a relaxed version of the problem (i.e., no coupled constraint rather carbon caps at individual level) are not significantly different from the solutions from basic projection algorithm. From the tables we observe that:

- (a) The decomposed algorithm underestimates the carbon consumption at OD level. This is valid for all three episodes and all user classes. However the extent of underestimation is negligible.
- (b) The highest difference we obtain is 0.114%. Most cases the difference is below 0.05% that is negligible.
- (c) For user class-1 the differences are high ( $\leq 0.114\%$ ) for DUE-episodes.

Table 5.4.: Comparison between two solution approaches

User	Carbon cost difference(%) from basic projection algorithm			
	OD-1	OD-2	OD-3	OD-4
DUE-1				
Class-1	-0.114	-0.115	-0.105	-0.098
Class-2	-0.038	-0.009	-0.005	-0.031
Class-3	-0.041	-0.0632	-0.058	-0.028
DUE-2				
Class-1	-0.084	-0.086	-0.078	-0.072
Class-2	-0.025	-0.004	-0.0005	-0.019
Class-3	-0.019	-0.037	-0.034	-0.01
DUE-3				
Class-1	-0.108	-0.112	-0.103	-0.093
Class-2	-0.034	-0.043	-0.005	-0.026
Class-3	-0.034	-0.055	-0.049	-0.022

With evidences from the cost vs. departure rate plots, the total time and cost values, and the carbon cost difference values at group levels, we conclude that the results obtained from decomposed algorithm are not significantly different from the basic projection algorithm. This is important because the basic projection algorithm

does not solve the reasonably sized networks efficiently whereas the decomposed algorithm can solve those networks at desired error tolerance. The next section describes the results from Sioux-Falls network obtained through the decomposed VI algorithm.

### 5.6 Results for Sioux-Falls network

This section describes the results from Sioux-Falls network. The six O-D pairs are: 540-550, 551-541, 540-570, 551-570, 571-541, and 571-550. For each O-D pair and each user class we define the trips demands to characterize the DUE-episodes. A three-episode PMCA-DUE is analyzed using the decomposed VI algorithm. Five user classes are defined: (a) Low income and work trip, (b) Medium income and work trip, (c) Medium income and grocery trip, (d) High income and work trip, and (e) High income and grocery trip. The value of travel time is used as a measure of the income level. The relative value of carbon cost is captured through the generalized cost function parameters.

The decomposed VI algorithm solves each DUE-episode separately. For brevity, we report the results for DUE-1 episode here. We test the PMCA-DUE model for 2%, 5%, and 7% carbon reduction from the base case where no carbon cap is introduced. First we report the cost vs. departure time plots for DUE-1 at 2%, 5%, and 7% reduction to examine the equilibrium conditions. Then we compare the O-D level carbon and travel time costs for each user class for each reduction level.

#### 5.6.1 PMCA-DUE-1 (different carbon reduction)

The total carbon cap is set at 98%, 95%, 93% level of the base case for each case respectively. Further, the cap is distributed at O-D level for each group. We cannot distribute the carbon cap uniformly because each user class has a unique generalized cost as parametric combination of carbon cost and travel cost. Therefore, we compute the carbon consumption of each user class for each O-D pair in the base case and set the carbon caps accordingly. Figure 5.10 reports the generalized cost vs.

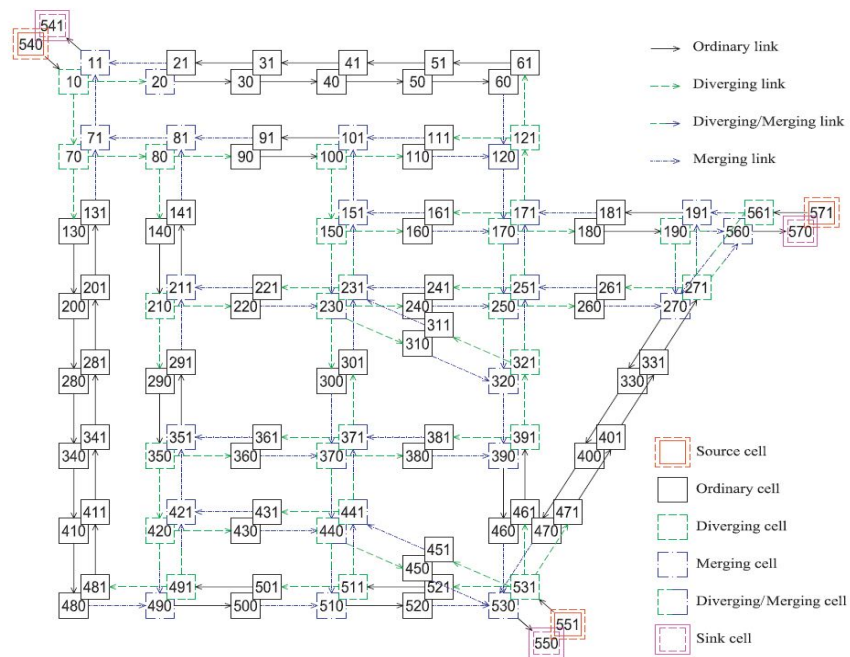


Figure 5.9.: Cell representation of Sioux Falls network [109]

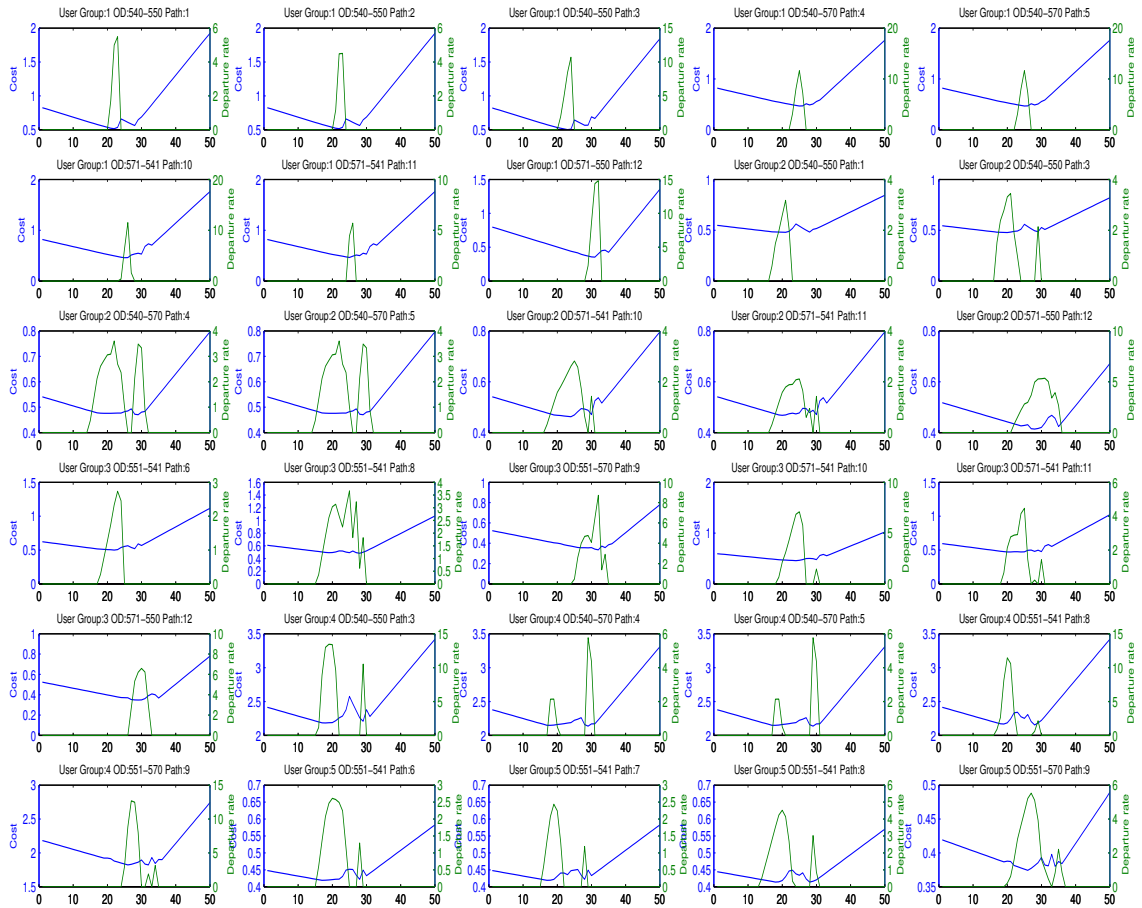


Figure 5.10.: PMCA-DUE-1 results: 2% reduction from base case

departure rate plots for the PMCA-DUE-1 with 2% reduction level. The plots show consistency in terms of the feature that higher departure rate occurs at lower cost reflecting DUE conditions. For few cases we observe multiple peaks in the departure rate vector. Most of those cases are accompanied with multiple troughs in the cost vector. Whenever the cost falls, the departure rate goes up. For user class-4 and class-5, this is more prominent. Similar trends can be found for the DUE-episodes with 5% and 7% reductions. For PMCA-DUE-1 at 7% reduction, we see multiple peaks in the departure rate vector more often. Since the carbon constraint becomes tight it may happen that the rate vector is distributed over multiple peaks to satisfy equilibrium.

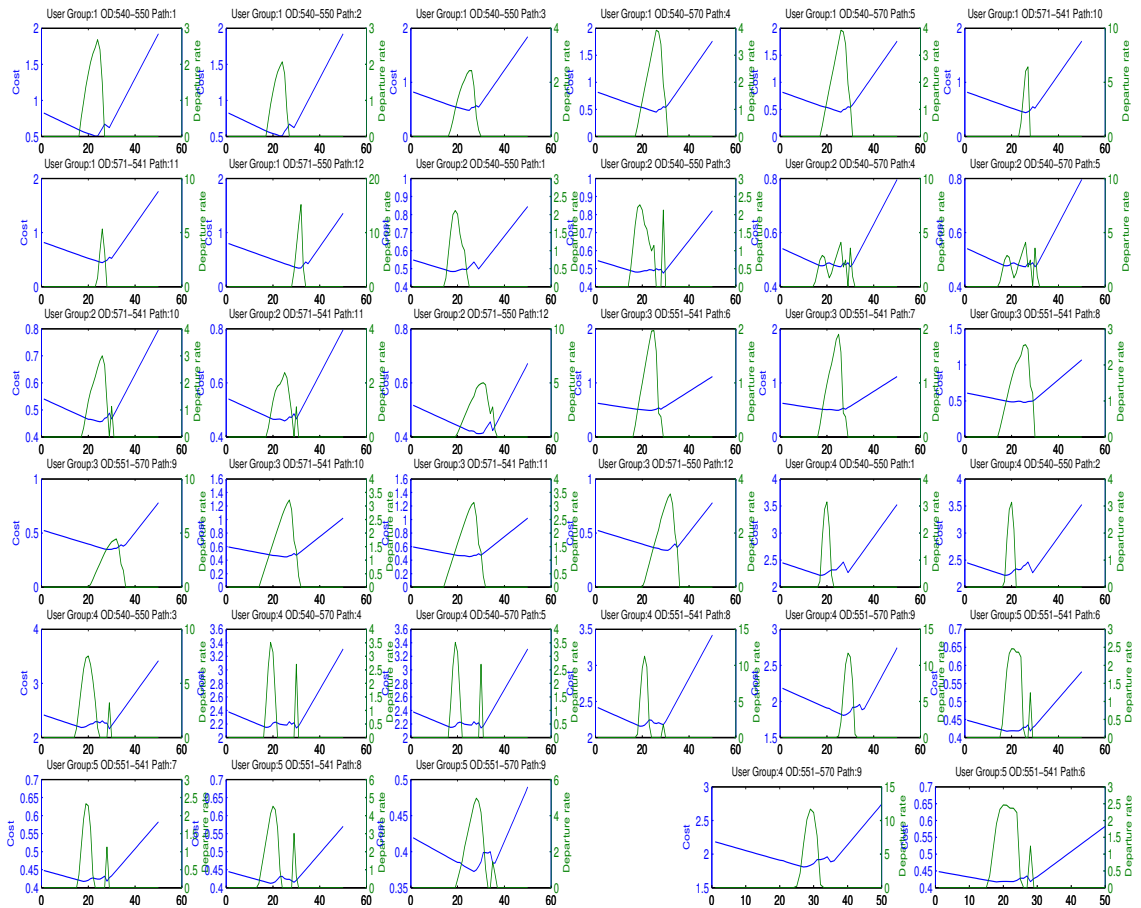


Figure 5.11.: PMCA-DUE-1 results: 5% reduction from base case

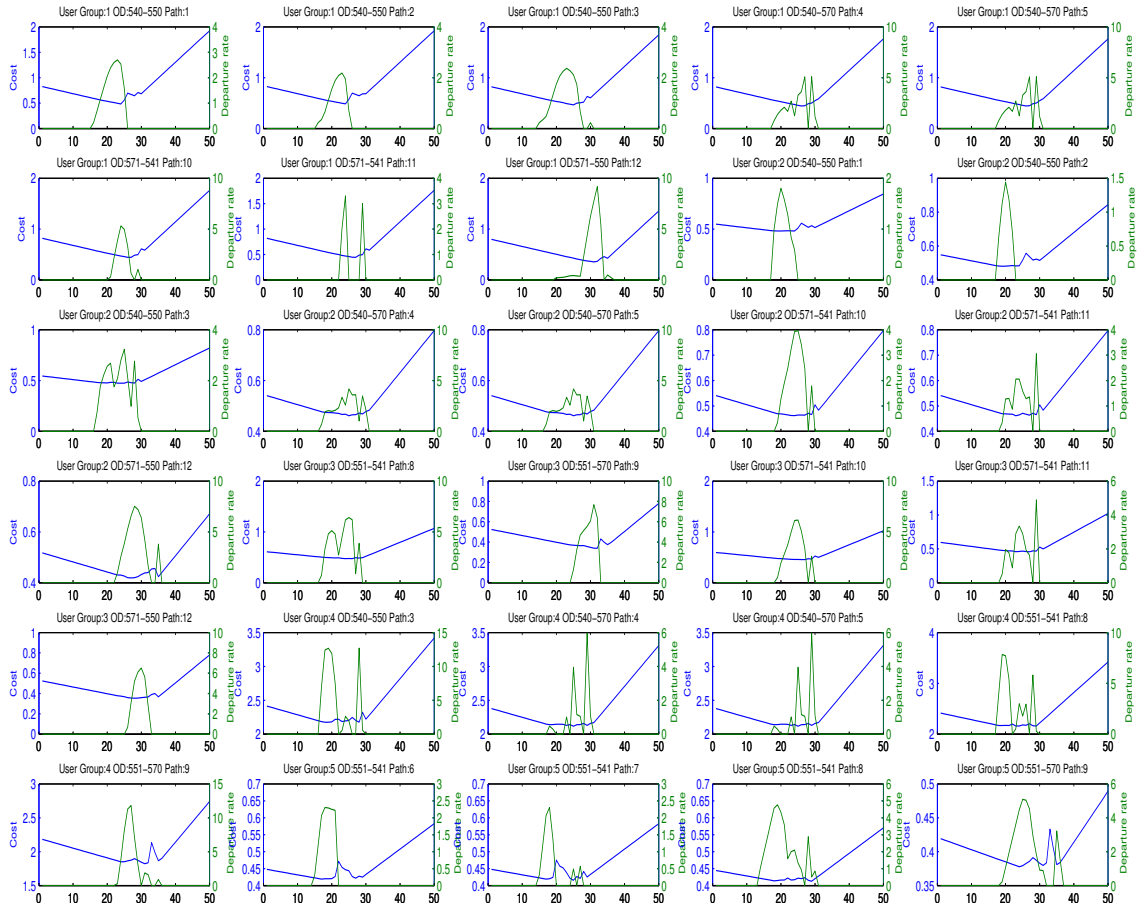


Figure 5.12.: PMCA-DUE-1 results: 7% reduction from base case



### 5.6.2 Comparison of OD level carbon and travel cost

This section compares the total carbon and travel cost at O-D level when PMCA is implemented at different reduction level. The goal here is to explore the effect of PMCA on total carbon consumption and system wide travel costs. Note that travel cost is not same as generalized cost. Travel cost is defined as the total cost accounting for travel time and penalties for early and late arrivals. The travel cost comparison shows the impact of PMCA when personal carbon allowance is introduced in the system.

We only compare the results for OD-1, OD-2, OD-3, and OD-5. Since OD-4 and OD-6 do not have any path choices, the results are not reported here.

Table 5.5 summarizes the results at O-D level. Carbon consumption at O-D level goes down as carbon cap constraints are introduced. This is valid for all O-D pairs and all reduction levels. The increase in travel cost is much higher as the carbon cap goes from 5% to 7%. This trend holds true for all O-D pairs. This indicates a non-linear pattern of travel cost increase as PMCA imposes carbon constraint.

For OD-2, the travel cost first decreases with 2% reduction. However, the travel cost increases as the reduction level rises. This can be explained with the effect of path flow redistribution and the conflicting nature of travel and carbon cost. With a smaller carbon cap, the PMAC-DUE model redistributes the flow to equilibrate the generalized cost that include both carbon and travel time cost. It is possible that this results into a better flow distribution in context of O-D level cost. However, with a higher cap, the model redistributes the flow so that carbon cap constraint is satisfied resulting into a higher travel cost compared with the base case. OD-5 exhibits the same feature.

### 5.6.3 Comparison of carbon consumption

Five user classes are defined with three attribute: (a) income level (value of travel time), (b) how many trips to make each week?, (c) purpose of the trip. The classes are:

Table 5.5.: OD level cost comparison

	<b>Carbon Cost</b>				<b>Travel Cost</b>			
		Reduction		level		Reduction		level
<b>Case:</b>	Base	2%	5%	7%	Base	2%	5%	7%
OD-1	56000	53261	53378	52600	3407	3424	3496	3739
OD-2	58651	53272	53268	52575	2671	2646	2687	2848
OD-3	51692	49737	49113	48980	4116	4119	4230	4978
OD-5	45756	43636	42807	42730	2534	2514	2576	2658

1. Low income, fewer weekly trips and work trip, 2. Medium income, moderate weekly trips, and work trip, 3. Medium income, moderate weekly trips, and grocery trip, 4. High income, high weekly trips, and work trip, 5. High income, high weekly trips, and grocery trip. The DUE-1 episode is the morning peak hour with work trips and grocery trips specific to OD pairs. Table 5.6 shows the total carbon consumptions for each user class. The results are categorized by OD pair and level of carbon reduction to demonstrate the effects of PMCA. The table reports % change only when the consumption is significantly large.

The decrease in carbon consumption for class-4 is much smaller compared with class-5 as seen in the results for OD-1 and OD-3. Class-4 and class-5 are differentiated by only trip purpose. For work trips the reduction levels is smaller. The largest decrease is 1.82% as observed for OD-3. On the other hand, the decrease for grocery trips ranges between 6-7.4%. This is intuitive because class-5 users have a high value of travel time for work trips compared with grocery trips. It is more likely that the users would be saving carbon credits more in the grocery trips.

The carbon consumption for class-2 gets smaller significantly (ranging from 7-11%) as carbon caps are introduced. However, the relative changes from 2% to 5% and 7% reductions are smaller. It is interesting to see that the reduction in carbon for grocery trips by class-3 (medium income) users is smaller compared with class-

5 (high income). Higher income (class-4 and class-5) users are characterized with higher trips compared to medium income (class-2 and class-3). It is more likely that higher income users (class-5) would be more sensitive to carbon saving in grocery trips compared with medium income users (class-2).

For class-1 users the carbon consumption decreases with higher carbon caps with the exception in OD-1. This can be explained by flow distribution mechanism at equilibrium. The value of time is low for class-1 users compared with other users. Equilibrium condition at the base case will push more flows from user class-1 to a relative higher travel time option (rate vector) resulting into lower carbon. With the carbon caps, the equilibrium state considers both carbon and travel costs. Accordingly, it is possible that flows from other user class are pushed to low-carbon (higher travel cost) option. This may cause higher carbon cost for the travel option compared to the base and the carbon consumption goes up for all classes using the travel option (specifically the users from class-1).

#### 5.6.4 Comparison of path level carbon cost

This section explores the changes in carbon cost specific to paths. The cumulative carbon cost is a parametric measure of the emissions level of the particular path contributed by a particular user class. We define 100 g of CO<sub>2</sub> equivalent to one carbon credit and the cost can be directly converted into emissions. One particular interest is to observe the change in the level of emissions at path levels. It is possible that the emissions level of a path significantly increases or decreases due to distribution of flows as PMCA-DUE satisfies equilibrium. Figure 5.13 shows the changes in carbon consumption (i.e., cumulative carbon cost) at path level for all O-D pairs.

For OD-1 (figure 5.13 top-right) the carbon consumption for path-3 decreases as we set the carbon consumptions caps. At the same time the carbon consumptions go up for path-1 and path-2. This trend continues up to 5% of reduction and at 7% reduction path-3 exhibits similar carbon consumption as that of 5%. However

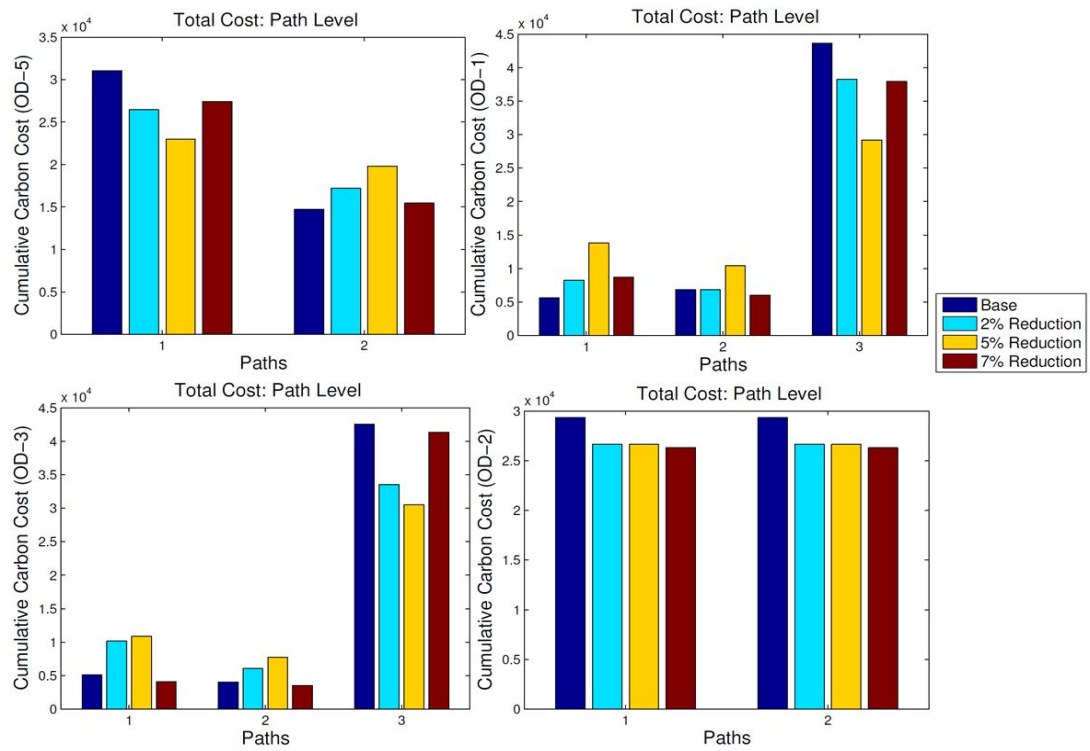


Figure 5.13.: Path level carbon cost at different carbon caps.

Table 5.6.: Comparison of carbon consumptions at user class level\*

OD-Pair	Total	Carbon	Cost
	Class-1	Class-2	Class-3
OD-1(Base)	18082	14620	363
OD-1-98	16379 (9.4%)	13038 (10.8%)	368
OD-1-95	16802 (7.07%)	13053 (10.72%)	361
OD-1-93	17160 (5.1%)	12964 (11.3%)	373
	Class-1	Class-2	Class-3
OD-2(Base)	23444	24906	348
OD-2-98	20357 (13%)	22622 (9.17%)	350
OD-2-95	19987 (15%)	22905 (8.03%)	359
OD-2-93	19487 (17%)	22674 (8.96%)	352
	Class-1	Class-2	Class-3
OD-3(Base)	414	415	17033
OD-3-98	387	365	16604 (2.51%)
OD-3-95	375	368	16303 (4.28%)
OD-3-93	369	368	16213 (4.81%)
	Class-1	Class-2	Class-3
OD-5(Base)	11069	14109	19871
OD-5-98	10232 (7.55%)	13071(7.35%)	19637 (1.18%)
OD-5-95	9868 (10.85%)	12903 (8.55%)	19340 (2.67%)
OD-5-93	9736 (12.04%)	12965(8.11%)	19438 (2.18%)

\*Values in the parentheses show the difference in % from base

the consumption is higher for path-1 and lower for path-2 when compared with 5% reduction level results.

For OD-2 (figure 5.13 bottom-right), flows are distributed between two paths. Lower carbon consumption can be observed when carbon cap constraints are intro-

duced. The carbon consumptions do not vary much at different levels of carbon cap. For OD-3 (figure 5.13, bottom-left) The total carbon consumptions increase for path-1 and path-2, whereas path-3 shows lower carbon consumption. The pattern changes for the case with 7% reduction. The carbon consumption goes up for path-3 while going down for path-2 and path-3. OD-5 (also with two paths) shows a different pattern compared with OD-2 (figure 5.13, top-left). The carbon consumption gets higher for path-2 at 2% and 5% reduction level and again goes down for 7% reduction level.

### 5.7 Concluding remarks

This research develops a multi-user class dynamic user equilibrium model, namely the PMCA-DUE model, incorporating the market based carbon reduction strategy described as personal mobility carbon allowance scheme. Consideration of carbon cost in addition to travel cost for path and departure time choice, requires a new generalized cost function and equilibrium condition. Also, the effects of initial allocation of carbon credits, value of travel time, and number of trips to make influence the travel decisions under PMCA scheme. It is obvious that these attributes are not homogeneous and a model capturing the heterogeneity is necessary. Accordingly we develop a multi-user dynamic equilibrium model where each user class has a distinct value of travel time, trip demand, different sensitivity to perceived carbon cost (see section 5.3.5).

This research makes several contributions to the literature. First, a multi-class dynamic user equilibrium model is formulated. Both complementarity and equivalent VI formulation is demonstrated. Second, we propose two solutions techniques: basic projection and decomposed VI algorithms. We solve two test networks and analyze the results. Third, the user and OD level travel and carbon costs are investigated. Carbon consumption patterns are explored. Finally, the impact PMCA scheme is investigated which provides insights for carbon allowance schemes in general.

The key findings from the analyses are as follows:

- (a) Introducing carbon cap through PMCA schemes can lower the system level travel time up to certain level of cap. Our results (table 5.3 and table 5.6) show that the cumulative travel costs are lower from the base case when PMCA scheme is in effect. This can be explained from the concept of congestion pricing and the conflicting nature of travel time minimization and carbon credit consumption. When the average trip speed is high, the carbon cost goes up. At the same time the travel cost goes down. Since the generalized cost in our model considers both, the model distributes the flows such a way that the generalized cost, which is a parametric combination of the carbon and travel cost, is minimized. At equilibrium it redistributes the flow by adjusting the departure rate vector. This results into a new equilibrium state with lower cumulative travel cost for a class. This does not necessarily decrease the travel cost for each path. Rather for some paths the costs increase and for some paths the cost decrease as exhibited by the figure 5.13. As a net effect, it is possible to have lower travel cost for the system at OD level.
- (b) Class-4 users (characterized by high value of travel time) are less sensitive to carbon constraint in context of work trips. Relatively higher value of time and higher penalties for late and early arrival may cause to exhibit this. For work trips class-4 users do not show significant reduction of carbon consumption as the carbon cap goes from 2% to 7%.
- (c) One important finding from our results is that the emissions level (parametric function of the carbon consumption) for paths changes with the levels of reduction. For air quality conformity this is important because PMCA leads reduction in carbon consumption for the network, however for some paths the emissions can be higher as seen in figure 5.13.
- (d) Carbon consumptions are lower for cases (OD-3) characterized by grocery trips compared with cases (OD-1) characterized by work trips. This is mainly because

of the nature the parameters in the generalized cost function. The parameters specific to grocery trips prioritize the savings of carbon credits so that it can be used for work trips later.

- (e) Our analysis indicates that the equilibrium state highly depends on the composition of trips characterized by purpose. A case with higher grocery trips will reach a different equilibrium compared with a case with higher work trips. This is because of the heterogeneity captured through the generalized cost function parameters.
- (f) The results also show the impact of setting initial distribution of carbon credits. The initial distribution is incorporated through the carbon cap constraint in the model. As we move from 5% to 7% reduction, the equilibrium state changes and we observe a new path cost pattern (see figure 5.13) and the OD level carbon consumptions are also affected (see table 5.3 and table 5.6).

This research has few limitations in terms of scope and transferability. First, the parameters for the generalized cost function are estimated specifically for the Sioux-Falls network. Although the models are applicable to other networks, one must estimate parameters specific to the transportation network. Second, the captured heterogeneity across population can be extended to have a comprehensive form through considering other trip types, finer level of income, and vehicle composition.

Finally, our solution technique solves only up to 7 % reduction for the Sioux-Falls network. It is possible that the problem becomes infeasible with higher carbon cap. We observe that the problem can be solved with lower trip demand keeping the carbon cap same indicating the allocated carbon for the system may not be sufficient for the original demand. The demand feasibility issue can be resolved through redistribution of the carbon credits based on the demands for specific groups at specific OD pairs. This alludes to another research question regarding the initial allocation of carbon credits with efficiency and equity. This is a potential future research direction that is critical for the implementation of the PMCA schemes.



## CHAPTER 6. LEARNING BASED TRAFFIC CONTROL

### 6.1 Introduction

Traffic congestion is ubiquitous in the 439 urban areas of the United States and is responsible for 2.9 billion gallons of additional fuel consumption in 2011 [19] 2010). The net congestion cost is 121 billion (in 2011 U.S. dollars) with about 5.5 billion hours of delay. Further, the transportation sector alone is responsible for about 76 percent of the total CO emissions and 50 percent of the total NO<sub>x</sub> [140] emissions in the United States. The U.S. Environmental protection agency (EPA) reports transportation sector as the fastest growing source of greenhouse gas (GHG) emissions indicating 47 percent net increase from 1990 to 2003 (EPA, 2006). The contribution of delay due to traffic signals is about 5 to 10 percent of the net delay (NTOC Report, 2012). National Traffic Signal Report Card (NTOC Report, 2012) gave C grade for the current traffic signal operations and emphasizes on optimized signal scheme implementation. Clearly, it is important to design signal control systems that can minimize travel delay, intersection delay, and number of stops at the intersections. Moreover, signal systems with reduced number of stops, intersection delay, and the variability in speed profiles can lead to less vehicular emissions for the network. Accordingly, this research aims to find signal control schemes that lead to sustainable mobility, i.e., reduced delay for the users and less vehicular emissions for the traffic network. Adaptive signal control schemes such as SCOOT [141], SCATS [142], PRODYN [143], OPAC [144], RHODES [145], UTOPIA [146], CRONOS [147], and TUC [148] are found to perform better than fixed and actuated signal timing plans. Nevertheless, adaptive schemes are often limited in terms of scalability and robustness ( [149, 150, 151]. Many of these control systems (e.g., SCOOT and SCATS) are centralized systems based on real time traf-

fic data and some (e.g., OPAC and RHODES) use dynamic optimization to obtain the signal settings. However, none of them adaptively learns from the environment and the computational complexity increase exponentially with network size. Further, researchers from the machine learning and artificial intelligence area have also applied algorithms that include (but not limited to) neuro-fuzzy networks [152], neural networks [153] (Li Mueck, 2010), Tabu search [154] (Hu Chen, 2012), self-organizing maps [155] (Li et al., 2011), emotional algorithm [156], and genetic algorithms [75]. Two limitations tied with most of these algorithms are: the requirement of large data to calibrate the parameters and exponential complexity of the problem for large scale networks [157]. To overcome these limitations, researchers from different area also looked at the prospects of using learning techniques as an alternative to using real time adaptive algorithms ([149, 151, 158, 159, 160, 161]).

Recent advances in CV environment offer useful technologies in detection and acquisition of high fidelity data that can be used for intelligent control for signalized intersections. Acknowledging the potential, the intelligent transportation system (ITS) program of the U.S. Department of Transportation (DOT) heavily emphasizes on CV research in the ITS Strategic Plan (2010-2014). CV environment facilitates communication platform where vehicles can talk to each other (Vehicle-to-Vehicle, V2V), to the infrastructure components (Vehicle-to-Infrastructure, V2I), and also infrastructure to infrastructure communication (I2I) is possible. We propose RL algorithm for signal control that allows an agent (i.e., signal controller) to share information with its neighbor controllers through I2I communication. Later we also show that, learning with information sharing improves the performance of the RL algorithm. To summarize, this research applies reinforcement-learning (RL) algorithm for signal control (namely, the R-Markov Average Reward Technique or RMART) at network level. Also, the algorithm takes advantage of the I2I communication to allow for information sharing among the neighborhood controllers. The remainder of the paper is organized as follows: the literature review section describes related works previously done by researchers, the problem definition section states the hypotheses and

research questions of this research, the methodology section explains the RL algorithm, the numerical results section explains the results obtained from test networks, and finally, we discuss the important contributions, limitations, and future directions of this research.

## 6.2 Literature Review

The implementation of RL in signal control area has been well studied in the last decade. Miakami and Kakazu [162] proposed cooperative signal control scheme with a combination of evolutionary algorithm and reinforcement learning techniques. Bingham [163] proposed rules based on fuzzy-logic that allocates green times based on the number of vehicles. Other than signal control researchers have also used it for other problems in transportation [164, 165, 166, 167]. Abdulhai et al. [149] applied off policy (Q-learning) algorithm to optimize signal control in an isolated intersection. Application to larger networks was challenging due to exponential increase in the joint state-action space. Later, Wiering et al. [158] proposed co-learning algorithms at network level accounting for the waiting time for the vehicles and used car-based value function that reduced the state space to a reasonable number. However, the prediction of waiting time is not accurate and the traffic simulator lacks important modules such as lane changing and dynamic route choice. Researchers ([159, 168, 169] have also studied cooperative multi agent system for urban traffic control. More recently, El-Tantawy et al. [161] proposed neighborhood coordinated RL based signal control and described a joint decision framework to present multi agent framework. Although Q-learning and SARSA are most widely used temporal difference techniques, researcher also applied other algorithms like actor-critic temporal difference, Q-learning with function approximation [170] and action dependent adaptive dynamic programming [171]. Although commonly used in long-term average reward specific algorithms, R-Markov Average Reward Technique (RMART) has not been applied potentially in the context of vehicular traffic control. Recognizing the potential to address long

term average reward this research applies RMART technique for signal control. The RL algorithms applied for signal control vary greatly with the definitions of state and reward. El-Tantawy et al. [161] provides an excellent discussion on the variations in state and reward definitions in context of signal control.

The most common definitions of state include number of arriving vehicles, queue lengths, average delay, and so on. Most of them do not consider information sharing among neighborhood controllers. Neighborhood information provides us with congestion status of the surrounding controllers. Including this information will help the controller to learn better. Consider a case when the adjacent intersections of a particular intersection are heavily loaded and in near future this intersection will experience heavy load. Using only local information, the agent does not have any idea of the immediate congestion that will appear. When the state definition includes congestion status of the adjacent intersections the agent learns to adjust signal settings when the nearby intersections are congested. Based on this idea, this research adds congestion information of the neighborhood intersections to the definition of state in the RL algorithm. This idea is different from the multi-agent coordination research ([151, 158, 159, 168] because multi-agent cooperative learning deals with the joint state-action space optimality. This research focuses on adding neighborhood information in the state definition without explicit coordination among the controllers.

Rewards in a RL algorithm can take different forms including number of stops made, intersection delay, and throughput for the intersection. The reward is defined in a static manner and the definition does not change over time. However, rewards can be dynamic as a response to the current state of the traffic network and multiple reward structure can be used [172]. Houli et al. [173] defined different reward functions such as stops, delay, and so on, for different congestion levels: free flow, saturated condition, etc. However, their approach is not truly dynamic because the congestion level is always known beforehand and rewards are predefined for different time of analysis. This study takes a different approach where the reward takes a dynamic form in the sense that reward definitions changes based on the congestion level in

real-time. In addition to static reward structure we also examine the performance of RL algorithms with this kind of dynamic structure. Finally, most research works relevant to learning techniques for signal control do not evaluate the benefits in terms of reducing vehicular emission. Although connected vehicle research area has some potential works [78, 79, 174] that evaluate benefits in terms of reducing emissions, however not in the context of applying learning techniques. To conclude, the goals of research are as follows:

- (a) To develop a learning based signal control scheme that minimizes emissions for the signalized intersections.
- (b) To apply RMART technique for traffic signal control that allows for neighborhood congestion information sharing within the CV environment and compare with fixed, adaptive, and other learning algorithms.
- (c) To demonstrate the benefits of learning based control algorithms in terms of reducing emissions from traffic network.

### 6.3 Reinforcement Learning Based Algorithms

Optimization of vehicular traffic control requires the determination of signal timing parameters: scheduling and allocation of green time to specific set of movements. A set of non-conflicting allowable movements is defined as phase or stage. In context of RL, traffic network is the environment and the traffic controllers act as agents. We define the action of an agent as the activation of a particular phase (predefined) at the decision interval. Thus, the traffic signal control problem has all the elements of MDP. Each time the agent takes an action that influences the current environment, the state of the environment changes. The problem is to find the optimal policy (mapping between the phase-activation and traffic states) that gives the largest reward that is commonly defined in terms of average delay, number of stops, etc. in the long-term.

The key idea of RL comes from DP and artificial intelligence (AI) based learning techniques. A detailed description can be found in Sutton and Barto [175] and Gosavi [176]. The two key elements of MDP are the reward and state transition probability. The RL technique is most appropriate when these elements are not deterministic. The solution methodology should contain components that determine the transition probabilities and rewards as a feedback from the environment. However, a simulator of the real environment can provide us with the reward and the transition of the states can be observed. This research uses VISSIM (PTV, 2012) as a traffic simulator that provides rewards and other performance.

#### 6.4 Elements of the RL-based algorithm

Reinforcement learning techniques follow sampling based approaches to solve the optimal control problems. RL systems contain basic components: the state, action, and reward. These components are specific to the problem at hand. Next, we define the state, action, and reward for the proposed RL algorithm.

##### 6.4.1 State of the system

Before defining state, we need to define the residual queuing state for each lane group served by the signal phases at the intersection. Residual queuing state for lane  $i$ , is defined as:

$$\omega_i^t = \frac{q_i^t}{J} \times \frac{1}{l_i} \quad (6.1)$$

$\omega_i^t$  = Residual queuing state for lane  $i$  at step  $t$ ,

$q_i^t$  = Queue length (in PCE units) for lane  $i$  at step  $t$ ,  $J$  = Jam density (190 PCE per lane mile)  $l_i$  = Length of lane (in miles)

Jam density is usually expressed in number of passenger car equivalent (PCE) per lane-mile. It refers to the density of a lane when speed equals to zero for all the vehicles on that lane. Highway Capacity Manual (HCM) suggests using 190 PCE

per lane-mile for freeway facilities. Note that, one should choose the value that is consistent with the existing network conditions. Now, the residual queuing state for the lane group served by phase  $p$  can be estimated by taking the average over all the lanes.

$$\pi_p^t = \frac{\sum_{i \in \text{lane group}, p} \omega_i}{\sum_{i \in \text{lane group}, p} i} \quad (6.2)$$

$\pi_p^t$  = Average residual queuing state for the lane group serving phase  $p$  at step  $t$ .

It can be seen that is continuous in nature and can take any value between 0 and 1. Next, the average residual state for a particular phase,  $p$  is labeled as low, high or medium using the following conditions:

$$\Pi_p^t = \left\{ \begin{array}{l} L, \text{ if } \pi_p^t < 0.4 \\ M, \text{ if } 0.4 \leq \pi_p^t < 0.7 \\ H, \text{ if } \pi_p^t \geq 0.7 \end{array} \right\}; L = \text{low}, H = \text{high}, M = \text{medium}. \quad (6.3)$$

The RQ state of the intersection is computed using the RQ states of the phases. Different values are assigned to the labels of RQ state of a particular phase. Here,  $\Pi_p^t$  = label of  $\pi_p^t$ .

$$\mu_p^t = \left\{ \begin{array}{l} 1, \text{ if } \Pi_p^t = L \\ 3, \text{ if } \Pi_p^t = M \\ 5, \text{ if } \Pi_p^t = H \end{array} \right\} \quad (6.4)$$

Now, the labels for RQ states of the intersection are defined as follows:

$$\Omega_j^t = \left\{ \begin{array}{l} \text{Free flow; if } \sum_{p \in \text{Phases}} \mu_p^t < 10 \\ \text{Average flow; if } 10 \leq \sum_{p \in \text{Phases}} \mu_p^t < 16 \\ \text{Saturated flow; if } \sum_{p \in \text{Phases}} \mu_p^t \geq 16 \end{array} \right\} \quad (6.5)$$

Note that these values in (3), (4), and (5) are arbitrary and depends on the judgment of the analyst and scope of the problem. We select these values through observation of congestion variation of our test cases.

### 6.4.2 System state of the RL

At any step of the RL algorithm, the state of the system is represented by three elements: (a) the average label of RQ states of the phases in signal timing plan, (b) the phase number with maximum queue length for the intersection, (c) the adjacent intersection number with maximum queue length. The state at step  $t$  for signal controller  $j$  can be represented as:

$$s_j^t = \left\{ \begin{array}{l} \text{average} (\Pi_p^t, \forall p \in P) \\ \arg \max_p (\Pi_p^t, \forall p \in P) \\ \arg \max_{\tilde{j}} (\Omega_{\tilde{j}}^t, \forall \tilde{j} \in \Gamma(j)) \end{array} \right\} \quad (6.6)$$

An example for the state: medium, phase 3, adjacent intersection no. 104 is interpreted as: a) the intersection has a medium congestion label in terms of residual queue, b) Phase 3 corresponds to the maximum queue length, c) Intersection 104 (straight northbound neighbor) has the maximum queue length. Where,

$P$  = Set of phases in the signal timing plan for intersection  $j$ ,

$\Gamma(j)$  = The set of adjacent intersection for intersection  $j$

### 6.4.3 Action selection strategy

The agents action is to switch on any of available phases in the signal-timing plan. Note that, there is no restriction on the sequence of the phases. Flexible sequence in signal timing plan has been used by previous researchers and has been implemented in real world signalized intersections. The algorithm follows the minimum and maximum green constraints. Currently, the thresholds for these parameters are assumed. Reinforcement learning algorithms in general require a balance between exploitation and exploration in the strategies for selecting optimal action. The simplest action rule is to select the action (or one of the actions) with the highest estimated state-action value (complete greedy behavior). In other words, the agent always tries to maximize the immediate reward using the immediate knowledge without any attempt



to explore other possible actions. To balance between exploitation and exploration Sutton and Barto [175] suggests two methods:

#### 6.4.4 $\epsilon$ -greedy method

In this method, the agents behaves greedily by choosing the action that gives the maximum state-action value in most cases except at some cases it chooses a random action. The probability of this random behavior is and the probability of selecting the optimal action converges to greater than  $1 - \epsilon$ . One should note that, the advantage of methods over the  $\epsilon$ -greedy methods is highly dependent on the type of problem.

#### 6.4.5 soft-max method

One limitation with the  $\epsilon$ -greedy method is that it gives equal priority to all actions while exploring. It is possible to choose the worst action instead of choosing the next best action. To resolve this, Softmax algorithms vary the action probabilities as a graded function of estimated value. Although, the greedy action has the highest selection probability the other are ranked and weighted according to the value estimates. In general, Gibbs or Boltzman distribution is used to define the probability. The probability for choosing action  $a$  in state  $s$ ,

$$P(a|\text{state} = s) = \frac{\exp(\frac{Q(s,a)}{\tau})}{\sum_{b=1}^{\text{all actions}} \exp(\frac{Q(s,b)}{\tau})} \quad (6.7)$$

$\tau$  =Positive parameter called the temperature. Higher values for the temperature can make the probability of choosing any of the actions nearly equal. On the other hand, lower value of the temperature will create a higher difference in the action selection probabilities. Another commonly used action strategy is the combination of the above mentioned strategies that is referred to as  $\epsilon$ -softmax. The agent behaves greedily with the probability of  $(1 - \epsilon)$  and the rest of the cases it selects an action using the probability computed from Softmax selection process.

#### 6.4.6 Reward function

Three separate reward functions have been used: Queue length (R1), average delay experienced by the intersection since previous action (R2), and Residual Queue (R3). In addition, we propose the multi reward structure that defines queue length as reward at free flow, average delay as reward over the time interval at medium level congestion, and residual queue as reward at near saturated condition.

#### 6.4.7 Multi-reward structure

The multi reward structure dynamically changes the reward function type based on the traffic congestion in real time. We consider the three categories of congestion states: (a) free flow to low congestion, (b) low to medium congestion and (c) medium congestion to high congestion (saturated condition). The algorithm identifies the congestion state in real time and uses the proper reward function in response. This research defines queue length as reward at free flow (to reduce the number of stops), average delay as reward over the time interval at medium level congestion, and residual queue as reward at near saturated condition (to avoid the gridlock and spill back condition).

### 6.5 Algorithm description

We applied three specific temporal-difference techniques:(a) Off-policy TD control (Q-Learning), (b) On-policy TD control (SARSA), and (c) Advanced off-policy TD. Like most RL based schemes, the proposed algorithm has two phases: learning phase and implementation phase. The learning takes place before the implementation. During the learning phase the agents update the state-action value through interacting with the environment. Balancing the exploration and exploitation is important at this phase. Initially, the algorithm starts with using higher probability for exploration. Then, gradually the value is decreased and at the end of the learning

phase we implement the Softmax method. During the implementation period, the algorithm emphasizes on exploitation with very small value.

### 6.5.1 Notations

$\rho$  = The average reward per time step.

$Q(s, a)$  = The value of state - action pair  $(s, a)$ .

$r(s, a, s')$  = Observed reward when the agent takes action  $a$  in state  $s$ , and moves to state  $s'$ .

$\alpha^{(k)}$  = Learning rate for the  $Q$  - values (scalar) at  $k$  - th iteration.

$\beta^{(k)}$  = Learning rate for the average reward at step,  $k$ .

$N$  = Maximum no. of iterations allowed (learning phase).

$\gamma$  = Discount factor for reward value.

### 6.5.2 RMART description

RMART does not divide the experience into separate episodes with finite returns. The value functions are defined with respect to the average expected reward per time step under the policy  $\kappa$  is defined as:

$$\rho^\kappa = \lim_{n \rightarrow \infty} \frac{1}{n} \sum_{t=1}^n E_\kappa(r_t) \quad (6.8)$$

RMART has the concept of average reward over long term instead of discounted reward used in Q-learning and SARSA. Tsitsikilis and Roy [177] provides an analytical comparison between the discounted (Q-learning) and average reward techniques and showed that as the discount factor approaches to 1, the value function by discounted technique approaches the differential value function by average reward technique. Average reward methods also offer computational advantages (Tsitsikilis and Roy [177]).

### 6.5.3 Pseudo Code

Since, Q-learning and SARSA have almost the same framework; we use a single algorithm separating out the update phase. In the learning phase the agent builds its state-action mapping table which can be used later to take decision (which phase to activate) in the implementation phase. Next, we present the pseudo codes for Q-Learning and SARSA, and RMART.

## 6.6 Implementation and numerical results

The RL-based algorithms are implemented in VISSIM using COM interface. Fig. 1 shows two networks: network-I (inside the rhombus) with eight junctions and network-II, with 18 junctions. VISSIM follows the psychophysical car-following models (Wiedemann74 and Wiedemann99) and its variants developed later. In our case, the networks are hypothetical with assumed geometry and flow conditions that resemble real world traffic networks. Therefore, we do not have to calibrate using field data. Further, we assume the same set of parameters for all simulation scenarios for all algorithms to have consistency in the results. For instance, RMART and Q-Learning have the same set of car following parameters.

### 6.6.1 Congestion level variation at intersection level

Algorithms are evaluated at three different congestion levels: low, medium, and high (near saturation). The trip rates for distinct origin-destination pairs are varied to create low to high congestion level. However, this is not the exact representation of the congestion experienced by the intersections. Two intersections can experience varying level of congestion state, even though the demand (network congestion level is same). Intersection-8 and intersection-11 in figure 6.3 experience different patterns of congestion, although the network congestion level is same. Table 6.1 shows the distribution of experienced states for these intersections.

---

**Algorithm 1** Q-Learning and SARSA

---

```

1: procedure INITIALIZATION
2:    $k = 0$  ▷ Iteration counter
3:    $Q(s, a) \leftarrow 0$  ▷ Initialize all Q-values as zero
4:    $\alpha^{(k)} = 10 \frac{\log(k+2)}{k+2}$  ▷ Learning Rate
5:    $\gamma = u$  ▷ Discount factor, we use  $u = 0.8$ 
6: end procedure
7: procedure UPDATE Q-VALUES
8:    $s \leftarrow$  Current State
9:   Select action  $a$  for State  $s$  ▷  $\epsilon - greedy$ 
10:  if Algorithm selected == Q-Learning then
11:    Observe Reward  $r$  for choosing action  $a$ 
12:    Determine resulting State  $\bar{s}$ 
13:     $Q(s, a) \leftarrow Q(s, a) + \alpha^{(k)}[r + \gamma \max_{(\bar{a})} Q(\bar{s}, \bar{a}) -$   

     $Q(s, a)]$ 
14:     $s \leftarrow \bar{s}$ 
15:  end if
16:  if Algorithm selected == SARSA then
17:    Observe Reward  $r$  for choosing action  $a$ 
18:    Determine resulting State  $\bar{s}$ 
19:    Choose action  $\bar{a}$  for State  $\bar{s}$ 
20:    Determine resulting  $Q(\bar{s}, \bar{a})$ 
21:     $Q(s, a) \leftarrow Q(s, a) + \alpha^{(k)}[r + \gamma Q(\bar{s}, \bar{a}) - Q(s, a)]$ 
22:     $s \leftarrow \bar{s}$ 
23:     $a \leftarrow \bar{a}$ 
24:  end if
25:   $k \leftarrow k + 1$ 
26: end procedure
27: procedure TERMINATION
28:  if  $k > N$  then ▷  $N$  is based on simulation period
29:    Stop
30:  else Continue Updating Q-Values
31:  end if
32: end procedure

```

---

Figure 6.1.: Algorithm: SARSA

---

**Algorithm 2** RMART
 

---

```

1: procedure INITIALIZATION
2:    $k = 0$  ▷ Iteration counter
3:    $Q(s, a) \leftarrow 0$  ▷ Initialize all Q-values as zero
4:    $\rho = 0$ 
5:    $\alpha^{(k)} = 10 \frac{\log(k+2)}{k+2}$  ▷ Learning Rate
6:    $\beta^{(k)} = \frac{A}{B+k}$  ▷ A, B are scalars
7: end procedure
8: procedure UPDATE Q-VALUES
9:    $s \leftarrow$  Current State
10:  Select action  $a$  for State  $s$  ▷  $\epsilon$ -greedy
11:  Observe Reward  $r$  for choosing action  $a$ 
12:  Determine resulting State  $\bar{s}$ 
13:   $Q(s, a) \leftarrow Q(s, a) + \alpha^{(k)}[r - \rho + \max_{(\bar{a})} Q(\bar{s}, \bar{a}) - Q(s, a)]$ 
14: end procedure
15: procedure UPDATE AVERAGE REWARDS
16:  if  $Q(s, a) == \max_a Q(s, a)$  then
17:     $\rho \leftarrow \rho + \beta^{(k)}[r - \rho + \max_{(\bar{a})} Q(\bar{s}, \bar{a}) - \max_a Q(s, a)]$ 
18:  end if
19: end procedure
20:  $s \leftarrow \bar{s}$ 
21:  $k \leftarrow k + 1$ 
22: procedure TERMINATION
23:  if  $k > N$  then ▷ N is based on simulation period
24:    Stop
25:  else Continue Updating Q-Values
26:  end if
27: end procedure

```

---

Figure 6.2.: Algorithm: RMART

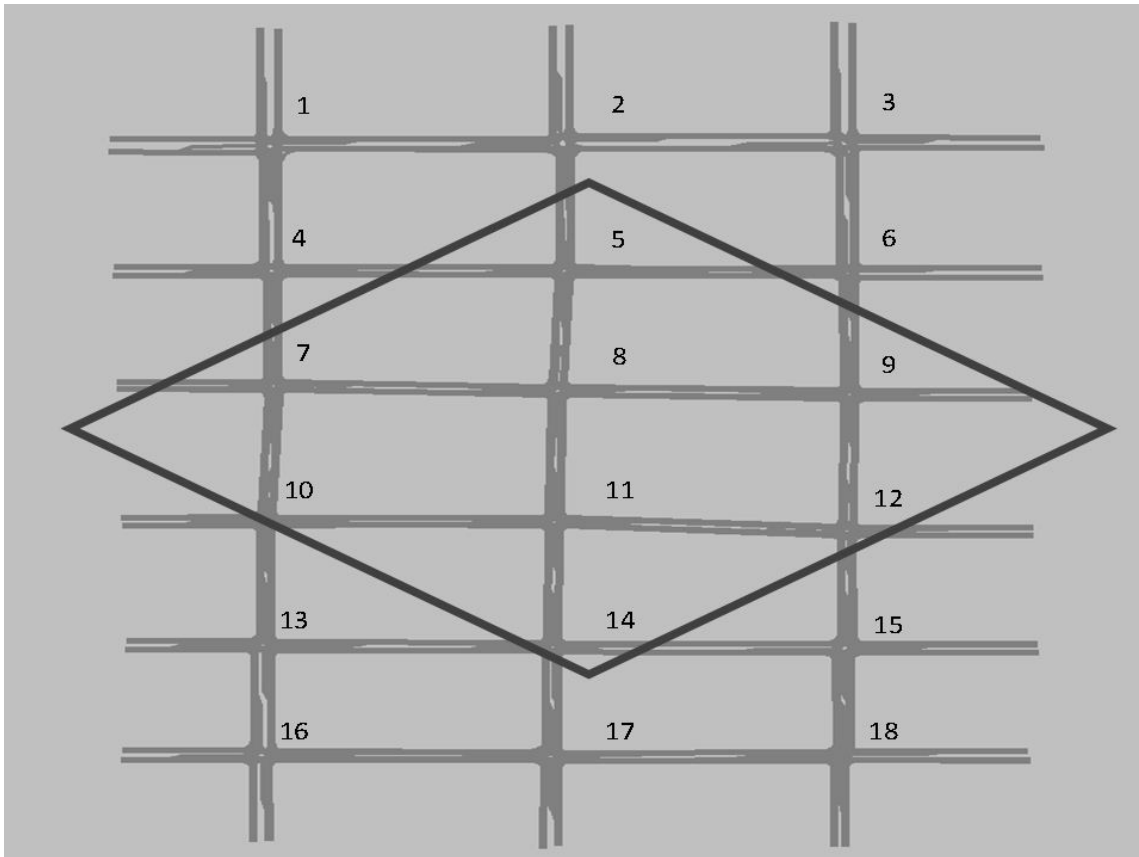


Figure 6.3.: Test network for evaluating the signal control algorithms.

Table 6.1.: Description Of Congestion Variation

Experienced State	Q-learning		SARSA		RMART	
	IS-8	IS-11	IS-8	IS-11	IS-11	IS-11
Low congestion (%)	45.74	45.74	22.87	37.67	27.81	78.92
Medium congestion (%)	39.91	49.78	45.3	57.85	43.49	20.18
High congestion (%)	14.35	4.48	31.83	4.48	2	0.9

### 6.6.2 Statistical tests

We obtain a sample from 10 simulation runs (for each scenario) in VISSIM using a different random seed each time. The sample size is  $N = 10$  with unknown standard deviation and accordingly, we use the Student  $t$  distribution for tests. First, we determine the mean value of the performance metrics (i.e., travel time, delay, and stops) at 95% confidence interval. The resulting values indicate the range of population mean at desired confidence interval (in our case 95%). For instance, the system delay of adaptive controller  $156.2 < \mu < 172.7$  indicates that we are 95% confident that the population mean for the system delay with adaptive controller lies between  $156.2 \times 10^4$  and  $172.7 \times 10^4$  seconds. Second, we test the validity of the claim that RMART performs better than other controller using statistical tests. For instance, with a predefined scenario we test whether the mean values of system delay for adaptive controller and RMART controller are significantly (statistically) different. Table 6.2 shows the results for high demand at network-II.

### 6.6.3 Performance comparison: Average Delay

Average delay, stopped delay, number of stops and network wide delay are chosen as the measures of effectiveness (MOE). Table 6.3 shows the sample comparison of average delay for different RL algorithms with different reward functions at different congestion levels for network-I. The results are reported for intersection-8, however



Table 6.2.: System performance for different control algorithms\*

	Fixed control	Adaptive control	RMART
System Delay			
Mean	173	164	130
(in seconds $\times 10^4$ )		(4.9% reduction)	(24.6% reduction)
Population mean range (at 95% confidence )	$167 < \mu < 178$	$156 < \mu < 172$	$121 < \mu < 139$
Stopped Delay			
Mean	118	114	85
(in seconds $\times 10^4$ )		(3.14% reduction)	(27.9% reduction)
Population mean range (at 95% confidence )	$114 < \mu < 122$	$106 < \mu < 121$	$77 < \mu < 92$

( $\mu =$  mean value) at high demand for network-II

(All the improvements are tested and we find  $p < 0.001$  with  $N = 10$ )

the trend is same for other intersections. At low congestion, Q-learning exhibits best performance with R1 and R2, and RMART performs better only with R3. The results are similar for both network-I and network-II. Due to space limitation, we report the results for network-I only. At high congestion, RMART outperforms all other algorithms with all types of reward functions. We made the following conclusions:

- (a) SARSA performs worse than the other two algorithms
- (b) At low congestion, Q-learning is a good choice. Note that, residual queue (R3) is a more appropriate reward, when the congestion level is higher, aiming at avoiding gridlock, however not directly related with delay.
- (c) At high congestion, RMART is the best choice that yields the minimal average delay.

Table 6.3.: Average Delay (seconds) Comparison

Reward	Congestion	Fixed control	Q-Learning	SARSA	RMART
Queue length (R1)	Low	155	135	142	139
		Decrease by	13%	8%	10%
	Medium	236	193	191	179
		Decrease by	18%	19%	24%
	High	353	265	291	227
		Decrease by	25%	18%	36%
Average delay (R2)	Low	155	136	149	145
		Decrease by	12%	4%	7%
	Medium	236	171	187	195
		Decrease by	28%	21%	17%
	High	353	297	290	277
		Decrease by	16%	18%	22%
Residual queue (R3)	Low	155	140	148	139
		Decrease by	10%	5%	10%
	Medium	236	167	201	176
		Decrease by	29%	15%	25%
	High	353	260	276	226
		Decrease by	26%	22%	36%

#### 6.6.4 Performance comparison: stopped delay

Table 6.4 reports the comparison of intersection delay along with percentage of improvement compared to fixed signal control. At low congestion, Q-learning performs best with R1 and R2 for both intersections, however SARSA performs better for intersection-8. At high congestion, RMART yields the best results with all reward functions for both the intersections. Similar to previous results, RMART is the best

choice to reduce stopped delay at signalized intersection at high congestion level of the network.

Table 6.4.: Comparison of Stopped Delay (seconds)

Reward definition	Congestion	Fixed control	Q-Learning	SARSA	RMART
Queue length (R1)	Low	113	91	112	96
		Decrease by	20%	1%	15%
	Medium	183	137	156	123
		Decrease by	25%	15%	33%
	High	284	189	208	156
		Decrease by	34%	27%	45%
Average delay (R2)	Low	113	94	105	104
		Decrease by	17%	7%	8%
	Medium	183	118	131	140
		Decrease by	36%	28%	24%
	High	284	216	207	201
		Decrease by	24%	27%	29%
Residual queue (R3)	Low	113	95	93	96
		Decrease by	16%	18%	15%
	Medium	183	110	118	121
		Decrease by	40%	36%	34%
	High	284	182	216	151
		Decrease by	36%	24%	47%

### 6.6.5 Comparison of system wide performance

Table 6.5 compares the system delays for different algorithms. Q-learning and RMART perform significantly better than the fixed control at all congestion levels.

SARSA has better performance at medium and high congestion levels. At high congestion level, RMART shows the highest percentage of improvement compared to fixed control.

Table 6.5.: Comparisons of system delay (seconds  $\times 10^3$ )

Congestion Level	Fixed Control	Q Learning	Reduce by(%)	RMART	Reduce by (%)	SARSA	Reduce by (%)
Low	235	229	2%	226	4%	235	0%
Medium	434	369	15%	376	14%	402	7%
High	774	622	20%	619	20%	638	18%

#### 6.6.6 Comparison with real time adaptive control

The RL algorithms are compared with a real time adaptive signal control, namely the Enhanced-Longest-Queue-First (ELQF) algorithm. The ELQF algorithm is based on a routing algorithm in data communication network and has been implemented by researchers in traffic control context (Arel et al.[178]; Wunderlich et al.[179]. Wunderlich et al. [179] proposed a variant of this algorithm, namely the Maximal Weight Matching algorithm. For the test purpose, we modified the algorithm to make it more efficient. The changes include provision for minimum and maximum green in the signal-timing plan and adjusting for repetitive phases for the case when a particular approach is highly congested compared to all other approaches. The LQF algorithm uses real time information to make signal control decision. ELQF activates the phase with longest queue size within the defined constraints. Queue size is defined as the number of stopped vehicles at the intersection on red.

Table 6.6 reports the comparison of RL algorithms with LQF algorithm. The RL algorithms perform better than the LQF algorithm in terms of both average delay and stopped delay (not reported due to space limitation). The results are similar for

Table 6.6.: Comparison with Adaptive (ELQF) Controllers

Congestion	Fixed Timing Plan	Adaptive (ELQF)	Q-Learning	RMART
	Intersection-8	Average Delay	(seconds)	
Low	144	177	132	132
Medium	203	207	160	175
High	357	294	270	232
	Intersection-11	Average Delay	(seconds)	
Low	155.13	198.338	145.86	134.53
Medium	236.42	223.947	176.79	177.42
High	353.47	279.32	263.95	228.06

both intersection-3 and intersection-6. Note that both RL and ELQF algorithms use real time traffic information to make signal control decision. The key difference is that, the RL based algorithm have the notion of learning i.e., the controllers learn to make the better decision with training. Similar results are found for network-II.

### 6.6.7 Value of information sharing among neighbors

Sharing traffic information among neighborhood controllers has been mentioned as one of the distinct feature of the proposed RL algorithm in this research. To justify the impact of information sharing we compare the results from two test cases: with and without information sharing. Table 6.7 shows the comparison results for different congestion levels. For Q-Learning, we see improvements at all congestion levels. For RMART, we see improvement for higher congestion and for SARSA negligible deterioration is observed at higher congestion level. It can be concluded that, sharing of neighborhood information helps to improve the performance of RL algorithms.

Table 6.7.: Benefits of information sharing

Test Case		Average			Stopped		
		Delay			Delay		
		With	W/O	Change	With	W/O	Change
		Info	Info.		Info	Info	
Off-policy (Q-Learning)	Low	132.39	133.58	0%	92.8	93.5	0%
	Medium	160.13	168.56	5%	111.3	118.29	6%
	High	270.12	270.37	0%	204.7	204.06	0%
RMART	Low	131.89	131.89	0%	93.09	93.09	0%
	Medium	174.98	172.52	-1%	123.81	121.31	-2%
	High	231.55	284.15	23%	168.42	218.03	30%
On Policy (SARSA)	Low	152.78	152.78	0%	111.43	111.43	0%
	Medium	184.55	192.88	5%	133.75	140.46	5%
	High	320.82	319.31	0%	247.58	245.92	0%

### 6.7 Emissions estimation using MOVES2010b

To evaluate the control algorithms from sustainability consideration, we estimate and compare emissions (CO, CO<sub>2</sub>, NO<sub>x</sub>, VOC, PM<sub>10</sub>) for the major seven roads. Since all the roads are two-ways, in total we have 14 road links. Motor Vehicle Emission Simulator (MOVES2010), developed by the U.S. EPA (EPA, 2012), is used to estimate the emission. EPA has regulated to use MOVES2010 for emission conformity analysis (except, California) for states in the U.S. MOVES2010 have the capability to estimate emission with time dependent speed profiles (Lin et al.[155]; Xie et al.[83]). We simulated the morning peak hour (8:00 am to 9:00 am) with higher level of congestion assuming the geographical and meteorological details of Tippecanoe County, Indiana for the year 2012. Only passenger cars with Gasoline type of fuel are used in the analysis. Although the values obtained are only for an hour, generally the analysis is done for the entire day or for the week. If we assume 4 hours of peak congestion

each day and assume the conditions prevail as we simulated through MOVES2010, then we see significant reduction in the emission level for a typical work week. Table 6.8 shows the results. It can be seen that RMART algorithm can significantly reduce emissions from road network.

Table 6.8.: Comparison of Emissions (Network-I)

Pollutants	Control Schemes			
	Fixed Timing	Adaptive	Q-Learning	RMART
CO (g/hour)	10683	4318	4394	4247
Weekly total (g)	213656	86357	87883	84935
NO <sub>x</sub> (g/hour)	732	312	308	302
Weekly total (g)	14632.34	6246.612	6155.406	6037.2
VOC (g/hour)	264	108	106	104
Weekly total (g)	5290	2151	2112	2079
PM <sub>10</sub> (g/hour)	38.1	16.33	16.2	15.78
Weekly total (g)	762.03	326.55	320.23	315.6072
CO <sub>2</sub> (g/hour)	841070.6	345631.6	339527.5	334037.4
Weekly total (g)	16821412	6912632	6790550	6680748
Energy consumption (j/hour) × 10 <sup>5</sup>	117032	48093	47244	46480
Equivalent fuel (in gallons per week)	1777	730	717	705

### 6.8 Summary and concluding remarks

The research presents and implements RL based signal control algorithm, namely RMART, which adapts with the traffic dynamics through learning from the stochastic environment. Our results show the total system delay and stopped delay are lower for RMART compared to fixed control and adaptive control (i.e., the variant of longest-queue-first). The obtained results are statistically significant ( $p < 0.001$ ). Adaptive controllers are quite different from the RL based controllers in terms of principle and implementation (Mirchandani and Head [145]; Abdulhai et al. [149]). The results from our empirical tests show that, learning based controls can perform better than the adaptive control. In addition, the RL controllers perform much better than the fixed timing plan. This implies that, learning is a useful and potential feature in the real time signal control algorithms and can improve the performance of the controllers.

The inclusion of neighborhood information sharing in the RL algorithms is found to improve the performance (H2) in most cases for the RL algorithms. Information sharing facilitates the controller to make decisions based on the overall congestion states of its neighborhoods. Without neighborhood information, the controller makes decision based on local information. However, the state of traffic flow of the neighbors affects the future traffic conditions (simplest example would be the arrival rate at the downstream intersection). This is particularly important at higher congestion level (near saturation).

To assess the benefits in terms of reducing vehicular emissions we compare the levels of emissions of RMART with other algorithms. The levels of emissions ( $\text{CO}$ ,  $\text{NO}_x$ ,  $\text{PM}_{10}$ ,  $\text{CO}_2$ ,  $\text{VOC}$ ) are significantly lower for the network when RMART is implemented (H4). The reduction in number of stops and average stopped delays at the intersections with RMART can be the major reasons behind lower level of emissions. Further, we also observe lower energy consumption for RMART compared to other algorithms. Therefore, RMART performs better than the other algorithms in terms of reducing vehicular emissions and energy consumption for the entire network.



Note that, our test cases do not indicate a better performance of the multi-reward structure. The random nature of on-road traffic (e.g., drastic changes from low congestion to high congestion due to an incident) is the key motivation behind the implementation of multi-reward structure. However, the multiple reward structure did not have better performance in our tests compared to the other learning algorithms. This phenomenon can occur due to the basic principle of the algorithms, i.e., learning over time. To test the algorithms, we applied varying demand over time and report the results for the last 15 minutes of the simulation. The algorithms with single reward structure learn over the simulation period. Accordingly, these algorithms are also able to take the best decision even in the most random environment (sudden change from low to high congestion). As a result, we do not observe significant improvement for the multi-reward based RL algorithm.

To conclude, the RMART algorithm as illustrated by the results has shown higher potential to reduce delay at highly congested states. In addition, this research shows the advantages of information sharing and potential of emissions reduction of the RL based algorithms.

## CHAPTER 7. INTEGRATED EMISSIONS TOOL

### 7.1 Introduction

A system or user level strategy that aims to reduce emissions from road networks requires a rigorous assessment of emissions inventory for the system to justify its effectiveness. In other words, it is necessary to estimate the total emissions for the transportation network before and after the implementation of a particular policy. For instance, a traffic signal control scheme that is optimized for environmental goal is expected to cause less emissions compared with the settings without any environmental goal. To assess the benefits of the new signal control scheme it is necessary to compare the emissions level with base case (i.e., scheme without any environmental goal). Further, air quality assessment is a requirement for the local agencies for conformity and funding decisions. The Clean Air Act section 176(c) requires transportation conformity to ensure that federally supported highway and transit project activities support and move towards the state air quality implementation plan (SIP). Federal Highway Administration (FHWA) requires transportation conformity studies to ensure that federal funded and approved projects are consistent with air quality goals set by National Ambient Air Quality Standards (NAAQS).

The previous chapters discuss strategies that include providing emissions related descriptive information (chapter 3), personal mobility carbon allowance schemes, learning based traffic signal control with environmental objectives. This chapter describes an integrated traffic-emissions simulator framework that can be used to assess the strategies described in the earlier chapters. The framework does not require any specific traffic simulator. Any micro-level simulator should fit in the framework that can provide outputs in second-by-second manner. Motor Vehicle Emissions Simu-

lator (MOVES) developed by the U.S. Environmental Protection Agency is used in the integrated framework. This is because, EPA has regulated to use MOVES to develop state implementation plans (SIPs) and regional or project-level transportation conformity analyses. MOVES is a modal-based emissions estimator that accounts for vehicle operating modes defined by factors like speed, acceleration, road grade, curvature, and so on. MOVES has the ability to include alternative types of fuel and different type of vehicles. MOVES can be used to conduct analysis at different scales including regional, state, and project level (e.g., small road network at county level). The development and refinement of MOVES will be an on-going process and MOVES will be considered as the standard tool for quantifying the emissions level of road networks in the United States.

Integration of MOVES with traffic simulator can be outlined as a input-output process. The second-by-second vehicular activities from traffic simulation serve as input for MOVES and the emissions inventory for a transportation network can be estimated [80, 81, 83, 84]. The input from traffic simulators can be any of the following formats: (I) Average speeds for the links in the network, (II) Link Driving Schedule (LDS) for each link of the network. LDS is the change in speed with time for a link in the network (generally done for a representative vehicle or by means of sampling), (III) Operating mode distribution of vehicles on the link. While option I is commonly used in practice, option II and option III can take the advantages regarding vehicular activity data and dynamic capability of MOVES to report time dependent emissions ([180]. Input data for MOVES for the analysis signalized intersections require more details and careful selection of vehicular activities. EPA suggests to use a series of LDS to represent cruise, acceleration, idle, and deceleration behavior in a congested intersection. Also notions of approach and departure link should be incorporated. Two challenges with this link segmentation technique are: (a) the overlapping of cruise, idle, acceleration, deceleration, and idle zone (e.g., the vehicular activity 100 ft. from the stop line at red and green phases), (b) Finding a single representative LDS that features all the vehicles within that segment for the analysis period (e.g.,

one may need to pick one LDS from 400 vehicles for a single hour analysis). Option III requires computing fractions of the fleet travel times spent in each mode of operations. The computation is based on ratios of mode travel times to total travel times and significant post processing is required [180].

Option II is commonly used because trajectories are relatively easy to obtain and can be converted into LDS for links. An alternative to the link segmentation technique is to input the second-by-second trajectory of the vehicles. This allows to overcome the first limitation of link segmentation technique. We do not have to separately model idling, cruise, acceleration, and deceleration because vehicular trajectories accommodates all possible activities. However, the challenge is to find the representative trajectory for a link that may be traversed by thousands of vehicles during the analysis period. Sampling techniques with carefully designed sample criteria can be used to reduce the size of the problem. However the computation becomes significantly expensive as the size of the problem grows. A sample of 5000 vehicles for 150,000 original data can take multiple hours (if not days). This makes the trajectory approach inefficient in terms of computation and obviously accuracy is compromised as the sample size is constricted.

This research proposes a novel technique based on similarity based clustering to find the representative vehicle trajectories. The technique uses the dynamic time warping distance as the similarity measure in clustering which is more appropriate for curve alignment compared with Euclidean distances and its variants which is more common in the literature. A recent approach by [181] applies K-means clustering with Euclidean distances. Two major limitation exists with this study. First, the Euclidean distance is not an appropriate similarity measure for time series type of clustering. Euclidean distance measures cannot account for this shift in time phase. Euclidean distance fails to provide a correct measure of similarity between two sequences because of its high sensitivity to changes in the time axis [182, 183]. Second, K-means algorithm requires the number of clusters to be predefined.

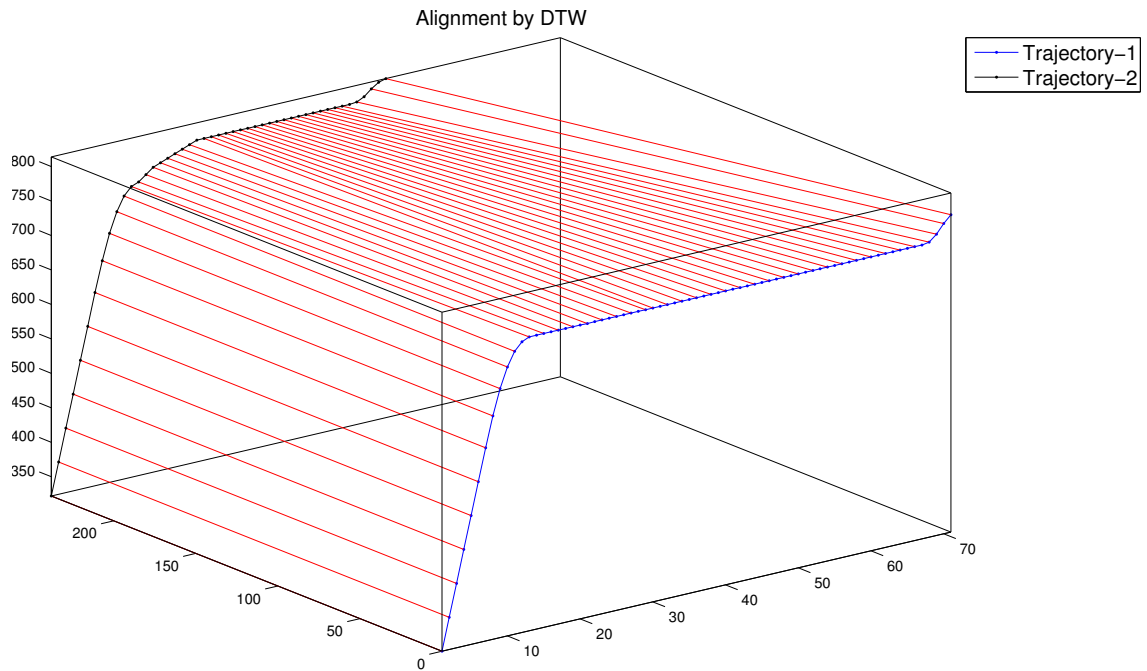


Figure 7.1.: Alignment by DTW

Our proposed technique overcomes both limitations. First, we use a dynamic time warping measure instead of Euclidean distance. The advantage DTW offers is that it can align two times series having similar shape but not aligned in time. DTW allows elastic shifting of the time axis to identify similar shapes with different phases. We applied agglomerative hierarchical clustering that does not require the number of clusters as input. The number of clusters is determined using inconsistency coefficient measure and also it is possible to assign maximum number clusters. Figure 7.1 illustrates the DTW similarity for two trajectories with different lengths. The trajectories are overall similar but shifted in time. Finally, our proposed technique reduces the computation requirement significantly with negligible compromise in the accuracy of estimation.

The goals for this research are as follows:

- (a) To present an integrated framework of traffic and emissions simulator (MOVES) that can be used to evaluate user and system level emissions and energy reduction policies
- (b) To develop a similarity based clustering technique that finds the representative link driving schedules for MOVES input from second-by-second trajectory data.
- (c) To demonstrate the applicability of the technique in terms of accuracy and computational efficiency for analyses of signalized intersections.

The rest of the chapter is organized as follows: section 8.2 provides an overview of MOVES2010, section 8.3 described the integration framework, section 8.4 and section 8.5 discuss the dynamic time warping based clustering technique in details, section 8.6 demonstrated the applicability of our proposed technique, and finally we discuss the limitations and future research direction in section 8.7.

## 7.2 EPA Regulated Estimation Tool: MOVES2010

MOVES (MOtor Vehicle Emission Simulator) developed by the U.S. EPA was first released in December 2009. In March 2010, MOVES was officially approved for use in state implementation plans (SIP) and transportation conformity analysis [184] outside California. MOVES2010b is the most recent update of the tool. We will use the term "MOVES" throughout the manuscript that refers to refer to MOVES2010b version. MOVES can be used both as an inventory model (estimation of total emissions for a network or region or even state). The VMT (vehicle miles traveled) and vehicle fleet composition information are used to compute the total emissions. If used as an emissions rate model MOVES only provides the emissions rates and post processing is required to obtain the total emissions. MOVES is one of the micro-scale vehicle emissions simulator that uses instantaneous (e.g., second-by-second) operations of individual vehicles on the road [185], [180]. Among the few microlevel emissions models, International Vehicle Emission (IVE) model [186] and Comprehensive Modal

Emissions Model (CMEM) [187], [17] are well known for estimating vehicular emissions. MOVES is one of the most sophisticated emissions models that can be applied at different modeling scales: from the micro-scale (project-level, e.g., parking lot) to the macro-scale, where national-scale inventories are being generated for precursor, criteria, and greenhouse pollutants from on-road mobile sources [185].

### 7.2.1 Estimation Method in MOVES

The emissions estimation in MOVES is primarily based on power demand of the vehicles. Two categorical bins are defined in the MOVES database: source bin and operating mode (op-mode) bin. The source bin is defined based on Vehicle characteristics (type of fuel, engine type, make and year, loaded weight, and engine size). The Operating mode bins are defined based on the second-by-second vehicle characteristics (idling, accelerating, cruising, decelerating, and so on). Vehicle Specific Power (VSP) is used as the measure of the power demand [188] placed on a vehicle under various driving modes. VSP is defined as the power demand on the engine per unit of vehicle mass to surmount the inertial acceleration (power demand), rolling resistance, road grade, and aerodynamic drag [188], [189]. Studies ([190], [191], [185]) show direct correlation between VSP and vehicular emissions. IVE [17], and CMEM [17] also use VSP based approach [186] to estimate emissions from road networks. VSP is differentiated based on driving cycles and vehicle characteristics. Other than the meteorological factors, vehicle characteristics highly impact the emissions estimation. Also, the aerodynamic drag varies by vehicle size, type, and loads. For instance, the aerodynamic drag for a compact car and for a full size car will be quite different [189]. Detail description on the emissions estimation method can be found in the MOVES user guide [180] and EPA guidelines for GHG and energy estimation from road networks [192].

### 7.2.2 Data input for MOVES

MOVES requires several traffic network related attributes for emissions estimation. These include

- Type of links (freeway, arterial, parking lot, truck terminal, and so on ) based on the type of access (restricted vs. unrestricted)
- Length of link, grade (slope), and average speed of vehicles on the link for the analysis period.
- Special treatment is applied for the analysis of signalized intersections. Generally, the link is divided into several segments to account for the stopping of the vehicles at red.

Currently, MOVES has five categories of road types. The default database contains: a) Rural roads with restricted and unrestricted access, b) Urban roads with restricted and unrestricted access, c) Off-network (this is primarily for the extended idle process in parking lots or truck terminals). Note that, the selected road type may or may not exist in the geographical bounds of selected county and MOVES only computes results for the existing road types for that county.

The time span including the year, month, day (weekday or weekend), and starting-ending hours needs to be defined precisely. The finest resolution is one hour in MOVES. For project level analysis, any county in the U.S. can be chosen for analysis. Further, one can customize the county level parameters using the option *custom domain*. The *custom domain* requires the following data:

- (a) GPA fraction which is defined as the fraction of the county within a fuel Geographic Phase-in Area (GPA).
- (b) Atmospheric pressure in units of Bar or Hg. The average for low altitude is 28.9 and average for high altitude is 24.6.
- (c) Vapor Adjust which is defined as the refueling vapor program adjustment fraction.



(d) Refueling Spill which is defined as the refueling spill program adjustment fraction.

The vehicle-fuel combination is required. Currently, MOVES has the following types of fuels Source Use Types (i.e., the types of vehicles). The available fuel types are as follows: Compressed Natural gas (CNG), diesel fuel, electricity, gasoline, and liquefied petroleum gas (LPG). The available vehicle types are: combination long-haul and short-haul truck, intercity bus, light commercial truck, motor home, motorcycle, passenger car and passenger truck, refuse truck, school bus, single unit long haul and short Haul truck, and transit bus. MOVES requires the age distribution of the vehicles on the network to be analyzed. The emissions are different for vehicles at different ages. The default database is available in EPA website that can be used when local data cannot be accessed. Similar to the vehicle-age distribution, distribution of fuel type use in the network is also required. MOVES provides a county level default database for fuel type composition.

### 7.3 Integration with Traffic Simulation

The recent advances in the emissions modeling allow to compute emissions accounting for second-by-second operation characteristics of a vehicle on a road segment [180], [81]. The instantaneous emissions models are useful for temporal and spatial analysis of different policies and emissions reduction strategies at fine-grained levels. These models overcome the under-estimation problem associated with the air quality models that assume emissions are evenly distributed along a road section [193]. Now, micro-scale models like MOVES require detailed and precise information regarding vehicle operation and location. Without the finesse of the data, expected accuracy level and accordingly the benefits are lost. On the other hand, collecting precise data on instantaneous vehicle operations for even a small network is tedious, expensive, and time consuming. An obvious solution to this problem is the use of micro level traffic simulation model that can effectively produce all the required inputs with desired details for the instantaneous emissions model.

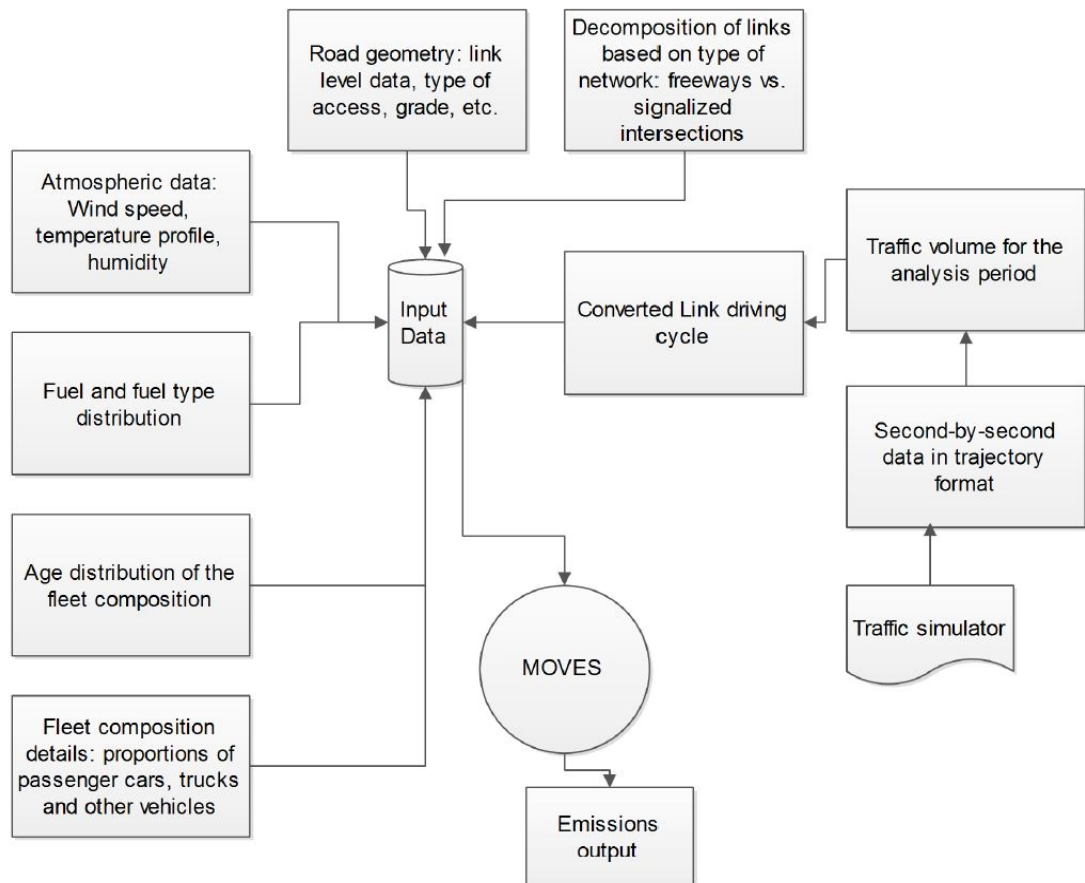


Figure 7.2.: Framework: integrated traffic and emissions simulator

This research provides a general framework to integrate MOVES with a traffic simulator. MOVES is build on Java platform and the databased is in MySQL format. In addition to the visual interface, MOVES can be executed from scripts in UNIX or LINUX or command prompt in Windows OS. Batch mode is possible as well for series of scenario analysis. The MOVES run specification is required to be saved as an XML file and later can be revoked from the system. Figure ?? shows the steps performed to integrate MOVES and the traffic simulator.

### 7.3.1 Applications of integrated tool

The potential applications of the integrate tool are as follows:

- Assessment of the air quality: The integrated tool will be able to output emissions level at link and network level in terms of emissions rate (gm/hour) or total emissions (in mass units). By means of an emissions dispersion model (for instance, the Gaussian dispersion model), the emissions concentrations will be reported.
- Effectiveness of provision of emissions information: The tool will allow us to assess the network state when descriptive emissions information will be provided to the system users. As described in chapter 4, we hypothesize that the travel decisions (departure time and route choice) are influenced by the information provision and this tool will help us to assess the resulting network state.
- Evaluation of signal control strategies
- Evaluation of pricing policies such as carbon budgeting for personal travel.

#### 7.4 Methodology: HC-DTW technique

The proposed methodology applies hierarchical clustering technique with dynamic time warping (DTW) (dis)similarity measures. Details on the methodology can be found in Everitt et al. [194]. Figure 7.3 shows the steps of the technique proposed in this research. Hereafter we refer to our clustering technique as hierarchical clustering with DTW or HC-DTW technique. The inputs are the vehicular trajectories of all links in the network. The DTW algorithm provides the shortest DTW path distance for any two trajectories. For a link we compute the DTW distances for all trajectories and then create a square matrix of size equals to number of trajectories. Each element in the matrix is the DTW measure with all other trajectories for the link. This matrix acts as the distance matrix for the hierarchical clustering. Note that we do not use k-means method because the objective is more curve alignment based on similarity measures. The k-means algorithms are more suitable for density based clustering where the focus is more on the location.

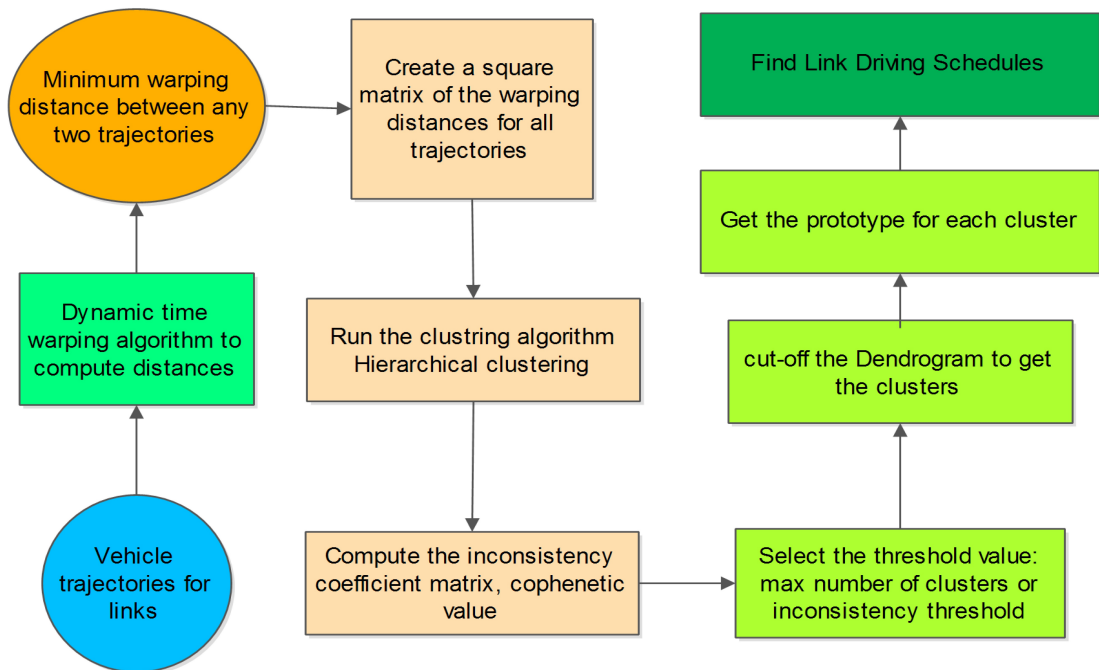


Figure 7.3.: Link Driving Schedule (LDS) finding methodology

Unlike k-means algorithm, hierarchical clustering does not require the number of clusters as an input. One can follow either agglomerative or divisive method to obtain hierarchical clusters. Both approaches provides the clusters and can be visualized using a dendrogram. This study follows agglomerative method. The clustering tree starts with all elements condensed in a single cluster on the top and each element a separate cluster at the bottom. One particular challenge is to find the optimal number of clusters. In other words, where should we cut the clustering tree? This research follows two approaches to cut the clustering tree: (a) inconsistency coefficients, (b) maximum number of clusters allowed. After obtaining the clusters, a prototype from each cluster is picked. The prototype trajectory is the member of the cluster that minimizes the distance with all other members within that cluster. The prototype trajectory is then converted into LDS by computing the instantaneous speed. The next subsections provide details

#### 7.4.1 Computing DTW measures

Dynamic time warping (DTW) [195, 196] is a similarity measure that can be applied for unsupervised clustering of time series. DTW has been used in several areas that include speech recognition, gesture recognition, data mining, robotics, and biometric data alignment problems. DTW finds an optimal alignment between any two time dependent sequences. The optimal alignment (also known as the minimum distance wrap path) is determined by assigning successive values of one sequence to a single value of the other. This enables DTW to find alignment even when the time series are of different lengths.

Consider two sequences  $u$  and  $v$  with lengths  $m$  and  $n$  respectively. The sequences are:  $u : \{u_1, u_2, \dots, u_i, \dots, u_m\}, v : \{v_1, v_2, \dots, v_j, \dots, v_n\}$ . A  $n \times m$  grid can be constructed where each element in the grid represents an alignment between any two objects from  $u$  and  $v$ . A warping path  $W^p$  is a sequence of elements from this grid ( $W^p = w_1, w_2, \dots, w_k, \dots, w_K$ ). Each element  $w_k$  is defined with element index

from  $u$  and  $v$ . The sequence  $W$  maps the elements of the  $u$  and  $v$ . Classical DTW path has several constraints:

- **Boundary conditions:** The warping path starts in first point of both sequences and ends in last point of both sequences. Mathematically,  $w_1 = (1, 1), w_K = (n, m)$
- **Continuity:** The warping path is restricted to the adjacent cells in all directions. Consider two sequential elements  $w_k = (u, v)$  and  $w_{k+1} = (\tilde{u}, \tilde{v})$  in  $W$ . Now the conditions  $\tilde{u} - u \leq 1, \tilde{v} - v \leq 1$  must hold.
- **Monotonicity:** The points in  $W$  are monotonically spaced in time.

Exponentially high number of warping paths are possible that satisfy the above conditions. DTW algorithm finds the path with minimal cost (distance).

$$DTW(u, v) = \min(1/K) \sqrt{\sum_{k=1}^K w_k} \quad (7.1)$$

Denote  $\lambda(i, j)$  as a cumulative distance defined as:

$$\lambda(i, j) = d(u_i, v_j) + \min\{\lambda(i-1, j-1), \lambda(i-1, j), \lambda(i, j-1)\} \quad (7.2)$$

Dynamic programming can be used to find this recurrence equation. Details on the algorithm can be found in Kruskall and Liberman [197].

Figure 7.4 shows an example of computing DTW minimum path for two vehicular trajectories of different lengths (45 seconds vs. 70 seconds).

#### 7.4.2 Hierarchical clustering

Hierarchical clustering partitions the data in sequential steps and the number of clusters is not predefined. The clustering method yields a series of partitions that may include a single object or all the objects in the data. Further classification of

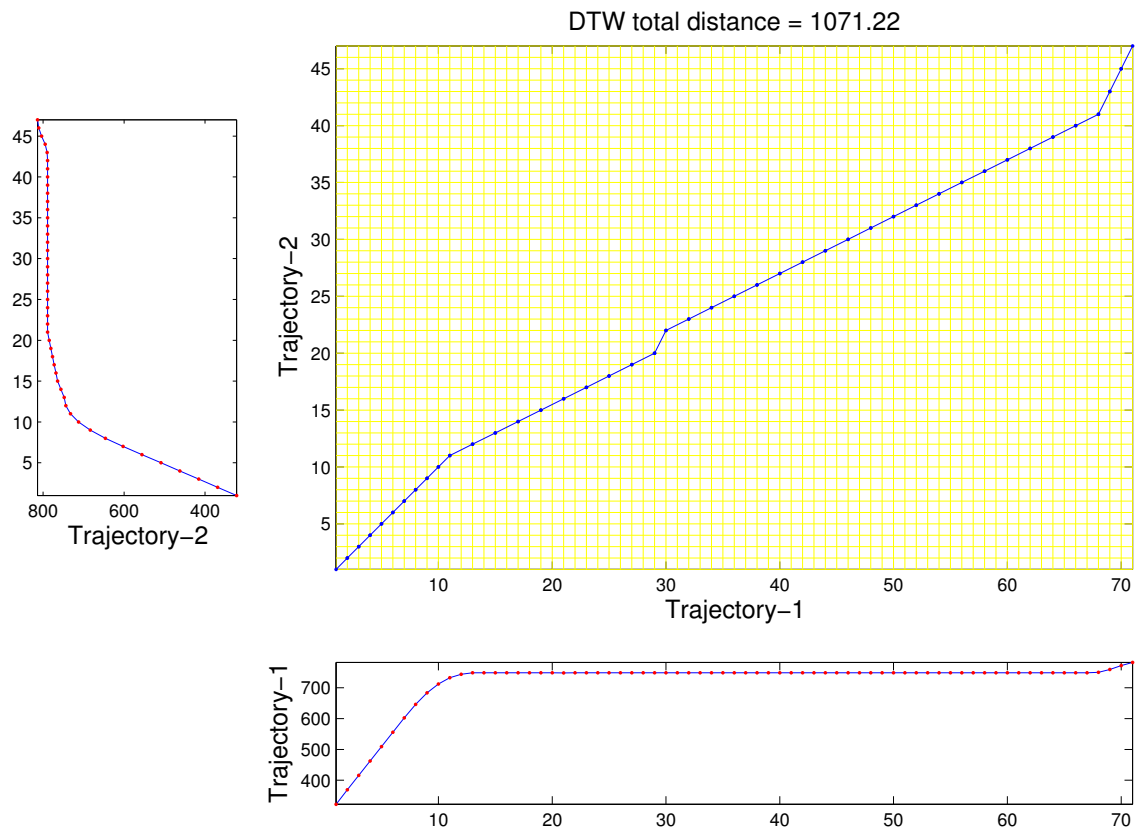


Figure 7.4.: DTW optimal path computation

hierarchical clustering leads to two subdivisions: agglomerative and divisive methods. This research follows agglomerative method that starts with all objects into a single cluster and ends with each object as a distinct cluster. At each stage of clustering agglomerative method fuses objects or groups which are most similar. The similarity measure dominates the patterns of partitioning. Finally, a binary hierarchical tree (linkage) is found. Clustering can be implemented with different specification of linkage. Single linkage (also known as *nearest neighbor*) defines the group distance as the distance between the closest pair of points of each group. Complete linkage (*farthest neighbor*) refers to the case where group distance is defined the distance between the farthest pair of points of each group. Average linkage clustering defines group distance as the average distance between all pairs of points. The results reported in this research are obtained from average linkage hierarchical clustering. After obtaining the dendrogram (binary tree) one needs to decide where to cut the tree (in other words we need to determine the number of clusters). This research follows two techniques: (1) cutting at an height that yields desired number of clusters, (2) cutting the inconsistent links using inconsistency coefficients.

#### 7.4.3 Consistency measures

The comparison of the height of each link in a cluster tree with the heights of neighboring links below it in the tree can provide a direction to determining optimal number of cluster in a tree (MATLAB statistical Toolbox, [194, 198]). If two links (vertically spaced) have almost the same height, the cluster distinction between these two levels is not significant. These links are characterized by higher level of consistency. Obviously links with lower level of consistency (or inconsistency) are desired. Higher level of inconsistency indicates that the distance between the objects being joined is approximately the same as the distances between the objects they contain. The links in the dendrogram that have significantly different height compared with the height of the links below can be identified as inconsistent. Outputs from hierar-



chical clustering can be used to determine the the relative consistency of each link that is denoted as the inconsistency coefficient. The coefficient is a ratio of the height of the link to the average height of all links that lie below the link. High value of inconsistency coefficient indicates the joining of distinctly featured clusters. On the other hand, low value indicates that the clusters may be insignificant and possibility of merging is high.

#### 7.4.4 (Dis)similarity measures

A property of a hierarchical cluster tree is that any two data objects must be connected to each other at some hierarchical levels of the tree. The *cophenetic* distance between any two objects is defined as the distance between the two clusters that contain these two objects. The distance between two clusters is measured as the height of the link in the tree. Intuitively, if the clustering is valid, the linking of objects in the cluster tree will be strongly correlated with the distances (DTW measures in our case) between objects in the original data. The *cophenetic correlation coefficient* measures this correlation between linkage distances and (dis)similarity distances ([199, 200]). A *cophenetic coefficient* closer to 1 indicates higher validity of the output from hierarchical clustering.

### 7.5 Demonstration of the technique

The applicability of the proposed technique is demonstrated with the data from of a corridor with five signalized intersections. The corridor is located in the city of West Lafayette, Indiana in the U.S. The trip demand and signal settings are obtained from a previous study [201]. The signal settings are based on Econolite controllers and designed for maximum congestion period. The network along with demand and signal settings is simulated using commercial traffic simulator VISSIM [202] and trajectories are collected for 15 minutes period.

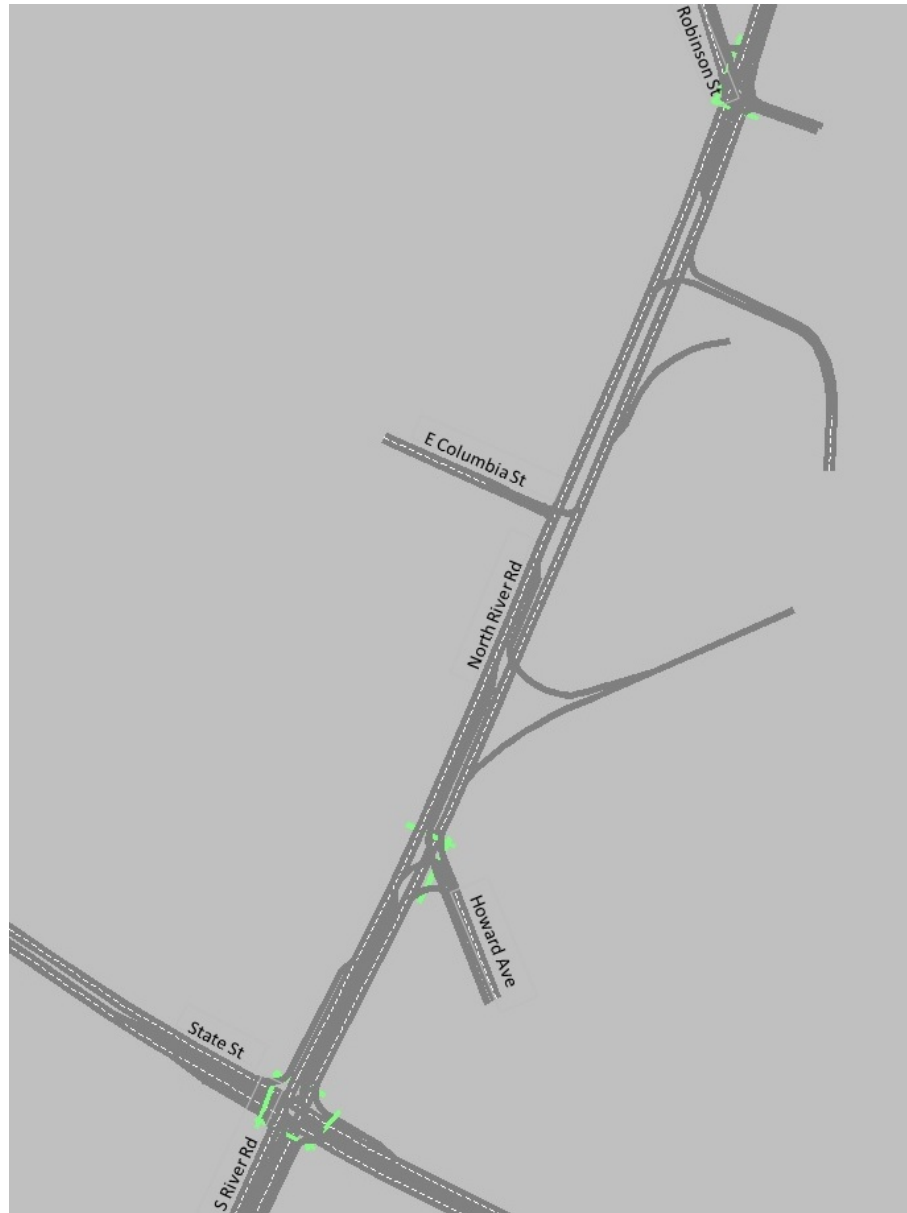


Figure 7.5.: Test network: five intersection corridor

### 7.5.1 Comparing the performance of HC-DTW

To demonstrate the applicability and benefits of the HC-DTW technique we compare the emissions estimates obtained from three different methods. The first method is the HC-DTW technique that uses the Link Driving Schedule (LDS) set obtained by clustering. Second method uses average speed of the link to estimate emissions which is the most commonly used technique in practice. The third method uses trajectories of all vehicles on a link as input for MOVES. The last technique provides the most accurate estimate of emissions from MOVES because the activity of each vehicle is considered as a separate link input into MOVES. For instance, if we have 1000 vehicles traversing on a link during the analysis period, we have to create 1000 instances of the link in the MOVES input file. Since each vehicle's activity is considered separately, different operating modes are considered by MOVES with higher accuracy. Hereafter we refer to this approach as the *exact method*. The goal of this section is to demonstrate that the emissions obtained from our proposed approach is not significantly different from the those obtained from *exact method*.

We tested our technique with seven scenarios with the trajectories from the links of the signalized corridor. The test cases are constructed in such a way that variation in vehicular activities, resulting from varying congestion level or simply due to the existence of traffic signals, on road links can be represented. Although many possible combinations of vehicular activities exist, six types of activities are considered: (I) Cruise-Decelerate-Idle, (II) Idle-Accelerate, (III) Cruise, (IV) Cruise-decelerate-Accelerate, (V) Idle-Accelerate-Decelerate-Idle, and (VI) Idle. Table 7.1 shows the percentage of each type of vehicular activities for each case considered in this study.

For case 1, 39 vehicles traverse the road segment during the analysis. To compute the emissions using the *exact method*, we input 39 LDS (one LDS for each vehicle) in MOVES and compute the emissions for the link. Next, we apply the HC-DTW technique and we find three representative clusters. A prototype from each cluster is obtained to find the LDS. These LDSs are used as input for MOVES with corresponding traffic volumes. Likewise we estimate the emissions for all other cases.

Further, we report the emissions estimated by inputting simply the average speed of the link for all cases (case 1 to case 7). Table 7.2 reports the emissions from these three approaches.

Further table 7.2 reports the percentage difference from the *exact method* for average speed and HC-DTW techniques. The differences for average speed method are found to be significantly higher compared with the HC-DTW technique. One intuitive cause is that the average speed method is not able to capture variations in speed profiles. For case 1, we observe 12 vehicles belong to a cluster where they do not have to stop on red phase of the signal or simply cruise through the link. The other two clusters (with 19 and 8 vehicles respectively) are characterized with acceleration, cruising, and then deceleration phase. Average speed for cluster-1 is about 22 mph and for the other two clusters the average speed is about 7.5 mph. The average speed method overestimates the speed for the link and uses a value of 13 mph and uses the corresponding driving cycle to estimate the emissions. This causes underestimation of emissions for that link. At lower speed (0-10 mph) the emissions are high, the average speed approach fails to capture that. Whereas by clustering we find representative speed profiles and emissions values are estimated with three LDS inputs that are close to *exact method* (table 7.2).

The difference values for  $PM_{10}$  is very high for cases 2, 3, and 7 with HC-DTW technique. However the difference values are still smaller compared with average-speed technique. The emissions estimate for  $PM_{10}$  are very small in terms of magnitude. It is possible to have accumulated error that leads to high percentage error although the absolute errors are small. HC-DTW provides one LDS for each cluster as a prototype of all vehicular activities in the cluster. Smaller difference in speed profiles between a member and the representative LDS can lead to higher degree of percentage difference as well.

Further we observe higher error percentage for CO emissions in case 2 and case 6. Both cases have higher percentage of cruise-decelerate-idle activity. It is possible that one single prototype of LDS cannot represent three activities: cruise, decelerate,

Table 7.1.: Description of test scenarios: vehicular activity proportions

Test Scenario	Vehicular Activity (%)					
	Cruise- Decelerate -Idle	Idle- Accelerate	Cruise	Cruise -Decelerate -Accelerate	Idle- -Accelerate Decel-Idle	Idle
Case 1	31		21	48		
Case 2	40			55		5
Case 3	51	8	41			
Case 4		44		41		15
Case 5				46	42	12
Case 6	48	5			47	
Case 7		9		51	40	

idle. Higher number of clusters to represent cruise-decelerate, decelerate-idle, and idle separately can improve the results. We observe that the difference is higher as we increase the number of links (compare case 1 and case 2). This is mainly because of the accumulation of errors for each vehicle. This can be addressed by increasing the number of clusters when number of vehicles gets higher.

Further, we tested the technique for a case where the variation of speed profiles is small. Three clusters with slight variation were chosen and all represent cruise-decelerate-idle activity. We found the difference with *Exact method* are 2% and 2.5% for HC-DTW and average-speed techniques respectively. This implies that the benefits of HC-DTW technique is marginal in cases where the vehicular activities do not vary much.

### 7.5.2 Computational time

We also observe significant reduction in running time when HC-DTW technique is applied. Table 7.3 shows the computational time for each cases. To conclude from our results, we do not have to compromise accuracy and obtain the solutions in much faster time. The running time is a function of the links in the network. For large networks with links in the order of thousands, the computational time can go up to days [180]. With the HTC-DTW technique it is possible to reduce the computational time. The analyst can define the error tolerance and the corresponding number of clusters to be used for large scale analysis. Further, it is possible to use real-world data as input to this algorithm and that will expedite the emissions estimation process for local transportation agencies while assessing air quality for transportation networks.

### 7.5.3 Results with two signalized intersections

This section illustrates results obtained for seven links (signalized intersections) using the HC-DTW technique. The results report clusters of trajectories. It is straight forward to convert a trajectory to a LDS, therefore we do not present results for LDS

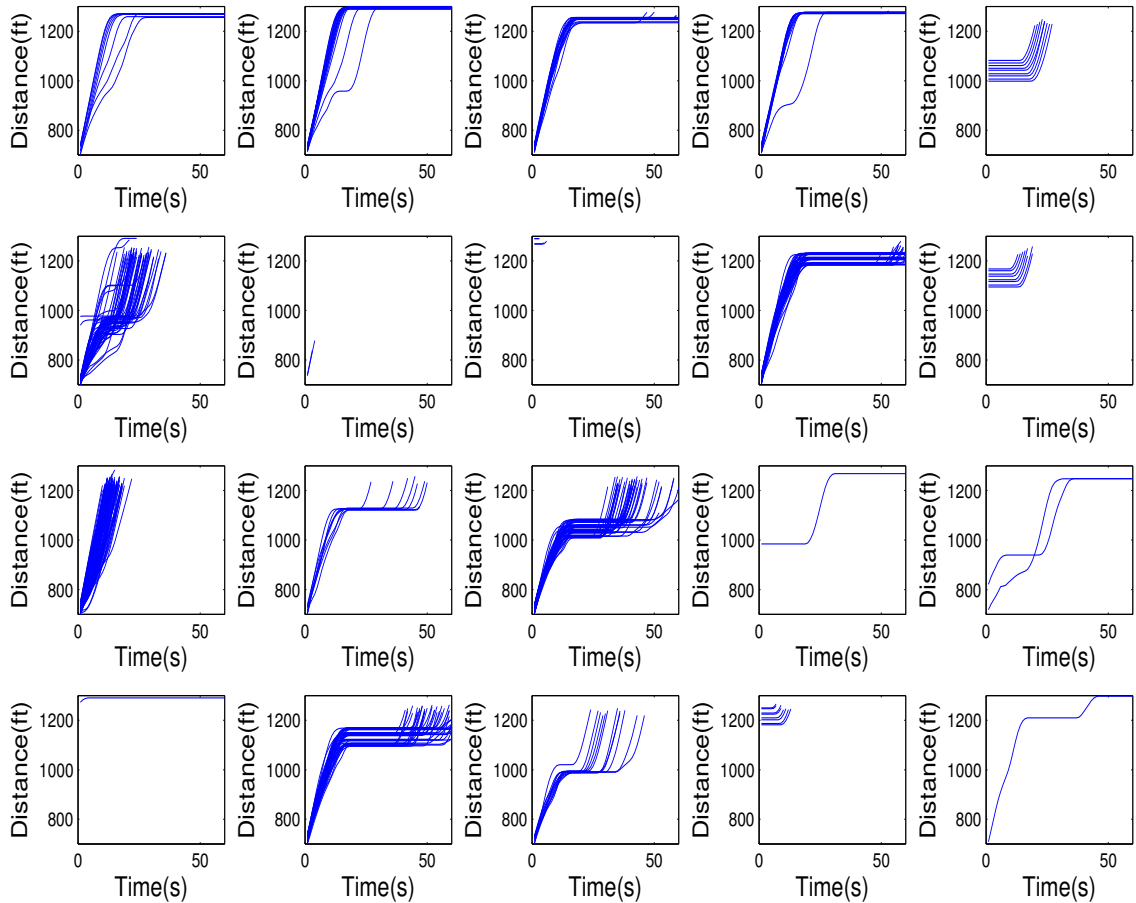


Figure 7.6.: Link-3 for intersection-1

objects. Table 7.4 summarizes the results for seven links from the test network. Figures 7.6 - 7.10 show examples of the clusters obtained and exhibit the heterogeneous vehicular activities on signalized intersections. Further the cophenetic coefficients have higher values close to 1 indicating higher degree of validity of the results obtained from clustering.

#### 7.5.4 Summary of findings

Several insights can be drawn from the observations. The major findings from our research are as follows:

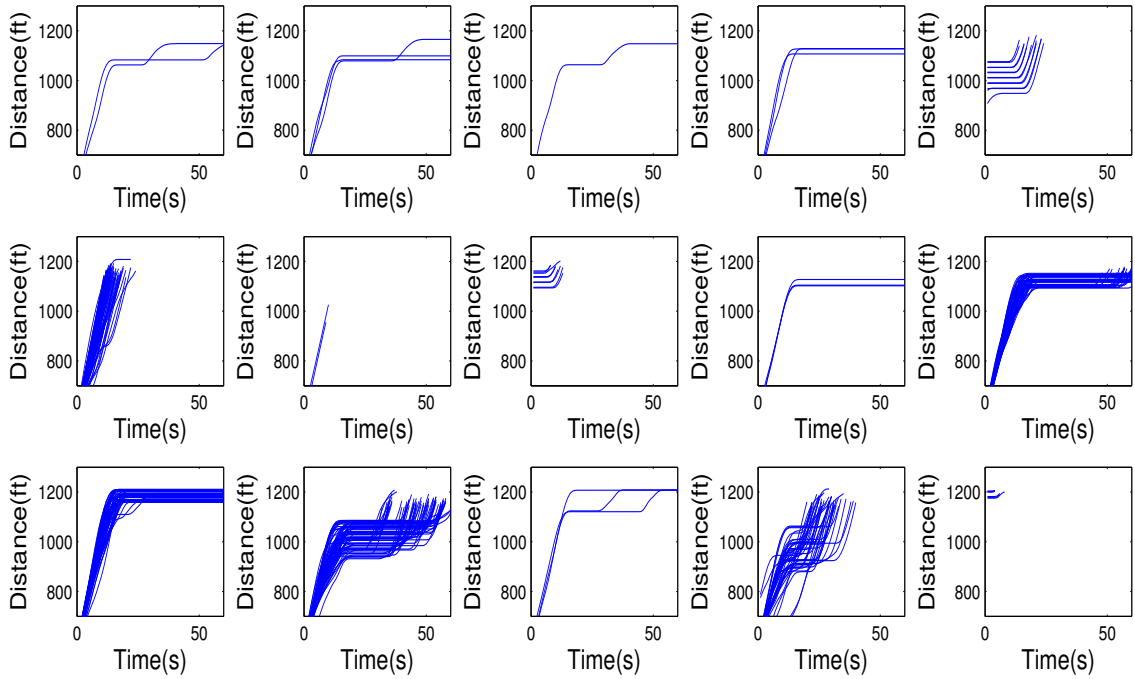


Figure 7.7.: Link-4 for intersection-1

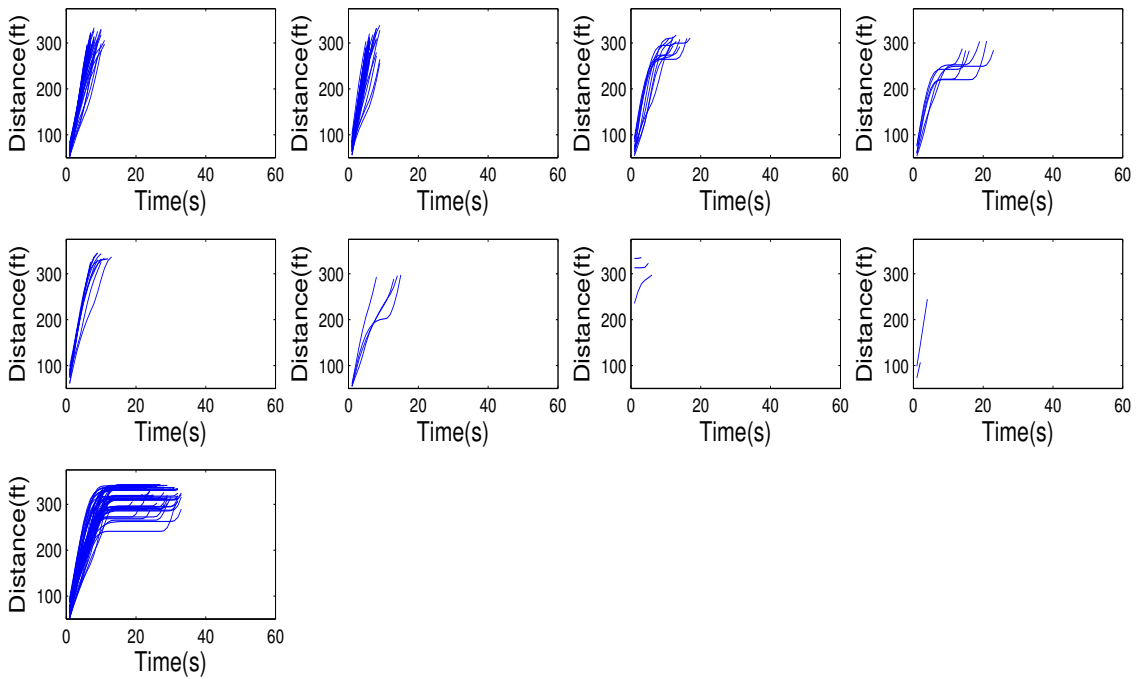


Figure 7.8.: Link-1 for intersection-4



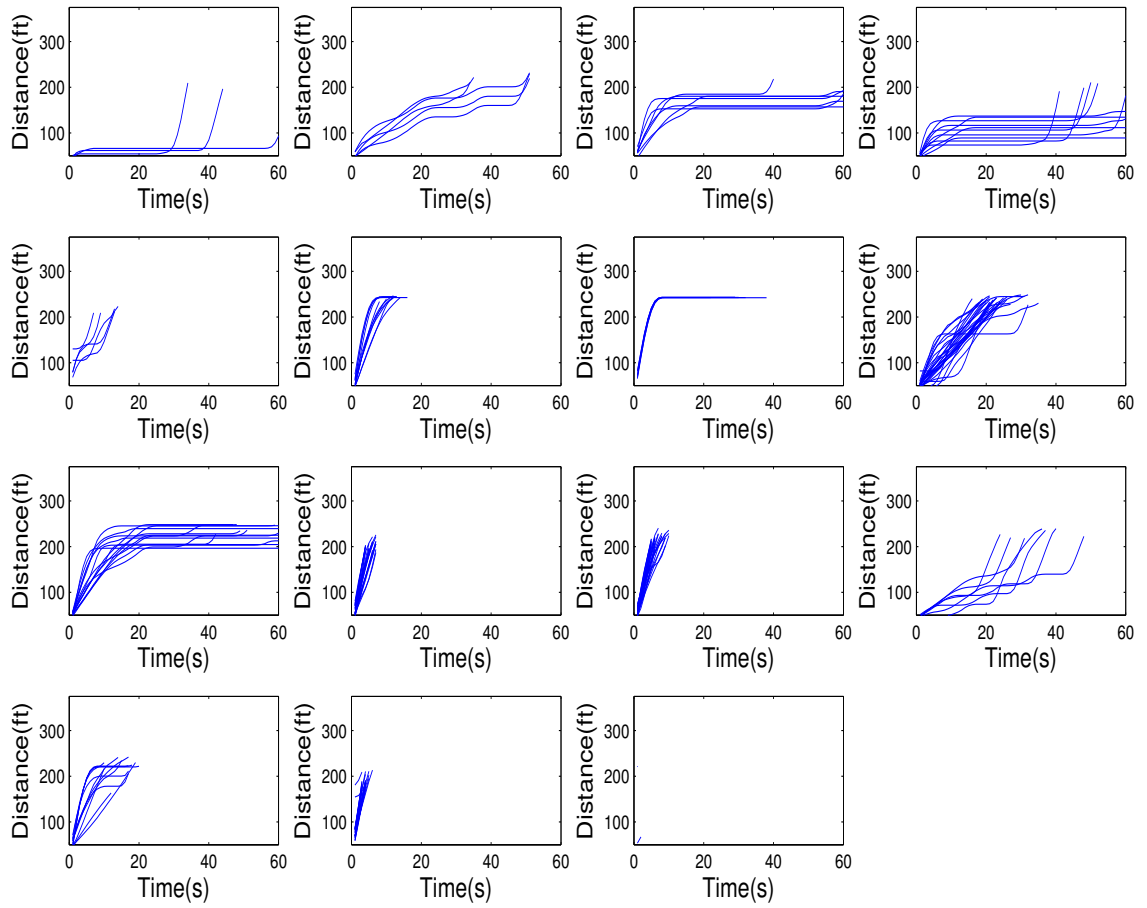


Figure 7.9.: Link-2 for intersection-4

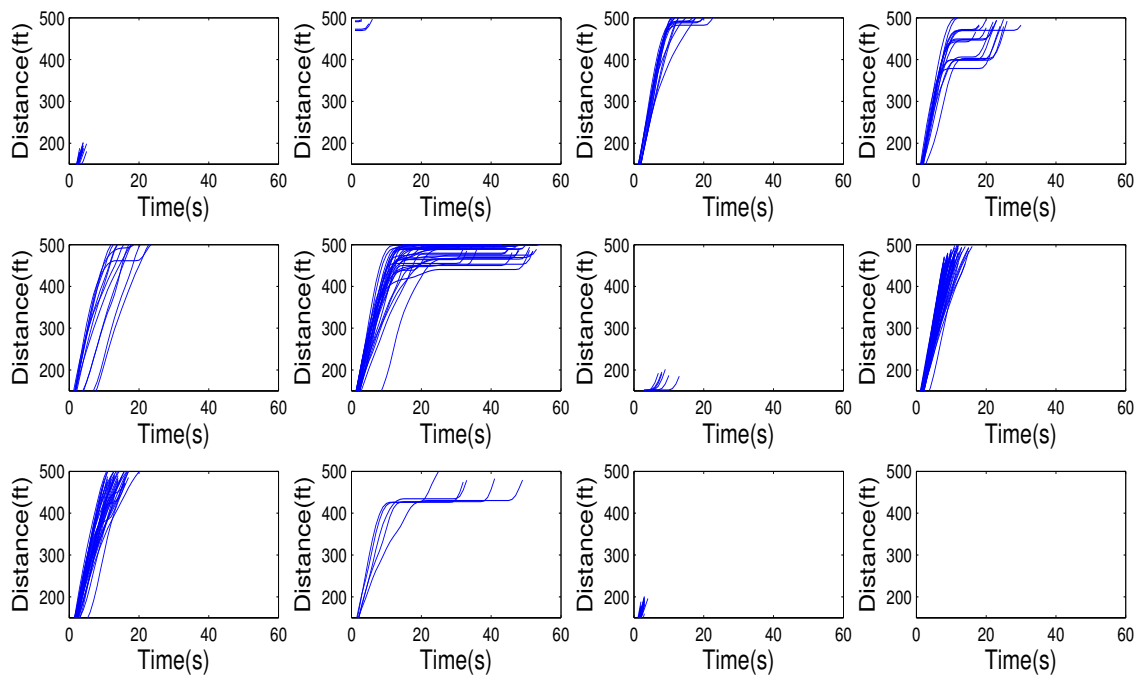


Figure 7.10.: Link-3 for intersection-4

- The HC-DTW technique provides higher accuracy compared with average-speed technique (table 7.2) as we see from our seven test cases.
- The error percentage for  $PM_{10}$  is found to very high in most cases.
- The number of links in a cluster affects the accuracy of the estimation. As the number of vehicle increases in a cluster, the degree of similarity (closeness) decreases. Although the average similarity remains same, some details are lost. Further, estimation with a very high volume traffic adds the accumulated error. This implies that the when the number of trajectories are reasonably high the analyst needs to carefully decide the number of clusters to include (section ??)as input to MOVES.
- Except  $PM_{10}$ , the error percentage ranges from 1% to 10% for all other pollutants. Case 2 and case 6 higher error for  $NO_x$ .
- HC-DTW is most effective when the variation in vehicular activities on a link is high which is typically found during peak hour conditions and in urban areas (section 7.5.1). If the congestion level is low, and the vehicular activities are similar, average speed technique provides estimation with reasonable accuracy.

Table 7.2.: Comparison of estimates for different approaches

		Case 1 (39 vehicles)			
Pollutants	<i>Exact method</i>	HC-DTW	**diff. (%)	Avg speed	**diff. (%)
CO <sub>2</sub> (g/hr)	3607.66	3692.06	2.33	2906.75	19.42
CO (g/hr)	32.75	30.98	5.41	23.99	26.74
PM <sub>10</sub>	0.1039	0.1059	1.91	0.0526	49.34
NO <sub>x</sub> (g/hr)	2.879	3.035	5.40	2.164	24.82
		Case 2 (62 vehicles)			
CO <sub>2</sub> (g/hr)	14884.44	13764.04	7.53	5939.55	60.10
CO (g/hr)	74.99	63.11	14.5	44.44	40.74
PM <sub>10</sub>	0.27	0.22	18.88	0.10	63.94
NO <sub>x</sub> (g/hr)	5.94	4.75	17.8	3.66	38.36
		Case 3 (42 vehicles)			
CO <sub>2</sub> (g/hr)	4692.43	4603.01	1.91	4291.64	8.54
CO (g/hr)	35.34	34.00	3.77	29.77	15.75
PM <sub>10</sub>	0.11	0.13	22.10	0.06	40.50
NO <sub>x</sub> (g/hr)	3.42	3.23	5.41	2.24	34.39
		Case 4 (34 vehicles)			
CO <sub>2</sub> (g/hr)	12469.52	11739.35	5.86	17401.29	39.55
CO (g/hr)	58.30	53.02	9.06	93.21	59.88
PM <sub>10</sub>	0.22	0.19	13.45	0.22	2.38
NO <sub>x</sub> (g/hr)	4.36	3.90	10.55	6.44	47.73
		Case 5 (26 vehicles)			
CO <sub>2</sub> (g/hr)	11704.87	11135.34	4.87	16588.73	41.73
CO (g/hr)	52.60	49.71	5.50	88.62	68.47
PM <sub>10</sub>	0.20	0.18	10.60	0.21	5.26
NO <sub>x</sub> (g/hr)	3.88	3.62	6.72	5.97	53.97
		Case 6 (36 vehicles)			
CO <sub>2</sub> (g/hr)	4282.95	3908.51	8.74	3738.09	12.72
CO (g/hr)	33.14	26.99	18.56	25.74	22.35
PM <sub>10</sub>	0.11	0.10	2.05	0.06	47.84
NO <sub>x</sub> (g/hr)	3.12	2.58	17.38	1.92	38.47
		Case 7 (34 vehicles)			
CO <sub>2</sub> (g/hr)	3893.57	3845.91	1.22	3570.03	8.31

Table 7.3.: Computational time comparison

Estimation method	No. of LDS	Computational time (minute)
Case 1		
Exact method	39	33
HC-DTW	3	less than a minute
Average-Speed	-	less than a minute
Case 2		
Exact method	62	39
HC-DTW	3	less than a minute
Average-Speed	-	less than a minute
Case 3		
Exact method	42	34
HC-DTW	3	less than a minute
Average-Speed	-	less than a minute
Case 4		
Exact method	34	25
HC-DTW	3	less than a minute
Average-Speed	-	less than a minute
Case 5		
Exact method	26	18
HC-DTW	3	less than a minute
Average-Speed	-	less than a minute
Case 6		
Exact method	36	29
HC-DTW	3	less than a minute
Average-Speed	-	less than a minute
Case 7		
Exact method	34	25
HC-DTW	3	less than a minute
Average-Speed	-	less than a minute

Conducted with 2.4 GHz, i5 4 core processor, 4 GB RAM machine

Table 7.4.: Sample results using HC-DTW technique

Link-ID	Total no. of Vehicles	No. of clusters	Min. no. of elements	Max. no of elements	Cophenetic coefficient
Link-1	195	8	19	58	0.83
Link-2	197	5	17	77	0.96
Link-3	400	9	17	116	0.76
Link-4	364	7	13	94	0.8
Link-5	181	5	12	47	0.78
Link-6	186	8	12	28	0.74
Link-7	249	8	15	62	0.86

## 7.6 Concluding remarks

This research develops a novel technique to find link driving schedules from vehicular trajectories that can be used as input for emissions simulator MOVES. First, we outline a framework that integrates traffic and emissions simulator. The traffic simulator can be any micro-level simulation that provides second-by-second vehicle activity data. Second, this research proposes a link driving schedule finding technique based on similarity based clustering that overcomes the general limitations of current approaches to estimate emissions using vehicle trajectories. The hierarchical clustering based dynamic time warping (HC-DTW) technique is shown to have negligible difference when compared with an exact method that requires to treat each vehicle's speed profile as a distinct LDS. Analysis with a link shows that the difference in emissions are very small. In addition, the computational time is significantly smaller than the exact method. The major contributions are as follows:

- (a) A similarity based clustering technique is proposed that finds the representative link driving schedules for MOVES input from second-by-second trajectory data.
- (b) The hierarchical clustering based dynamic time warping (HC-DTW) technique does not compromise accuracy at a higher degree. This is particularly important for networks with highly varying congestion states. Traditional approaches such as average speed based techniques tend to under or over estimate the emissions, whereas HC-DTW technique is expected to have estimated emissions with very small difference with the exact method.
- (c) The computational time decreases significantly because HC-DTW only uses cluster prototypes as the LDS for MOVES input. Since the number of link-instances gets lower, the computation is faster.

The proposed technique can be used with any traffic simulation tool that provides second-by-second data. Moreover, real-world trajectory data can be easily processed and converted into LDS using our HC-DTW technique. The computational time also

depends on the choice of number of clusters. However this will be decided by the analyst depending on the scope of the study.

For HC-DTW we observe that, the error level ranges from 2% to 18% in most cases. We observe the error level goes up with higher links in a cluster. This can be an issue if we estimate emissions for clusters with very high number of links. This can be addressed by increasing the number of clusters so that each cluster does not have a very high number of links. Also, more tests are required to have a stronger conclusion on the savings of computational time. Further, the technique is more promising to links with higher variability of vehicular activities. Nevertheless, the HC-DTW technique will significantly benefit the estimation of emissions using MOVES in terms of efficiency and accuracy and serve as a useful tool for the practitioners in context of air quality conformity analysis.



## CHAPTER 8. CONCLUSIONS

### 8.1 Major contributions

The general theme of the dissertation underscores the potential of influencing travel related decisions that can lead to significant reduction in greenhouse gas emissions. This dissertation proposes user and system level strategies, critically analyzes the impact of the strategies on the state of the transportation networks, and develops an evaluation framework to assess the effectiveness of the strategies. The broader impact of this dissertation is the innovation and assessment of the behavior based *soft* policies to reduce GHG emissions and fossil fuel consumptions from road networks. Further, each research work has its distinct contribution to the literature.

- The analysis of trade-off between emissions and travel time (**chapter 3**) at different contexts of daily travel is one of the first studies that investigates travel decision making when emissions related information is available. We estimate random parameter models accounting for correlation across repeated observations to find the trade-off between emissions and travel. The results can significantly assist to find policies that encourage travel behavior leading to less emissions for road networks. We observe that different groups of people have different trade-off values and accordingly one need to consider the population mix before consideration of any scheme.
- The PMCA scheme described in **chapter 4** is a novel market based strategy to reduce carbon consumptions originating from personal travel. This research contributes to literature in several ways. The developed game is a handy tool to collect data for cases that require interaction among users in real time. Without a market integration, analysis of the tradable schemes is incomplete. Further,

the sensitivity analysis using the estimates mode random parameter models provides insights on the effect of travel option attributes and market conditions on travel choices.

- The PMCA-DUE model (**chapter 5**), is one of the first dynamic user equilibrium models incorporating the travel behavior under carbon allowance scheme. The complementarity based formulation provides a novel way to describe equilibrium under PMCA scheme. Two solutions techniques: basic projection and decomposed VI algorithms are proposed. In addition, we examine the effects of different levels of initial allocation as set by carbon reduction goals (e.g., 2%, 5%, 7%).
- We developed learning based signal control algorithms (**chapter 6**) that can reduce emissions from road networks. The levels of emissions (CO, NO<sub>x</sub>, PM<sub>10</sub>, CO<sub>2</sub>, VOC) are found to be less with the learning based signal controllers. The reduction in number of stops and average stopped delays at the intersections with learning based control can be the major reasons behind lower level of emissions.
- The link driving schedule finding technique (**chapter 7**) is a significant contribution to the emissions assessment methodologies when integrated with traffic simulation. The HC-DTW techniques significantly reduce the computational time. At the same time the level of accuracy is reasonable. This technique is also useful when real world trajectory data are collected. With the availability of trajectory data irrespective of the source, HC-DTW can provide link driving schedules and the estimation using MOVES can be done with shorter computational time.

## 8.2 Future works

- The trade-off values can be further explored at different dimensions such as bike-sharing, zip-cars, electric vehicles, and accounting for trip-chains.
- The PMCA scheme can be extended to combine energy consumptions in household utility and personal travel. Instead of focusing on travel we can explore the general energy consumption behavior. The market component will be same. However more decisions have to be incorporated in the first segment of the experimental game developed here (see chapter 4). The question of interest would be the evolving patterns of energy consumptions as a result of interaction between travel and household energy related activities,
- Agent based models can be an alternative to the PMCA-DUE model to assess network state under PMCA. Incorporating user heterogeneity at a large scale is possible,
- Coordinated signal control schemes that balance the delay and emissions can be developed. The basic methodology will be same. However the state space will be larger and the actions require to be coordinated aligned with the objectives,
- The integrated emissions-traffic simulator can be extended to make investment and project planning decisions.

## BIBLIOGRAPHY

## Bibliography

- [1] US EPA. National emissions inventory (nei) air pollutant emissions trends data (1970-2012). url:<http://www.epa.gov/ttn/chief/trends/index.html>, accessed: July, 2012. 2012.
- [2] US EPA. Greenhouse gas emissions from the us transportation sector, 1990 2003. transportation ghg emissions report. 2006.
- [3] Matthew E. Kahn. New evidence on trends in vehicle emissions. *The RAND Journal of Economics*, 27(1):183–196, 1996.
- [4] Yafeng Yin and Siriphong Lawphongpanich. Internalizing emission externality on road networks. *Transportation Research Part D: Transport and Environment*, 11(4):292–301, 2006.
- [5] Thomas Dietz, Gerald T. Gardner, Jonathan Gilligan, Paul C. Stern, and Michael P. Vandenbergh. Household actions can provide a behavioral wedge to rapidly reduce us carbon emissions. *Proceedings of the National Academy of Sciences*, 106(44):18452–18456, 2009.
- [6] Kyoungho Ahn and Hesham Rakha. The effects of route choice decisions on vehicle energy consumption and emissions. *Transportation Research Part D: Transport and Environment*, 13(3):151–167, 2008.
- [7] Liya Guo, Shan Huang, and Adel W. Sadek. An evaluation of environmental benefits of time-dependent green routing in the greater buffaloniagara region. *Journal of Intelligent Transportation Systems*, 17(1):18–30, 2012.

- [8] Kyounggho Ahn and Hesham A. Rakha. Network-wide impacts of eco-routing strategies: A large-scale case study. *Transportation Research Part D: Transport and Environment*, 25:119–130, 2013.
- [9] K. Boriboonsomsin, M. J. Barth, Zhu Weihua, and A. Vu. Eco-routing navigation system based on multisource historical and real-time traffic information. *Intelligent Transportation Systems, IEEE Transactions on*, 13(4):1694–1704, 2012.
- [10] David A. Hensher. Climate change, enhanced greenhouse gas emissions and passenger transport what can we do to make a difference? *Transportation Research Part D: Transport and Environment*, 13(2):95–111, 2008.
- [11] John K. Stanley, David A. Hensher, and Chris Loader. Road transport and climate change: Stepping off the greenhouse gas. *Transportation Research Part A: Policy and Practice*, 45(10):1020–1030, 2011.
- [12] Anna Nagurney. Congested urban transportation networks and emission paradoxes. *Transportation Research Part D: Transport and Environment*, 5(2):145–151, 2000.
- [13] J. Lin and Y. E. Ge. Impacts of traffic heterogeneity on roadside air pollution concentration. *Transportation Research Part D: Transport and Environment*, 11(2):166–170, 2006.
- [14] K. G. Ahn and H. Rakha. The effects of route choice decisions on vehicle energy consumption and emissions. *Transportation Research Part D: Transport and Environment*, 13(3):151–167, 2008.
- [15] Yunlong Zhang, Jinpeng Lv, and Qi Ying. Traffic assignment considering air quality. *Transportation Research Part D: Transport and Environment*, 15(8):497–502, 2010.

- [16] Matthew Barth and Kanok Boriboonsomsin. Real-world carbon dioxide impacts of traffic congestion. *Transportation Research Record: Journal of the Transportation Research Board*, 2058:163–171, 2008.
- [17] Matthew Barth, George Scora, and Theodore Younglove. Modal emissions model for heavy-duty diesel vehicles. *Transportation Research Record: Journal of the Transportation Research Board*, 1880:10–20, 2004.
- [18] David Fleming and Shaun Chamberlin. Teqs(tradable energy quotas): A policy framework for peak oil and climate change. *London: All-Party Parliamentary Group on Peak Oil, and The Lean Economy Connection.*, 2011.
- [19] David Schrank, Bill Eisele, and Tim Lomax. Ttis 2012 urban mobility report. Technical report, Texas A&M Transportation Institute, The Texas A&M University System, December, 2012.
- [20] Hani S. Mahmassani. Dynamic models of commuter behavior: Experimental investigation and application to the analysis of planned traffic disruptions. *Transportation Research Part A: General*, 24(6):465–484, 1990.
- [21] Moshe Ben-Akiva, Andre De Palma, and Kaysi Isam. Dynamic network models and driver information systems. *Transportation Research Part A: General*, 25(5):251–266, 1991.
- [22] Chris Caplice and Hani S. Mahmassani. Aspects of commuting behavior: Preferred arrival time, use of information and switching propensity. *Transportation Research Part A: Policy and Practice*, 26(5):409–418, 1992.
- [23] Hani S. Mahmassani and PeterShen-Te Chen. An investigation of the reliability of real-time information for route choice decisions in a congested traffic system. *Transportation*, 20(2):157–178, 1993.

- [24] Roger Chen and Hani Mahmassani. Travel time perception and learning mechanisms in traffic networks. *Transportation Research Record: Journal of the Transportation Research Board*, 1894:209–221, 2004.
- [25] G. Ramadurai and Satish Ukkusuri. Dynamic traffic equilibrium: Theoretical and experimental network game results in single-bottleneck model. *Transportation Research Record: Journal of the Transportation Research Board*, 2029:1–13, 2007.
- [26] Caspar G. Chorus, Theo A. Arentze, Eric J. E. Molin, Harry J. P. Timmermans, and Bert Van Wee. The value of travel information: Decision strategy-specific conceptualizations and numerical examples. *Transportation Research Part B: Methodological*, 40(6):504–519, 2006.
- [27] P. Wesley Schultz, Jessica M. Nolan, Robert B. Cialdini, Noah J. Goldstein, and Vidas Griskevicius. The constructive, destructive, and reconstructive power of social norms. *Psychological Science*, 18(5):429–434, 2007.
- [28] Yuko Heath and Robert Gifford. Extending the theory of planned behavior: Predicting the use of public transportation. *Journal of Applied Social Psychology*, 32(10):2154–2189, 2002.
- [29] Ayako Taniguchi, Haruna Suzuki, and Satoshi Fujii. Mobility management in japan: Its development and meta-analysis of travel feedback programs. *Transportation Research Record: Journal of the Transportation Research Board*, 2021(-1):100–109, 2007.
- [30] T Garling and Satoshi Fujii. Travel behavior modification: Theories, methods, and programs. *The expanding sphere of travel behaviour research*, pages 97–128, 2009.
- [31] C Thompson. Thompson thinks: Desktop orb could reform energy hogs. *Wired*, 15(8), 2007.



- [32] Juan de Dios Ortzar and Gonzalo Rodriguez. Valuing reductions in environmental pollution in a residential location context. *Transportation Research Part D: Transport and Environment*, 7(6):407–427, 2002.
- [33] Jean-Daniel M. Saphores, Hilary Nixon, Oladele A. Ogunseitan, and Andrew A. Shapiro. California households' willingness to pay for green electronics. *Journal of Environmental Planning and Management*, 50(1):113–133, 2007.
- [34] C Choudhury, T TSANG, P Burge, and R SHELDON. Measuring willingness to pay for green options. *EUROPEAN TRANSPORT CONFERENCE 2008; PROCEEDINGS*, 2008.
- [35] Martin Achtnicht. German car buyers willingness to pay to reduce co2 emissions. *Climatic Change*, 113(3-4):679–697, 2012.
- [36] David Gaker, Yanding Zheng, and Joan Walker. Experimental economics in transportation. *Transportation Research Record: Journal of the Transportation Research Board*, 2156:47–55, 2010.
- [37] David Gaker, David Vautin, Akshay Vij, and Joan L Walker. The power and value of green in promoting sustainable transport behavior. *Environmental Research Letters*, 6(3):034010, 2011.
- [38] R. H. Coase. The problem of social cost. *Journal of Law and Economics*, 3(ArticleType: research-article / Full publication date: Oct., 1960 / Copyright 1960 The University of Chicago):1–44, 1960.
- [39] J.H. Dales. Pollution, property, and prices. *University of Toronto Press, Toronto*, 1968.
- [40] W. David Montgomery. Markets in licenses and efficient pollution control programs. *Journal of Economic Theory*, 5(3):395–418, 1972.

- [41] Tom Tietenberg. The tradable-permits approach to protecting the commons: Lessons for climate change. *Oxford Review of Economic Policy*, 19(3):400–419, 2003.
- [42] Adriaan Perrels. User response and equity considerations regarding emission cap-and-trade schemes for travel. *Energy Efficiency*, 3(2):149–165, 2010.
- [43] David Fleming. Tradable quotas: using information technology to cap national carbon emissions. *European Environment*, 7(5):139–148, 1997.
- [44] Richard Starkey and Kevin Anderson. Domestic tradable quotas: A policy instrument for reducing greenhouse gas emissions from energy use. *Tyndall Centre for Climate Change Research Norwich,, UK*, 2005.
- [45] Mayer Hillman, Tina Fawcett, and Sudhir Chella Rajan. How we can save the planet: Preventing global climate catastrophe. *St. Martin's Griffin*, 2008.
- [46] Tina Fawcett. Carbon rationing and personal energy use. *Energy & Environment*, 15(6):1067–1083, 2004.
- [47] D. Niemeier, Gregory Gould, Alex Karner, Mark Hixson, Brooke Bachmann, Carrie Okma, Ziv Lang, and David Heres Del Valle. Rethinking downstream regulation: California's opportunity to engage households in reducing greenhouse gases. *Energy Policy*, 36(9):3436–3447, 2008.
- [48] E. Verhoef, P. Nijkamp, and P. Rietveld. Tradeable permits: their potential in the regulation of road transport externalities. *Environment and Planning B: Planning and Design*, 24(4):527–548, 1997.
- [49] Kara M. Kockelman and Sukumar Kalmanje. Credit-based congestion pricing: a policy proposal and the publics response. *Transportation Research Part A: Policy and Practice*, 39(79):671–690, 2005.
- [50] Charles Raux. Downstream emissions trading for transport. *Transport Moving to Climate Intelligence:Springer New York*, pages 209–226, 2011.

- [51] Zia Wadud. Personal tradable carbon permits for road transport: Why, why not and who wins? *Transportation Research Part A: Policy and Practice*, 45(10):1052–1065, 2011.
- [52] Anna Nagurney, Padma Ramanujam, and Kanwalroop Kathy Dhanda. A multi-modal traffic network equilibrium model with emission pollution permits: compliance vs noncompliance. *Transportation Research Part D: Transport and Environment*, 3(5):349–374, 1998.
- [53] Anna Nagurney. Alternative pollution permit systems for transportation networks based on origin/destination pairs and paths. *Transportation Research Part D: Transport and Environment*, 5(1):37–58, 2000.
- [54] Hai Yang and Xiaolei Wang. Managing network mobility with tradable credits. *Transportation Research Part B: Methodological*, 45(3):580–594, 2011.
- [55] Xiaolei Wang, Hai Yang, Daoli Zhu, and Changmin Li. Tradable travel credits for congestion management with heterogeneous users. *Transportation Research Part E: Logistics and Transportation Review*, 48(2):426–437, 2012.
- [56] Yu Nie. Transaction costs and tradable mobility credits. *Transportation Research Part B: Methodological*, 46(1):189–203, 2012.
- [57] Xiaolei Wang and Hai Yang. Bisection-based trial-and-error implementation of marginal cost pricing and tradable credit scheme. *Transportation Research Part B: Methodological*, 46(9):1085–1096, 2012.
- [58] Di Wu, Yafeng Yin, Siriphong Lawphongpanich, and Hai Yang. Design of more equitable congestion pricing and tradable credit schemes for multimodal transportation networks. *Transportation Research Part B: Methodological*, 46(9):1273–1287, 2012.
- [59] Yu Nie and Yafeng Yin. Managing rush hour travel choices with tradable credit scheme. *Transportation Research Part B: Methodological*, 50(0):1–19, 2013.

- [60] Linxi Chen and Hai Yang. Managing congestion and emissions in road networks with tolls and rebates. *Transportation Research Part B: Methodological*, 46(8):933–948, 2012.
- [61] A. Chen, Z. Zhou, and S. Ryu. Modeling physical and environmental side constraints in traffic equilibrium problem. *International Journal of Sustainable Transportation*, 5(3):172–197, 2011.
- [62] W. Y. Szeto, X. Jaber, and S. C. Wong. Road network equilibrium approaches to environmental sustainability. *Transport Reviews*, 32(4):491–518, 2012.
- [63] Erin M. Ferguson, Jennifer Duthie, and S. Travis Waller. Comparing delay minimization and emissions minimization in the network design problem. *Computer-Aided Civil and Infrastructure Engineering*, 27(4):288–302, 2012.
- [64] Anna Nagurney and Ding Zhang. Dynamics of a transportation pollution permit system with stability analysis and computations. *Transportation Research Part D: Transport and Environment*, 6(4):243–268, 2001.
- [65] H. M. Abdul Aziz and Satish Ukkusuri. Tradable emissions credits for personal travel: a market-based approach to achieve air quality standards. *International Journal of Advances in Engineering Sciences and Applied Mathematics*, 5(2-3):145–157, 2013.
- [66] Simon Roberts and Joshua Thumim. A rough guide to individual carbon trading: The ideas, the issues and the next steps, report to defra. 2006.
- [67] Helen Harwatt, Miles Tight, Abigail L. Bristow, and Astrid Guhnemann. Personal carbon trading and fuel price increases in the transport sector: an exploratory study of public response in the uk. *European Transport Trasporti Europei*, (47):47–70, 2011.
- [68] Tina Fawcett. Personal carbon trading: A policy ahead of its time? *Energy Policy*, 38(11):6868–6876, 2010.

- [69] Nagui M Roupail, H Christopher Frey, James D Colyar, and Alper Unal. Vehicle emissions and traffic measures: exploratory analysis of field observations at signalized arterials. *80th Annual Meeting of the Transportation Research Board, Washington, DC*, 2001.
- [70] Alper Unal, Nagui Roupail, and H. Frey. Effect of arterial signalization and level of service on measured vehicle emissions. *Transportation Research Record: Journal of the Transportation Research Board*, 1842:47–56, 2003.
- [71] K. Ahn, H. Rakha, A. Trani, and M. Van Aerde. Estimating vehicle fuel consumption and emissions based on instantaneous speed and acceleration levels. *Journal of Transportation Engineering*, 128(2):182–190, 2002.
- [72] H. Rakha and Y. Ding. Impact of stops on vehicle fuel consumption and emissions. *Journal of Transportation Engineering*, 129(1):23–32, 2002.
- [73] J Van Mierlo, G Maggetto, E Van de Burgwal, and R Gense. Driving style and traffic measures-influence on vehicle emissions and fuel consumption. *Proceedings of the Institution of Mechanical Engineers, Part D: Journal of Automobile Engineering*, 218(1):43–50, 2004.
- [74] Hesham Rakha, Michel Van Aerde, K. Ahn, and Antonio Trani. Requirements for evaluating traffic signal control impacts on energy and emissions based on instantaneous speed and acceleration measurements. *Transportation Research Record: Journal of the Transportation Research Board*, 1738:56–67, 2000.
- [75] A. Stevanovic, J. Stevanovic, K. Zhang, and S. Batterman. Optimizing traffic control to reduce fuel consumption and vehicular emissions integrated approach with vissim, cmem, and visgaost. *Transportation Research Record*, (2128):105–113, 2009.

- [76] Byungkyu Park, Ilsoo Yun, and Kyoungho Ahn. Stochastic optimization for sustainable traffic signal control. *International Journal of Sustainable Transportation*, 3(4):263–284, 2009.
- [77] T. Umedu, Y. Togashi, and T. Higashino. A self-learning traffic signal control method for co2 reduction using prediction of vehicle arrivals. *Intelligent Transportation Systems (ITSC), 2012 15th International IEEE Conference on*, pages 421–426, 2012.
- [78] Jaeyoung Kwak, Byungkyu Park, and Jaesup Lee. Evaluating the impacts of urban corridor traffic signal optimization on vehicle emissions and fuel consumption. *Transportation Planning and Technology*, 35(2):145–160, 2012.
- [79] S. Huang, A. W. Sadek, and Y. Zhao. Assessing the mobility and environmental benefits of reservation-based intelligent intersections using an integrated simulator. *Intelligent Transportation Systems, IEEE Transactions on*, PP(99):1–14, 2012.
- [80] Michael Mahut and Michael Florian. Traffic simulation with dynameq. In Jaume Barcel, editor, *Fundamentals of Traffic Simulation*, volume 145 of *International Series in Operations Research and Management Science*, pages 323–361. Springer New York, 2010.
- [81] J. Lin, Chiu Yi-Chang, S. Vallamsundar, and Bai Song. Integration of moves and dynamic traffic assignment models for fine-grained transportation and air quality analyses. In *Integrated and Sustainable Transportation System (FISTS), 2011 IEEE Forum on*, pages 176–181, 2011.
- [82] Guohua Song, Lei Yu, and Yanhong Zhang. Applicability of traffic microsimulation models in vehicle emissions estimates. *Transportation Research Record: Journal of the Transportation Research Board*, 2270:132–141, 2012.

- [83] Yuanchang Xie, Mashrur Chowdhury, Parth Bhavsar, and Yan Zhou. An integrated modeling approach for facilitating emission estimations of alternative fueled vehicles. *Transportation Research Part D: Transport and Environment*, 17(1):15–20, 2012.
- [84] Liu Hao, Liang Shuang, Yao Zhuo, Wei Heng, Y. Jeffrey Yang, and Wang Xinhao. Framework for integrating traffic-source emission estimates into sustainability analysis. In *CICTP 2012*, pages 3612–3619. American Society of Civil Engineers, 2012.
- [85] H. M. Abdul Aziz and Satish V. Ukkusuri. Integration of environmental objectives in a system optimal dynamic traffic assignment model. *Computer-Aided Civil and Infrastructure Engineering*, 27(7):494–511, 2012.
- [86] L. Smith Vernon. An experimental study of competitive market behavior. *Journal of Political Economy*, 70(2):111–137, 1962.
- [87] L. Smith Vernon. Microeconomic systems as an experimental science. *The American Economic Review*, 72(5):923–955, 1982.
- [88] L. Smith Vernon. Economics in the laboratory. *The Journal of Economic Perspectives*, 8(1):113–131, 1994.
- [89] Filippos Exadaktylos, Antonio M. Espn, and Pablo Braas-Garza. Experimental subjects are not different. *Sci. Rep.*, 3, 2013.
- [90] Daniel McFadden and Kenneth Train. Mixed mnl models for discrete response. *Journal of applied Econometrics*, 15(5):447–470, 2000.
- [91] Kenneth Train. *Discrete choice methods with simulation*. 2009.
- [92] Simon P Washington, Matthew G Karlaftis, and Fred L Mannering. *Statistical and econometric methods for transportation data analysis*. 2011.

- [93] Chandra R. Bhat. Simulation estimation of mixed discrete choice models using randomized and scrambled halton sequences. *Transportation Research Part B: Methodological*, 37(9):837–855, 2003.
- [94] P. C. Anastasopoulos and F. L. Mannering. An empirical assessment of fixed and random parameter logit models using crash- and non-crash-specific injury data. *Accident Analysis and Prevention*, 43(3):1140–1147, 2011.
- [95] D. R. Cox. Further results on tests of separate families of hypotheses. *Journal of the Royal Statistical Society. Series B (Methodological)*, 24(2):406–424, 1962.
- [96] Gudmundur F. Ulfarsson and Fred L. Mannering. Differences in male and female injury severities in sport-utility vehicle, minivan, pickup and passenger car accidents. *Accident Analysis & Prevention*, 36(2):135–147, 2004.
- [97] John C. Milton, Venky N. Shankar, and Fred L. Mannering. Highway accident severities and the mixed logit model: An exploratory empirical analysis. *Accident Analysis & Prevention*, 40(1):260–266, 2008.
- [98] J. K. Kim, G. F. Ulfarsson, V. N. Shankar, and F. L. Mannering. A note on modeling pedestrian-injury severity in motor-vehicle crashes with the mixed logit model. *Accident Analysis & Prevention*, 42(6), 2010.
- [99] Richard H. M. Emmerink, Peter Nijkamp, Piet Rietveld, and Jos N. Van Ommeren. Variable message signs and radio traffic information: An integrated empirical analysis of drivers’ route choice behaviour. *Transportation Research Part A: Policy and Practice*, 30(2):135–153, 1996.
- [100] Mark Bradley, John L. Bowman, and Bruce Griesenbeck. Sacsim: An applied activity-based model system with fine-level spatial and temporal resolution. *Journal of Choice Modelling*, 3(1):5–31, 2010.



- [101] Wafaa Saleh and Sona Farrell. Implications of congestion charging for departure time choice: Work and non-work schedule flexibility. *Transportation Research Part A: Policy and Practice*, 39(79):773–791, 2005.
- [102] Mark W. Horner and Morton E. OKelly. Is non-work travel excessive? *Journal of Transport Geography*, 15(6):411–416, 2007.
- [103] Meiping Yun, David van Herick, and Patricia Mokhtarian. Nonwork travel behavior changes during temporary freeway closure. *Transportation Research Record: Journal of the Transportation Research Board*, 2231:1–9, 2011.
- [104] Eran Ben-Elia and Yoram Shiftan. Which road do i take? a learning-based model of route-choice behavior with real-time information. *Transportation Research Part A: Policy and Practice*, 44(4):249–264, 2010.
- [105] Fred L. Mannering and Mohammad M. Hamed. Occurrence, frequency, and duration of commuters’ work-to-home departure delay. *Transportation Research Part B: Methodological*, 24(2):99–109, 1990.
- [106] Chandra R. Bhat. Covariance heterogeneity in nested logit models: Econometric structure and application to intercity travel. *Transportation Research Part B: Methodological*, 31(1):11–21, 1997.
- [107] Hai Yang. Multiple equilibrium behaviors and advanced traveler information systems with endogenous market penetration. *Transportation Research Part B: Methodological*, 32(3):205–218, 1998.
- [108] Hani S. Mahmassani and R. Jayakrishnan. System performance and user response under real-time information in a congested traffic corridor. *Transportation Research Part A: General*, 25(5):293–307, 1991.
- [109] Satish Ukkusuri, Lanshan Han, and Kien Doan. Dynamic user equilibrium with a path based cell transmission model for general traffic networks. *Transportation Research Part B*, 46(10):1657–1684, 2012.

- [110] Charles Raux and Grgoire Marlot. A system of tradable co2 permits applied to fuel consumption by motorists. *Transport Policy*, 12(3):255–265, 2005.
- [111] T Grayling and T Gibbs. Tailpipe trading: how to include road transport in the eu emissions trading scheme (eu ets). *Institute for Public Policy Research, LowCVP Low Carbon Road Transport Challenge*, 2006.
- [112] Mark Keppens and Lode Vereeck. The design and effects of a tradable fuel permit system. *PROCEEDINGS OF THE EUROPEAN TRANSPORT CONFERENCE (ETC) 2003 HELD 8-10 OCTOBER 2003, STRASBOURG, FRANCE*, 2003.
- [113] Stuart Bryce Capstick and Alan Lewis. Effects of personal carbon allowances on decision-making: evidence from an experimental simulation. *Climate Policy*, 10(4):369–384, 2010.
- [114] Tina Fawcett and Yael Parag. An introduction to personal carbon trading. *Climate Policy*, 10(4):329–338, 2010.
- [115] Abigail L. Bristow, Mark Wardman, Alberto M. Zanni, and Phani K. Chintakayala. Public acceptability of personal carbon trading and carbon tax. *Ecological Economics*, 69(9):1824–1837, 2010.
- [116] Vernon L Smith. An experimental study of competitive market behavior. *The Journal of Political Economy*, 70(2):111–137, 1962.
- [117] Report US DOT. The value of travel time savings: Departmental guidance for conducting economic evaluations (revision 2). *US Department of Transportation* (<http://ostpxweb.dot.gov/policy/reports.htm>), 2011.
- [118] Charles R Plott. Industrial organization theory and experimental economics. *journal of Economic Literature*, 20(4):1485–1527, 1982.
- [119] Alvin E Roth and John Henry Kagel. *The handbook of experimental economics*, volume 1. Princeton university press Princeton, 1995.

- [120] Siddhartha Chib and Rainer Winkelmann. Markov chain monte carlo analysis of correlated count data. *Journal of Business and Economic Statistics*, 19(4):428–435, 2001.
- [121] Eun Park and Dominique Lord. Multivariate poisson-lognormal models for jointly modeling crash frequency by severity. *Transportation Research Record: Journal of the Transportation Research Board*, 2019:1–6, 2007.
- [122] Jonathan Aguero-Valverde and Paul Jovanis. Bayesian multivariate poisson lognormal models for crash severity modeling and site ranking. *Transportation Research Record: Journal of the Transportation Research Board*, 2136:82–91, 2009.
- [123] Fabrizio Durante and Carlo Sempi. Copula theory: An introduction. In Piotr Jaworski, Fabrizio Durante, Wolfgang Karl Hrdle, and Tomasz Rychlik, editors, *Copula Theory and Its Applications*, Lecture Notes in Statistics, pages 3–31. Springer Berlin Heidelberg, 2010.
- [124] Pravin K Trivedi and David M Zimmer. *Copula modeling: an introduction for practitioners*. Now Publishers Inc, 2007.
- [125] Hai Yang and Hai-Jun Huang. The multi-class, multi-criteria traffic network equilibrium and systems optimum problem. *Transportation Research Part B: Methodological*, 38(1):1–15, 2004.
- [126] Hai Yang and Michael G.H. Bell. Models and algorithms for road network design: a review and some new developments. *Transport Review: A transnational Transdisciplinary Journal*, 18(3):257–278, 1998.
- [127] Erik T. Verhoef and Kenneth A. Small. Product differentiation on roads: constrained congestion pricing with heterogeneous users. *Journal of Transport Economics and Policy*, 38(1):127–156, 2004.

- [128] Carlos F. Daganzo. The cell transmission model: a simple dynamic representation of highway traffic. *Transportation Research Part B*, 28(4):269–287, 1994.
- [129] Carlos F. Daganzo. The cell transmission model, part ii: Network traffic. *Transportation Research Part B*, 29(2):79–93, 1995.
- [130] W. Y. Szeto. Cell-based dynamic equilibrium models. *Advances in Dynamic Network Modeling in Complex Transportation Systems*, 2:163–192, 2013.
- [131] Lanshan Han, Satish Ukkusuri, and Kien Doan. Complementarity formulations for the cell transmission model based dynamic user equilibrium with departure time choice, elastic demand and user heterogeneity. *Transportation Research Part B: Methodological*, 45(10):1749–1767, 2011.
- [132] Satish V. Ukkusuri, Lanshan Han, and Kien Doan. Dynamic user equilibrium with a path based cell transmission model for general traffic networks. *Transportation Research Part B: Methodological*, 46(10):1657–1684, 2012.
- [133] Deepak K. Merchant and George L. Nemhauser. A model and an algorithm for the dynamic traffic assignment problems. *Transportation Science*, 12(3):183–199, 1978.
- [134] Athanasios K. Ziliaskopoulos. A linear programming model for the single destination system optimum dynamic traffic assignment problem. *Transportation Science*, 34(1):37–49, 2000.
- [135] Gitakrishnan Ramadurai and Satish Ukkusuri. Dynamic traffic equilibrium: Theoretical and experimental network game results in single-bottleneck model. *Transportation Research Record: Journal of the Transportation Research Board*, 2029:1–13, 2007.
- [136] G. Ramadurai. *Novel dynamic user equilibrium models: analytical formulations, multi-dimensional choice, and an efficient algorithm*. PhD thesis, RPI, 2009.

- [137] Lauren M. Gardner, Melissa Duell, and S. Travis Waller. A framework for evaluating the role of electric vehicles in transportation network infrastructure under travel demand variability. *Transportation Research Part A: Policy and Practice*, 49(0):76–90, 2013.
- [138] Lanshan Han, Satish V. Ukkusuri, and Kien Doan. Complementarity formulations for the cell transmission model based dynamic user equilibrium with departure time choice, elastic demand and user heterogeneity. *Transportation Research Part B*, 45(10):1749–1767, 2011.
- [139] X. Zhan and S. V. Ukkusuri. Multi-user class, simultaneous route and departure time choice dynamic traffic assignment with an embedded spatial queuing model. *5th International Symposium on Dynamic Traffic Assignment*, Salerno:Italy, 2014.
- [140] USA EPA. U.s. transportation sector greenhouse gas emissions: 1990-2011. *Office of Transportation and Air Quality*, EPA-420-F-13-033a, 2013.
- [141] P. B. Hunt, D. I. Robertson, R. D. Bretherton, and M. C. Royle. The scoot on-line traffic signal optimisation technique. *Traffic Engineering and Control*, 23(4):p. 190–192, 1982.
- [142] P. R. Lowrie. Scats:the sydney coordinated adaptive traffic system principles, methodology, algorithms. *Proceedings of the IEE international conference on road traffic signaling*, pages 66–70, 1982.
- [143] J. Farges, J. Henry, and J. Tufal. The prodyn real-time traffic algorithm. *Proceedings of the fourth IFAC symposium on transportation systems*, pages 307–312, 1983.
- [144] N. H. Gartner. Opac: A demand-responsivestrategy for traffic signal control. *Transportation Research Record*, (906):p. 75–81, 1983.

- [145] Pitu Mirchandani and Larry Head. A real-time traffic signal control system: architecture, algorithms, and analysis. *Transportation Research Part C: Emerging Technologies*, 9(6):415–432, 2001.
- [146] V. Mauro and D. Taranto. Utopia. *Proceedings of the sixth IFAC/IFIP/IFORS symposium on control, computers, communications on transportation*, pages 245–252, 1989.
- [147] Florence Boillot, Sophie Midenet, and Jean-Claude Pierrele. The real-time urban traffic control system cronos: Algorithm and experiments. *Transportation Research Part C: Emerging Technologies*, 14(1):18–38, 2006.
- [148] Christina Diakaki, Markos Papageorgiou, and Kostas Aboudolas. A multi-variable regulator approach to traffic-responsive network-wide signal control. *Control Engineering Practice*, 10(2):183–195, 2002.
- [149] Baher Abdulhai, Rob Pringle, and Grigoris J. Karakoulas. Reinforcement learning for true adaptive traffic signal control. *Journal of Transportation Engineering*, 129(3):278–285, 2003.
- [150] J C Medina and R F Benekohal. Traffic signal control using reinforcement learning and the max-plus algorithm as a coordinating strategy, 2012.
- [151] Samah El-Tantawy and Baher Abdulhai. Towards multi-agent reinforcement learning for integrated network of optimal traffic controllers (marlin-otc). *Transportation Letters: the International Journal of Transportation Research*, 2(2):89–110, 2010.
- [152] D. Srinivasan, Choy Min Chee, and R. L. Cheu. Neural networks for real-time traffic signal control. *Intelligent Transportation Systems, IEEE Transactions on*, 7(3):261–272, 2006.

- [153] Xueqian Li, Qinmin Wu, Jin Li, and Daoli Zhu. Congestion transportation network and optimal environmental link tolls. *Networked Computing (INC), 2010 6th International Conference on*, pages 1–4, 2010.
- [154] T. Hu and L. Chen. Traffic signal optimization with greedy randomized tabu search algorithm. *Journal of Transportation Engineering*, 138(8):1040–1050, 2012.
- [155] Yan Li, Jie Yang, Xiucheng Guo, and Montasir M. Abbas. Urban traffic signal control network partitioning using self-organizing maps. *Transportation Research Board 90th Annual Meeting Transportation Research Board*, page 20p, 2011.
- [156] H. Ishihara and T. Fukuda. Traffic signal networks simulator using emotional algorithm with individuality. *Intelligent Transportation Systems, 2001. Proceedings. 2001 IEEE*, pages 1034–1039, 2001.
- [157] P. G. Balaji, X. German, and D. Srinivasan. Urban traffic signal control using reinforcement learning agents. *Intelligent Transport Systems, IET*, 4(3):177–188, 2010.
- [158] M. Wiering, J. Vreeken, J. van Veenen, and A. Koopman. Simulation and optimization of traffic in a city. *Intelligent Vehicles Symposium, 2004 IEEE*, pages 453–458, 2004.
- [159] Ana L. C. Bazzan, Denise de Oliveira, and Bruno C. da Silva. Learning in groups of traffic signals. *Engineering Applications of Artificial Intelligence*, 23(4):560–568, 2010.
- [160] J. C. Medina and R. F. Benekohal. Traffic signal control using reinforcement learning and the max-plus algorithm as a coordinating strategy. *Intelligent Transportation Systems (ITSC), 2012 15th International IEEE Conference on*, pages 596–601, 2012.

- [161] Samah El-Tantawy, Baher Abdulhai, and Hossam Abdelgawad. Design of reinforcement learning parameters for seamless application of adaptive traffic signal control. *Journal of Intelligent Transportation Systems*, 18(3):227–245, 2013.
- [162] S. Mikami and Y. Kakazu. Genetic reinforcement learning for cooperative traffic signal control. *Evolutionary Computation, 1994. IEEE World Congress on Computational Intelligence., Proceedings of the First IEEE Conference on*, 1:223–228, 1994.
- [163] Ella Bingham. Reinforcement learning in neurofuzzy traffic signal control. *European Journal of Operational Research*, 131(2):232–241, 2001.
- [164] Dai Xiaohui, Li Chi-Kwong, and A. B. Rad. An approach to tune fuzzy controllers based on reinforcement learning for autonomous vehicle control. *Intelligent Transportation Systems, IEEE Transactions on*, 6(3):285–293, 2005.
- [165] C. Desjardins and B. Chaib-draa. Cooperative adaptive cruise control: A reinforcement learning approach. *Intelligent Transportation Systems, IEEE Transactions on*, 12(4):1248–1260, 2011.
- [166] M. Abdoos, N. Mozayani, and A. L. C. Bazzan. Traffic light control in non-stationary environments based on multi agent q-learning. *Intelligent Transportation Systems (ITSC), 2011 14th International IEEE Conference on*, pages 1580–1585, 2011.
- [167] Lin Wei-Song and Sheu Jih-Wen. Metro traffic regulation by adaptive optimal control. *Intelligent Transportation Systems, IEEE Transactions on*, 12(4):1064–1073, 2011.
- [168] Lior Kuyer, Shimon Whiteson, Bram Bakker, and Nikos Vlassis. *Machine Learning and Knowledge Discovery in Databases*, volume 5211 of *Lecture Notes in Computer Science*. Springer Berlin Heidelberg, Berlin, Heidelberg, September 2008.



- [169] Ana L. C. Bazzan. A distributed approach for coordination of traffic signal agents. *Autonomous Agents and Multi-Agent Systems*, 10(2):131–164, 2005.
- [170] L. A. Prashanth and S. Bhatnagar. Reinforcement learning with function approximation for traffic signal control. *Intelligent Transportation Systems, IEEE Transactions on*, 12(2):412–421, 2011.
- [171] Li Tao, Zhao Dongbin, and Yi Jianqiang. Adaptive dynamic programming for multi-intersections traffic signal intelligent control. *Intelligent Transportation Systems, 2008. ITSC 2008. 11th International IEEE Conference on*, pages 286–291, 2008.
- [172] D. C. K. Ngai and N. H. C. Yung. A multiple-goal reinforcement learning method for complex vehicle overtaking maneuvers. *Intelligent Transportation Systems, IEEE Transactions on*, 12(2):509–522, 2011.
- [173] Duan Houli, Li Zhiheng, and Zhang Yi. Multiobjective reinforcement learning for traffic signal control using vehicular ad hoc network. *EURASIP J. Adv. Signal Process*, 2010:1–7, 2010.
- [174] Joyoung Lee and Byungkyu Park. Development and evaluation of a cooperative vehicle intersection control algorithm under the connected vehicles environment. *Intelligent Transportation Systems, IEEE Transactions on*, 13(1):81–90, 2012.
- [175] Richard S Sutton and Andrew G Barto. *Reinforcement learning: An introduction*, volume 1. Cambridge Univ Press, 1998.
- [176] Abhijit Gosavi. *Simulation-Based Optimization: Parametric Optimization Techniques & Reinforcement Learning*. Springer, 2003.
- [177] John N. Tsitsiklis and Benjamin Van Roy. On average versus discounted reward temporal-difference learning. *Mach. Learn.*, 49(2-3):179–191, 2002.

- [178] I Arel, C. Liu, T. Urbanik, and AG. Kohls. Reinforcement learning-based multi-agent system for network traffic signal control. *Intelligent Transport Systems, IET*, 4(2):128–135, June 2010.
- [179] R Wunderlich, Liu Cuibi, I Elhanany, and T Urbanik. A Novel Signal-Scheduling Algorithm With Quality-of-Service Provisioning for an Isolated Intersection. *Intelligent Transportation Systems, IEEE Transactions on*, 9(3):536–547, 2008.
- [180] United States Environmental Protection Agency EPA. Motor vehicle emission simulator: User guide for moves2010b. 37(EPA-420-B-12-001b), June 2012.
- [181] Robert Chamberlin, Ben Swanson, Eric Talbot, Jeff Dumont, and Stephen Pesci. Analysis of moves and cmem for evaluating the emissions impact of an intersection control change. In *Transportation Research Board 90th Annual Meeting*, 2011.
- [182] S. Chu, E. Keogh, D. Hart, and M. Pazzani. Iterative deepening dynamic time warping for time series. *Proceedings of the 2002 SIAM International Conference on Data Mining*, pages 195–212, 2002.
- [183] Eamonn J Keogh and Michael J Pazzani. Scaling up dynamic time warping to massive datasets. In *Principles of Data Mining and Knowledge Discovery*, pages 1–11. Springer, 1999.
- [184] U.S. EPA. Epa releases moves2010 mobile source emissions model: Questions and answers. Technical Report EPA-420-F-09-073., 2009.
- [185] Huan Liu and Matthew Barth. Identifying the effect of vehicle operating history on vehicle running emissions. *Atmospheric Environment*, 59(0):22–29, 2012.
- [186] J. Lents and N. Davis. International vehicle emission (ive) model users manual. Technical report, 2004.

- [187] M. Barth, F. An, T. Younglove, G. Scora, C. Levine, M. Ross, and T. Wenzel. Development of a comprehensive modal emissions model. Technical report, 2000.
- [188] J. L. Jimenez-Palacios. *Understanding and quantifying Motor vehicle emissions with vehicle specific power and TILDAS remote sensing*. PhD thesis, MIT, Cambridge, MA., 1999.
- [189] H. Christopher Frey, Kaishan Zhang, and Nagui M. Roupail. Vehicle-specific emissions modeling based upon on-road measurements. *Environmental Science and Technology*, 44(9):3594–3600, 2010.
- [190] Ameya Bapat and H. Oliver Gao. Diesel particulate matter number emissions: Evaluation of existing modal emission modeling approaches. *Journal of Transportation Engineering*, 136(2):93–101, 2010.
- [191] Tao Huai, Thomas D. Durbin, Ted Younglove, George Scora, Matthew Barth, and Joseph M. Norbeck. Vehicle specific power approach to estimating on-road nh3 emissions from light-duty vehicles. *Environmental Science and Technology*, 39(24):9595–9600, 2005.
- [192] U.S. EPA. Using moves for estimating state and local inventories of on-road greenhouse gas emissions and energy consumption. Technical Report EPA-420-B-12-068, 2012.
- [193] P. G. Boulter and I. S. McCrae. The links between micro-scale traffic, emission, and air pollution models. Technical Report Transport Research Laboratory, PPR 269, 2007.
- [194] Brian S Everitt, Sabine Landau, Morven Leese, and Daniel Stahl. Hierarchical clustering. *Cluster Analysis, 5th Edition*, pages 71–110, 2001.

- [195] H. Sakoe and S. Chiba. Dynamic programming algorithm optimization for spoken word recognition. *Acoustics, Speech and Signal Processing, IEEE Transactions on*, 26(1):43–49, 1978.
- [196] Donald J Berndt and James Clifford. Using dynamic time warping to find patterns in time series. In *KDD workshop*, volume 10, pages 359–370. Seattle, WA, 1994.
- [197] JB Kruskall and M Liberman. The symmetric time warping algorithm: From continuous to discrete. *Time Warps, String Edits and Macromolecules*, 1983.
- [198] D Gerbec, S Gasperic, I Smon, and F Gubina. An approach to customers daily load profile determination. *Power Engineering Society Summer Meeting, 2002 IEEE*, 1:587–591, 2002.
- [199] James S. Farris. On the cophenetic correlation coefficient. *Systematic Biology*, 18(3):279–285, 1969.
- [200] V. Parker Lessig. Comparing cluster analyses with cophenetic correlation. *Journal of Marketing Research*, 9(1):82–84, 1972.
- [201] Andrew Nichols and Darcy Bullock. Design guidelines for deploying closed loop systems. *Joint Transportation Research Program*, No. FHWA/IN/JTRP-2001/11,, 2001.
- [202] Vision PTV America. 5.4 user manual. *PTV Vision*, 2012.

VITA

## VITA

H M. Abdul Aziz is originally from the splendid and the most happening Dhaka city, Bangladesh. He obtained B.Sc. degree in civil engineering from Bangladesh University of Engineering and Technology (BUET). Later, he received M.S.E degree in transportation engineering from the University of Texas at Austin in December 2009. He joined the Ph.D. program in Transportation Engineering at Purdue University from Spring 2010 and completed all requirements for the Ph.D. degree by August 2014. He worked in the interdisciplinary Transportation Modeling and Analytics Lab at Purdue where he has the role as a team leader in projects funded by National Science Foundation and the US DOT. His current areas of interests include: Network modeling of energy-efficient transportation systems, carbon allowance schemes for personal mobility, signal control with vehicle to vehicle/infrastructure (V2V and V2I) information exchange, application of econometrics and machine learning techniques in traffic safety analysis and agent-based simulation. He has several publications in peer-reviewed journals and conferences. He is a recipient of the 2014 Outstanding Graduate Student Award, presented by the Lyles School of Civil Engineering at Purdue University.